

ESD TDR 65-76
Vol I
ESTI FILE COPY

ESD-TDR-65-76

SPIRAL DECAY AND SENSOR CALIBRATION
DIFFERENTIAL CORRECTION PROGRAMS

Volume I. Program Development

TECHNICAL DOCUMENTARY REPORT NO. ESD-TDR-65-

31 JANUARY 1965

ESD RECORD COPY

RETURN TO
SCIENTIFIC & TECHNICAL INFORMATION DIVISION
(ESTI), BUILDING 1211

T. G. Gaa
C. G. Hilton
P. A. VanderStucken
L. G. Walters

COPY NR. _____ OF _____ COPIES

ESTI PROCESSED

DDC TAB PROJ OFFICER

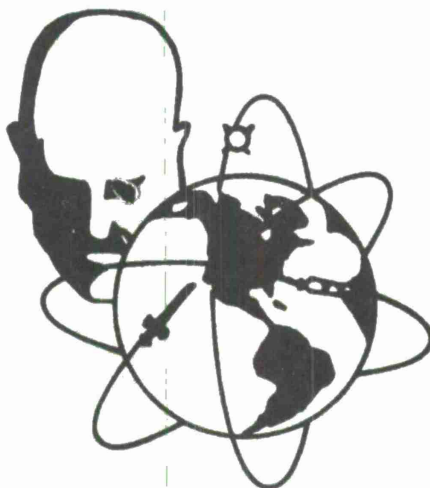
ACCESSION MASTER FILE

DATE _____

ESTI CONTROL NR AL 45280

CY NR _____ OF _____ CYS

496L SYSTEM PROGRAM OFFICE
ELECTRONIC SYSTEMS DIVISION
AIR FORCE SYSTEMS COMMAND
UNITED STATES AIR FORCE
L. G. Hanscom Field, Bedford, Massachusetts



Prepared under Contract No. AF 19(628)-3377 by Aeronutronic,
a Division of Philco Corporation, Newport Beach, California

AD0613279

When US Government drawings, specifications or other data are used for any purpose other than a definitely related government procurement operation, the government thereby incurs no responsibility nor any obligation whatsoever; and the fact that the government may have formulated, furnished, or in any way supplied the said drawings, specifications, or other data is not to be regarded by implication or otherwise, as in any manner licensing the holder or any other person or corporation, or conveying any rights or permission to manufacture, use, or sell any patented invention that may in any way be related thereto.

Copies available at Office of Technical Services, Department of Commerce.

DDC AVAILABILITY NOTICE

Qualified requesters may obtain copies from Defense Documentation Center (DDC). Orders will be expedited if placed through the librarian or other person designated to request documents from DDC.

SPIRAL DECAY AND SENSOR CALIBRATION
DIFFERENTIAL CORRECTION PROGRAMS

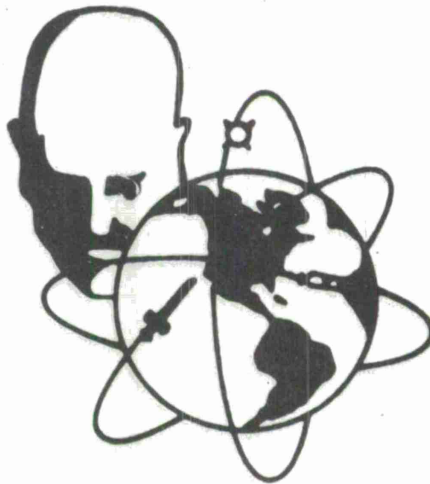
Volume I. Program Development

TECHNICAL DOCUMENTARY REPORT NO. ESD-TDR-65-

31 JANUARY 1965

T. G. Gaa
C. G. Hilton
P. A. VanderStucken
L. G. Walters

496L SYSTEM PROGRAM OFFICE
ELECTRONIC SYSTEMS DIVISION
AIR FORCE SYSTEMS COMMAND
UNITED STATES AIR FORCE
L. G. Hanscom Field, Bedford, Massachusetts



Prepared under Contract No. AF 19(628)-3377 by Aeronutronic,
a Division of Philco Corporation, Newport Beach, California

FOREWORD

This Technical Documentary Report has been prepared in four volumes, as follows:

<u>Volume</u>	<u>Title</u>	<u>Contractor's Publication Number</u>
I	Program Development	U- 3005
II	Operating Instructions	U- 3006
III	Programmer's Manual	U- 3007
IV	Operations Summary (U)	S- 2990

Publication of this technical documentary report does not constitute Air Force approval of its findings or conclusions. It is published only for the exchange and stimulation of ideas.

SPIRAL DECAY AND SENSOR CALIBRATION
DIFFERENTIAL CORRECTION PROGRAMS

ABSTRACT (U)

This document presents the theory, operation, and coding details of and experience with a computer program for the accurate prediction of the reentry corridor of an earth satellite undergoing orbital decay due to atmospheric friction. This program is also useful in the precision prediction of satellite positions for other purposes such as sensor calibration and weapon systems.

CONTENTS

SECTION		PAGE
1	INTRODUCTION	1
2	ORBIT DETERMINATION PROGRAM	6
	2.1 Differential Correction Procedure	6
	2.2 Programming System	9
	2.3 Ephemeris Integration	9
	2.4 Differential Correction	13
3	SENSOR CALIBRATION PROGRAM.	15
4	SPIRAL DECAY EXPERIMENTATION	19
	4.1 Objects 632 and 707 Decay	19
	4.2 Object 803 Decay	23
APPENDIX		
I	EPHEMERIS AND DIFFERENTIAL CORRECTION PROCEDURE	27
	I.1 Variation-of-Parameter Ephemeris Computation	27
	I.2 Weighted Differential Correction	40
II	JACCHIA-NICOLET DYNAMIC ATMOSPHERE MODEL	50
	II.1 Relation of Solar, Geomagnetic and Geographic Phenomena to Temperature	51
	II.2 Application of Nicolet's Steady-State Model	54
	II.3 Interpolation Formulas	54
	II.4 Density Above 1000 KM	55
III	SCALAR DIFFERENTIAL EXPRESSIONS FOR ORBIT PARAMETERS	57
	III.1 Selection of Orbit Parameters	58
	III.2 The Differential Relationships	60
IV.	SCALAR DIFFERENTIAL EXPRESSIONS FOR DRAG	74
	IV.1 Determination of Density Variations Along Path	74
	IV.2 Secular Variation in Semi-Major Axis	76
	IV.3 Secular Variation in Eccentricity	81
	IV.4 Scalar Differential Expressions	81

APPENDIX		- PAGE
V	SCALAR DIFFERENTIAL EXPRESSIONS FOR SENSOR CALIBRATION	84
	V.1 Scalar Differential Expressions for Sensor Locations	84
	V.2 Scalar Differential Expressions for Time and Observation Bias	89
VI	VARIATION-OF-PARAMETERS FOR NON EQUATORIAL ORBITS	94
VII	LIST OF SYMBOLS	106

ILLUSTRATIONS

FIGURE		PAGE
1	Spiral Decay Program Flow Chart	7
2	Sensor Calibration Procedure	16
3	Cosmos 31 (Object 803) Decay	25

APPENDIX I

I-1	Variation-of-Parameters Method for Ephemeris Computation	28
I-2	Position of Satellite With Respect to Earth's Shadow. .	34
I-3	Vector Relationships	44

APPENDIX II

II-1	Relation of Vehicle Latitude to Subsolar Bulge	53
------	--	----

APPENDIX III

III-1	Projection of Orbit on Celestial Sphere	59
III-2	Observational Framework	67

APPENDIX IV

IV-1	Height Above Oblate Earth	75
------	-------------------------------------	----

APPENDIX V

V-1	Position Relationship of Observer, Satellite and Dynamic Center	86
V-2	Meridian Cross-Section of Earth	92

APPENDIX VI

VI-1	Osculating Orbit Definition	95
VI-2	Vector Relations	105

TABLES

NUMBER		PAGE
I	Spiral Decay Program Specifications	2
II	Variability of Dynamic Atmosphere Terms	12
III	Correlation of Visual Observations and Ephemeris . . .	20
IV	Spacetrack Object 632 Decay	22

APPENDIX I

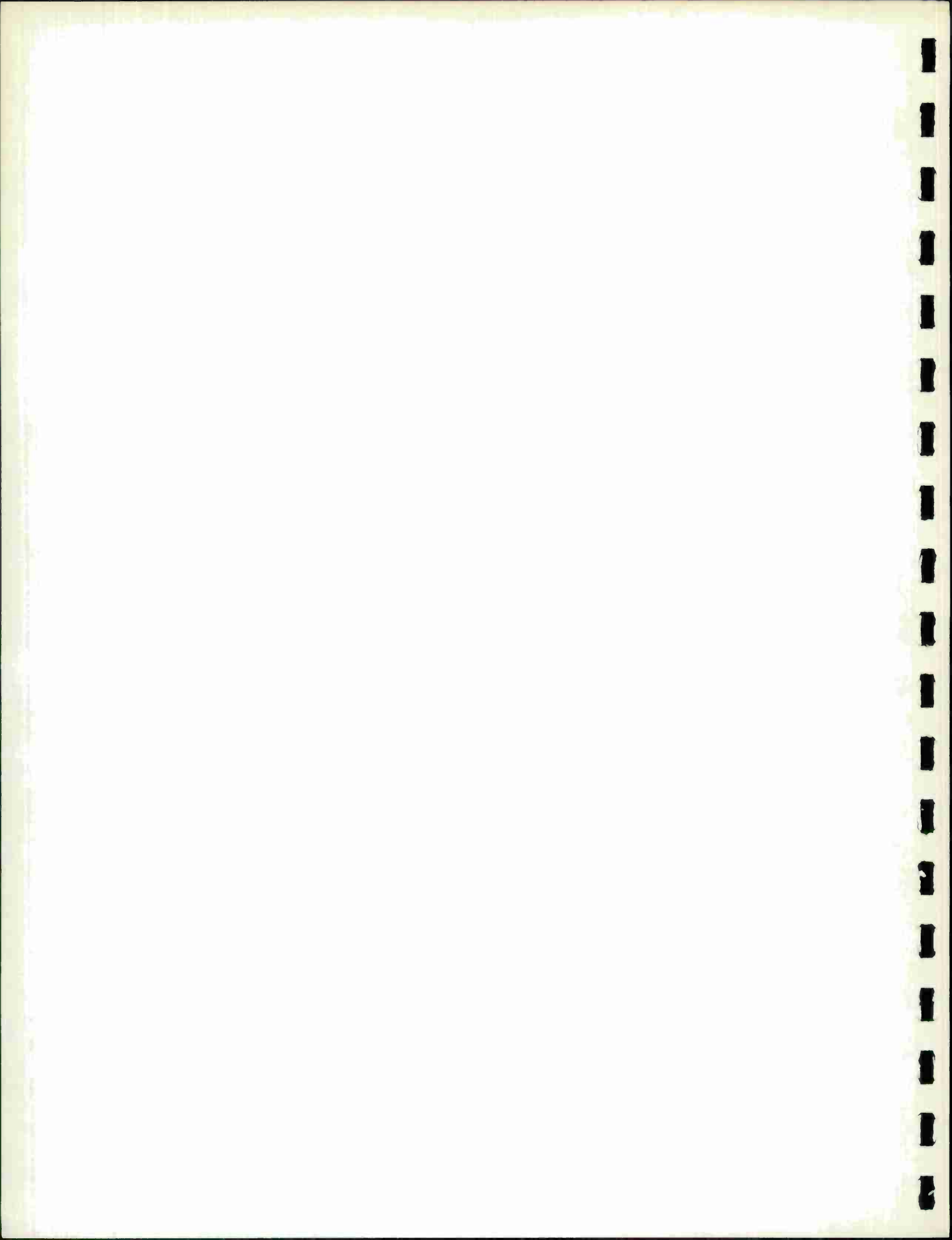
I-1	Expressions for g_S , g_E , and g_r	29
I-2	Associated Legendre Functions and Their Derivatives . .	31

APPENDIX IV

IV-1	Bessel Functions of Imaginary Argument	79
IV-2	Expression for Secular Variation in Semi-Major Axis . .	80
IV-3	Expression for Secular Variation in Eccentricity . . .	80

APPENDIX V

V-1	Scalar Differential Expressions for Sensor Calibration	90
-----	--	----



SECTION 1

INTRODUCTION

This report documents Aeronutronic's approach to the formulation of a computer program for high-precision orbit determination within the SPACETRACK computational environment. Although originally intended for terminal decay corridor determination for satellites executing spiral decay, this program has evolved, within the limitations imposed by the Spiral Decay Technique Development Contract, as a highly effective tool for a majority of the high-precision requirements of the SPACETRACK center, including spiral decay, weapon command and control, and sensor calibration. Through an extended period of joint contractor and SPACETRACK analyst application of this class of programs to the rapidly-changing spectrum of operational requirements on the SPACETRACK center, a high degree of analyst proficiency and operational utility have also been developed.

Specifications for the Spiral Decay class of programs are conveyed in Table I. Two programs are involved:

- (1) Spiral Decay (SPIRDEC) is an orbit determination and prediction program, with weighted differential correction capability for osculating elements and ballistic coefficient. Current limitations are to non-equatorial satellites with eccentricities less than 0.9* (no ballistic coefficient correction) and 0.1 (with ballistic coefficient correction).

* For the higher eccentricities, lunar and solar perturbations become increasingly important. These are not included in the current version of the program.

TABLE I. SPIRAL DECAY PROGRAM SPECIFICATIONS

Operating System	SPS B-3 / Philco 2000 Schedule Tape Mode
Ephemeris Integration	Variation of Parameters Cowell Entry Option
Numerical Integration	Sixth-order Adams-Bashforth with Runge-Kutta Start Automatic Interval Control
Initialization	SPACETRACK Mean Elements Osculating (<u>M</u> , <u>N</u>) Elements Geocentric Position and Velocity
Geopotential	Zonal Harmonics Inclusive of Fifth- order Non-zonal Harmonics Inclusive of Fourth-order
Atmosphere	Jacchia-Nicolet Dynamic Model Above 120 Kilometers COESA 1962 Static Model Below 120 Kilometers
Differential Correction (Weighted)	Six Osculating Parameters (<u>M</u> , <u>N</u> Formulation) Ballistic Coefficient Sensor Location Timing and Observation Biases (Using CALIB Program)
Sensor Input Data	Internally Compiled Table for Biases and Weights, with Optional Override
Observation Capacity	Up to 984 Observations; Sorting Internal to Program
Prediction Capability	Geographic and/or Geocentric Cartesian Coordinates
Acquisition Capability	Binary Ephemeris Tape for XYZLA Program
Restart Capability	Punches Parameter Cards for Both Spiral Decay and Calibration Programs

- (2) Sensor Calibration (CALIB) is a differential correction program for determining biases in sensor location, timing, and observed quantities, utilizing a reference orbit determined from an independent sensor network (normally either PRELORT or Baker-Nunn data), using the SPIRDEC program.

The SPIRDEC program has been compiled in both SPS B-2 and SPS B-3 versions to accommodate the SPACETRACK system change to be installed during January 1965. Although the operating instructions conveyed with this report reflect a B-3 capability for the CALIB program as well, delivery of a B-3 version coincident with this report is not planned. In the interim, the SPS A-1 version of the SPIRDEC and CALIB programs, documented in the Milestone II report,* shall be available.

In the development of the Spiral Decay class of programs, particular attention has been paid to those factors considered limiting in a useful spiral decay and weapon command and control capability. Important considerations which have influenced the program design include:

- (1) Environmental factors which influence the trajectory, primarily the atmospheric density and gravitational perturbations, must be carefully considered. Such considerations lead to the inclusion of a dynamic model atmosphere and longitude-dependent (tesseral) harmonics in the geopotential, inclusive of fourth-order.**
- (2) The rational application of statistical weights to ADC sensor data cannot be made without first providing for the large known biases in these sensors. The Spiral Decay program will accept and process both weight and bias data for sensors and, through the interfacing Sensor Calibration program, will determine location, timing and observation biases for selected sensors, utilizing either ADC or independent (PRELORT, Baker-Nunn) sensors as a reference network.

* "Spiral Decay and Sensor Calibration Differential Correction Programs - Milestone II Draft", 31 March 1964, Aeronutronic Publication U-2559.

** The fifth zonal harmonic is also included. A subroutine is now in checkout which extends the potential to the ninth-order zonal and sixth-order non-zonal harmonics. A change note to this documentation will be issued upon completion.

- (3) Since this class of programs will normally provide nearly real-time support to SPACETRACK spiral-decay and weapon-oriented requirements, every effort has been expended to provide a precision orbit capability of the highest computational efficiency. This is reflected in the choice of the variation-of-parameters method for ephemeris calculation, and in the derivation and application of analytical differential correction equations.*

To accomplish these ultimate objectives while providing a meaningful interim capability, a series of programming milestones was established. These milestones, with technical and programming targets, are listed below:

<u>Milestone</u>	<u>Technical and Programming Target</u>
I (31 December 1963)	Demonstrate the application of the variation-of-parameters approach, with analytic correction equations, to a decaying satellite (object 292)
II (31 March 1964)	Demonstrate, in the live SPACETRACK computation and data environment, an interim capability for Spiral Decay calculations (objects 632, 707)
III (30 June 1964)	Deliver an interim operational (SPS B-2) capability for Spiral Decay calculations. Demonstrate an interim sensor calibration capability (objects 759, 811)
IV (30 September 1964)	Demonstrate a weapon support capability in the SPACETRACK environment.
V (31 December 1964)	Deliver "final" operational (SPS B-3) capability for Spiral Decay and weapon support.

* This approach has been demonstrated, in the SPACETRACK environment, to exceed the computational speed of the competitive COWELL approach by a factor of four or more, with better accuracy.

Highlights in the development of these capabilities include the scheduled visual confirmation of two satellite decays during the Milestone II demonstration (See Section 4) and the subsequent scheduling of four additional visual confirmations.

This report documents the Milestone V program status. Subsequent sections and appendices provide a detailed technical description of the Spiral Decay and Sensor Calibration programs.

SECTION 2

ORBIT DETERMINATION PROGRAM

Except in the somewhat trivial case of a point mass moving in a pure central force-field, the so-called "Two Body Problem," it is generally impossible to derive orbital elements from observations by direct analytical means. The process usually employed is to create a dynamical model of the motion and then to adjust the constants introduced into this model until the best possible fit to the observations is obtained in the sense of least squares. The problem is very similar to the one faced in classical celestial mechanics; the solutions discussed here draw heavily from the theory and practice of celestial mechanics.

The principal differences between modern orbital theory of artificial satellites and classical celestial mechanics theories arise in part from the fact that the artificial satellite environment includes perturbative forces such as aerodynamic drag, earth-bulge, and the like, and in part from the availability of high-speed computing equipment and electronic instrumentation providing range and range-rate data, as well as angles.

2.1 DIFFERENTIAL CORRECTION PROCEDURE

Reduced to its simplest form, the differential correction technique involves the following five steps (identified in Figure 1):

- Step 1. Raw observation data is corrected for known systematic errors (biases) as determined from calibration efforts.

Differential Corrections To:

Six Orbit Parameters
Ballistic Drag Parameter

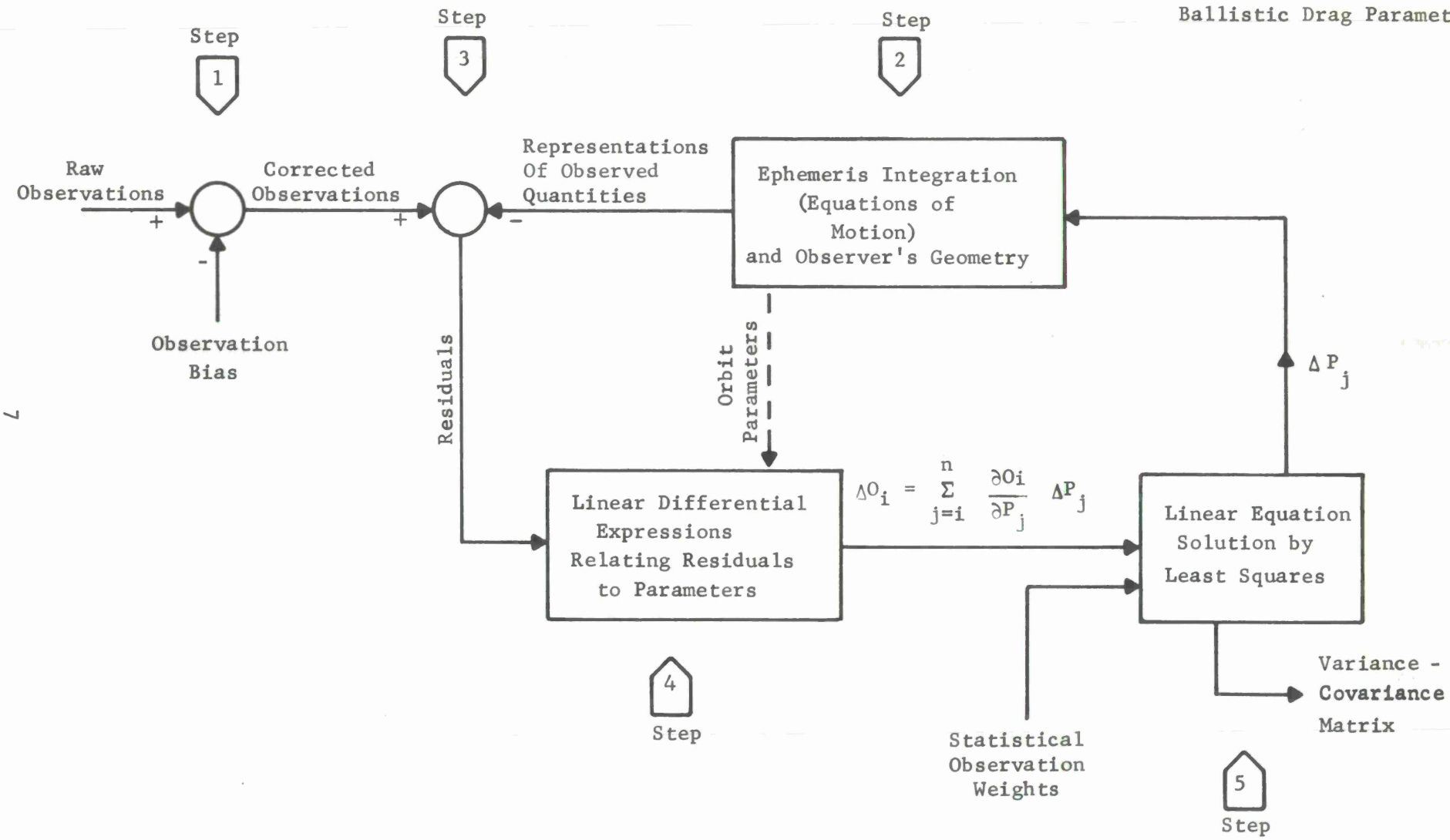


FIGURE 1. SPIRAL DECAY PROGRAM FLOW CHART

- Step 2. Beginning with a tentative estimate of the injection conditions and other "constants" entering into the equations of motion, an ephemeris is produced by integrating these equations. At each time for which an observation exists, this ephemeris is translated into a "representation" for those observations available from the particular sensor.
- Step 3. In the absence of unknown observation errors, and for exact knowledge of the injection conditions and environment governing the motion, the representations and corrected observations would be identical. In practice, however, they are not identical, and their differences, or "residuals," serve as a basis for differentially correcting the initial constants, as shown in the following steps 4 and 5.
- Step 4. Cause and effect relations between injection conditions and subsequent observations are highly nonlinear. Where corrections to these injection conditions and subsequent changes in residuals are small, the problem is readily linearized. For each observed quantity, a scalar differential expression relating the known residual to the unknown changes in injection conditions and other parameters defining the motion is derived.
- Step 5. The system of linear equations, one for each observed quantity and normally heavily overdetermined, is solved in the sense of weighted least squares for the differential corrections to the injection parameters. Some insight into the convergence of the procedure is available by examining the weighted sum-of-squares of the residuals, and the variance-covariance matrix of the differential corrections.

Normally, steps 2 through 5 will be repeated until the weighted sum-of-squares of the residuals becomes stationary. During this iterative process, observations which do not fit the orbit may be rejected.

Execution of the foregoing five basic operations is quite involved and requires meticulous attention to detail. Such items as the atmospheric model, geopotential, and choice of reference systems must be correctly handled to ensure the greatest precision.

2.2 PROGRAMMING SYSTEM

To facilitate the eventual application of the Spiral Decay Program within the ADC Spacetrack Center, yet permit interim experimentation and simulation at 496-L (Bedford, Massachusetts), Aeronutronic and the ADC Spacetrack Center, the Semiautomatic Programming System (SPS), A-1 version, was utilized in the first milestone. The successful demonstration of the Milestone II version in the ADC environment, and the desire on the part of ADC personnel to utilize these procedures, made an interruptable (B-2) version of this program desirable. Thus, the Milestone II program was prepared in two versions:

- (1) An interruptable (B-2) version of the Spiral Decay module, permitting application of this procedure during periods where the ADC computer(s) are providing backup for other ADC functions.
- (2) A noninterruptable (A-1) version of the Spiral Decay and Sensor Calibration modules, in which the executive system has been modified to prevent truncation of time. This latter feature is considered essential to meaningful calibration work.

The operating instructions for both A-1 and B-2 program versions, operating in the Schedule Tape Mode, were conveyed in the Milestone II draft of the present report.*

The present report applies to programs operating under the control of the B-3 system, which is interruptable and uses new formats accommodating five-digit satellite numbers.

2.3 EPHEMERIS INTEGRATION

The ephemeris integration represents a major portion of the computational burden for spiral decay calculations. Since no satisfactory theory is yet available to perform this integration by general perturbations (development of the perturbations into series and integrating term-by-term) for orbits highly perturbed by drag, the special perturbations technique (numerical step-by-step integration) has been employed.

* Aeronutronic Publication U-2559, 31 March 1964

The coordinates are referred to the mean equinox of a fixed epoch and the true equator of date. For detail refer to the definitions of I, J, K, etc., in Appendix VII.

Of the several formulations available in special perturbations, the variation-of-parameters method has been employed for two reasons:

- (1) The technique suppresses the dominant central gravitation term in the geopotential by integrating parameters which, in the absence of perturbative effects, are constant.
- (2) The parameters integrated in the variation-of-parameters method may be related, through scalar differential expressions, to observed coordinates at future times, thereby permitting a fully analytical development of the differential correction.

These factors contribute to computational efficiency by (1) permitting large integration step size (or fewer derivative evaluations per revolution) and (2) facilitating communication between the ephemeris and differential correction modules of the program.

Of the several available formulations for variation-of-parameters, the a, h formulation* has been used, since it exhibits no zero-eccentricity singularities.

During the last revolution of a satellite executing spiral decay, the perturbative accelerations become too large to be efficiently accommodated by the variation-of-parameters method. A transition to the Cowell formulation of the equations of motion during this revolution is provided.

a. Numerical Integration Method

The variation-of-parameters method leads to seven first-order differential equations, with time or one of the anomalies as the independent variable.

* A complete derivation of the equations is given in Appendix VI. The mathematical steps involved in both ephemeris integration and differential correction are conveyed in Appendix I.

Prior to Milestone IV, expediency dictated program compilation with the Runge-Kutta integration subroutine, a fourth-order technique requiring four (4) derivative evaluations per step. This self-starting technique permits great flexibility in specification of time interval, but at the expense of running time. Comparable precision and stability, however, is available with higher-order predictor-corrector methods requiring fewer derivative evaluations per revolution. The final program thus is compiled with such an alternative numerical integration subroutine, Adams-Bashforth. The Runge-Kutta technique will continue to be used for starting purposes.

Representation of observations for residual computation demands that satellite coordinates at arbitrary observation times be calculated. Initially, and again for expediency, the program numerically integrates to each observation time. For situations where a large number of observations exist, such as sensor calibration work utilizing raw data derived from the AF Satellite Control Facilities, the additional integration step for each observation becomes inefficient. To avoid this unnecessary computational burden, a fifth-order divided difference interpolation procedure has been included, permitting the interpolation for observation times in an ephemeris table of arbitrary time interval (as determined by the integration error control).

b. Drag Perturbations

A number of atmospheric models, which include dynamic terms to represent deviations from "standard" models, are in use. Those dynamic effects which have been identified from satellite acceleration studies include seasonal and longitude-dependent terms, as well as those correlated with solar radiation and planetary magnetic effects.

At altitudes below 300 km., representing the region of interest during the last few days of spiral decay, the variations in density due to important dynamic terms are given in Table II.

TABLE II. VARIABILITY OF DYNAMIC ATMOSPHERE TERMS*
(orders of magnitude)

<u>Altitude</u>	<u>Diurnal</u>	<u>Seasonal</u>	<u>Solar (F_{10})</u>	<u>Magnetic (A_p)</u>
150 km	0	0	0.14	0
200 km	0	0.07	0.54	0.05
250 km	0.06	0.10	0.86	0.09
300 km	0.14	0.12	1.00	0.14

At higher altitudes, these effects are even greater.

These considerations have led to the incorporation of a dynamic model atmosphere in the spiral decay program. The Jacchia-Nicolet model** has been utilized; this model includes significant geometric and solar radiation terms above 120 km. The formulation of the Jacchia-Nicolet atmosphere subroutine is given in Appendix II.

c. Gravitational Model

In the selection of terms to be included in the gravitational model for the earth, careful consideration must be given to terms which either (1) lead to secular and/or long period terms which, if neglected, would be aliased into other effects, or (2) can lead to short period radial displacements with consequential drag coupling.

Based upon these considerations, zonal, sectorial, and tesseral terms have been included in the gravitational model. For Milestones I and II, the J_{22} term was implemented. A general expression for the earth model permitting the inclusion of a consistent set of the harmonics through $n,m = 4,4$ is now used. The formulation of this earth model is conveyed in Appendix I. The values of the coefficients of the non-zonal harmonics, which are still undergoing redefinition by several investigators, are specified by two parameter cards in the program input.

* H. K. Paetzold, "Model for the Variability of the Terrestrial Atmosphere above 150 km", submitted to COSPAR working group IV, "Reference Atmosphere", 1962 January.

**L. G. Jacchia, "Temperature Above the Thermopause", Smithsonian Inst. Astrophysical Observatory Special Report No. 150, April 22, 1964.

2.4 DIFFERENTIAL CORRECTION

The differential correction involves the formulation of scalar differential expressions relating observation residuals to corrections to the parameters defining the representation; these parameters normally include six initial conditions or elements defining the orbit and a seventh parameter related to the interaction of the satellite with drag environment. Where sufficient observation redundancy exists to permit the determination of additional parameters, sensor biases (range, angles, timing) or geometric factors entering into the representation (such as geocentric coordinates of the observer) may also be determined.

The scalar differential expressions take the following form:

$$\Delta O_i = \sum_{j=1}^n \frac{\partial O_i}{\partial p_j} \Delta p_j$$

where O_i are observed coordinates and the p_j are parameters to be corrected. Two conditions must be met to solve for the Δp_j , namely:

- (1) There must be at least as many observations as parameters ($i \geq n$) to solve the system of linear equations, and
- (2) The selected parameters must be capable of being related to observed coordinates by linear differential expressions, without singularities at critical parameter values.

The first condition is readily met with modern electronic instrumentation, and the overdetermined system of equations is solved in the sense of weighted least squares. This approach assumes that observation errors are statistically uncorrelated, a reasonable assumption for SPACETRACK observations if the biases can be predetermined. Under these conditions, the variance-covariance matrix of orbit parameters reveals the quality of the determination and may be printed out for inspection.

The second condition above implies that the partial derivatives exist for the complete range of parameter values encountered in the differential correction. Attempts to differentially relate, for example, the orbit eccentricity and perigee argument to observed coordinates through linear differential expressions must fail at zero eccentricity for the eccentricity is, by definition, non-negative and the perigee argument indeterminate. A number of parameter sets exist which can be successfully related to observed coordinates through linear differential expressions at this critical eccentricity*. Some of these sets, such as the M, N pattern

* See, for example, Aeronutronic Report U-880.

utilized in the Spiral Decay Program, may be differentiated to provide a completely analytical formulation for the differential correction, thereby leading to substantial economies in computational time.

With the exception of the drag parameter, the \underline{M} , \underline{N} form for the differential correction has been adequately documented*. Analytical differential expressions for the drag parameter have also been derived, and this derivation is included as Appendix IV to this report.

In addition to the differential correction features cited above, the Milestone III version was to have included limited differential correction in the Cowell entry option. It has been demonstrated (see Section 6), however, that the variation-of-parameters method will accommodate tracking data extending into the incendiary region of decay. Experimentation has also established the desirability of including geometric terms in the drag correction equations arising from earth flattening, which can lead to density variations equivalent to a scale height. The formulation of these expressions is given in Appendix IV.

*In addition to U-880, sources include the Proceedings of the JPL Seminar on Tracking Programs and Orbit Determination, 22-26 February 1960, and Koelle, "Handbook of Astronautical Engineering" McGraw-Hill, 1961, Section 8.112.

SECTION 3

SENSOR CALIBRATION PROGRAM

In Appendix V, scalar differential expressions have been developed which relate observation residuals — in range, range-rate, azimuth and elevation — to biases in sensor location, time reference and observed coordinates. This theory has been implemented in a Sensor Calibration Program, designated CALIB, operating in the Schedule Tape Mode, A-1 system. This Section presents a description of the procedure; operating instructions are given in Volume II. Results of operational applications of these techniques are conveyed in the Operations Summary, Volume IV.

The calibration procedure involves the consecutive application of two differential correction procedures as shown in Figure 2.

The first step involves the definition of a highly precise reference orbit derived by processing tracking data from sources of high confidence level and redundancy. The most appropriate tracking system for this purpose is the network of PRELORT radars operated by the 6594th Aerospace Test Wing (Sunnyvale, California) in support of AFSC satellite programs. These radars track a cooperative S-band beacon carried by most AFSC satellites, and the tracking data rate for this network is in excess of 1500 observations/day even for relatively low (100 n.m.) satellites. The quality of these data and of the earth and atmospheric model used to define the satellite motion is demonstrated by the ability to fit these data, even over relatively long time spans, to the order of 100 meters. To facilitate the utilization of these data within the ADC computation environment. AFSC has contracted for preparation of a 160A computer program to translate PRELORT data tapes into SPADAT BCD card format, and to prepare a standard teletype tape for transmission into SPACETRACK.

Additional data sources can be exploited for performing this calibration function, either to complement the PRELORT data or to replace it where the satellite does not carry an active S-band beacon. Baker-Nunn camera data, for example, lacks the redundancy and intrinsic metric desirable for calibration exercises, but will strengthen the PRELORT data, where greatest emphasis is placed upon range data.

The design of the Spiral Decay differential correction program provides for the definition of the reference orbit to the desired precision. The necessary interface between the SPIRDEC and CALIB programs, as shown in Figure 2, is a vector defining the parameters of the reference orbit; provision has been made in the SPIRDEC program to format and print the parameter card images for control of CALIB directly.

The second step in the Sensor Calibration procedure also involves a differential correction procedure. Beginning with the reference ephemeris and with observations derived from the sensor undergoing calibration, a weighted least-squares determination is made of those sensor properties — sensor location, time, and observation biases — which lead to the best fit of the tracking data to the reference ephemeris. This step is performed by the CALIB differential correction program, which permits the selective determination of any combination of the seven sensor properties, data permitting. In addition to these biases, CALIB also determines RMS values for the individual observation types, to be used as weights in subsequent applications of the sensor data.

Although these procedures could have been assembled as a single program, the following considerations influenced the decision to prepare two programs with a simple, program-defined interface:

- (1) More flexible use of memory is permitted, particularly in subsequent B-2 and B-3 versions of these programs, where certain memory regions are denied.
- (2) The simultaneous determination of biases and orbit parameters, in a single pass involving both PRELORT and ADC sensor data, may alias the reference orbit parameters unless the freedom to determine all biases in the candidate sensor is permitted. Few such data situations will exist.

It is important to note that the earth model and atmosphere constants must be identical in the two programs, to permit the accurate reconstruction of the reference ephemeris in the CALIB program.

The current operational version of the calibration procedure operates in the Schedule Tape Mode, A-1 version. Restriction to the A-1 operating system was necessitated by the manner in which time is processed in executive modules of the B-2 system, where the representation of time since 1950.0 as a floating point number introduces errors in tens of milliseconds. In the A-1 master tape utilized at ADC/496L for calibration work, these modules have been modified to represent time in fixed point and double precision, thereby avoiding this source of error. These modifications have now been introduced into the B-2 and B-3 executive modules, paving the way for the subsequent compilation of the CALIB program in these systems.

SECTION 4

SPIRAL DECAY EXPERIMENTATION

During the application at ADC of procedures developed under this study for spiral decay corridor determination, six visual confirmations of decay were successfully scheduled. Four of these represented Russian satellites which, by virtue of their lower inclinations, were more likely to decay over the populated middle and equatorial latitudes. Two of these scheduled visuals (on objects 632 and 707) were made during the demonstration at ADC of the spiral decay capability in March, 1964, while a third provided the first visuals on two consecutive revolutions. These three satellites are discussed in detail in this section.

The visuals described above involved observers in North America and represent the best documented observations. Additional visuals were scheduled through the 1127th Field Activities Group, Fort Belvoir, including object 834, 1 August, 1964, at Carnarvon, Australia; and object 796, 27 May, 1964, at Maracaibo, Venezuela. The visuals on 911 were made by both ground observers and SAC aircraft commanders, above the Arctic circle, and were scheduled through NORAD.

4.1 OBJECTS 632 and 707 DECAY

To evaluate the performance of the Spiral Decay program, Milestone II version, in the ADC data and computation environment, the tracking records of two Russian Cosmos Satellites, Spacetrack Objects 707 and 632, were reduced on a real-time basis in ADC centers at L. G. Hanscom Field and Colorado Springs. Both exercises were successful beyond expectations, resulting in visual confirmation of decay in each case. Equally gratifying was the performance of the variation-of-parameters method, coupled with the analytic differential correction technique which (in the case of Object 632) converged readily on tracking data extending into the incendiary region of decay.

Object 707 was a cylindrical body of low area-to-mass ratio. The data reduction for this exercise was performed at L. G. Hanscom Field by SCAF and Aeronutronic personnel. The success of this venture may be measured by results presented in Table III. The low area/mass ratio of this object

TABLE III

CORRELATION OF VISUAL OBSERVATIONS AND EPHEMERIS

SPACETRACK OBJECT 707 DECAY
 (Based upon data over 3/26 0208Z - 3/26 2225Z)

<u>TIME</u> (Day: Time)	<u>POSITION</u>	<u>OBSERVER</u>	<u>COMMENTS</u>
27:0128Z	44 ^o .2N 115 ^o .W 94km	--	--
27:0129Z	45 ^o .7N 110 ^o .0W 89km	--	--
27:0130Z	47 ^o .0N 105 ^o .0W 82km	Finley AF WX Station Finley, N.D.	"Dim object report moving SW to NE"
27:0131Z	47 ^o .9N 100 ^o .W 70.0km	Baudette, Minn. Duluth, Minn. (SAGE Direction Center, 4 observers)	"Red-orange object directly overhead; pieces falling off." "Three objects; visible trail lasting 5 sec. behind first object; one object appeared to descent in local area."
27:0132.54Z	*	Madison, Wisconsin (Moonwatch)	"Sparking object, 4 ^o elev., 355 ^o azimuth"

* The ephemeris for object was based upon a single drag coefficient implying structural integrity. The low W/C_DA and confirmed breakup would permit pieces to go beyond the impact area corresponding to the intact object.

and its shape suggest a collection of dense components (rocket motor, payload) joined by light structural components and tankage. One would expect the aerothermodynamic environment to rapidly strip away these lighter structural components, creating a variety of objects of differing area/mass ratio, each following an independent course. This speculation is supported by visual evidence, which verified the onset of high heating rates (Fargo, N.D.), the breakup of the satellite (Baudette, Minn.), and the independent decay of at least three objects (Duluth, Minn.). The correlation between these phenomena and the ephemeris provided by the Spiral Decay program is excellent, as demonstrated in the Table.

The decay exercise for Object 632 was conducted at Colorado Springs. The area/mass ratio of 632 was also quite low, as noted in Table IV. Nine fits were obtained over the last 72 hours of lifetime, each requiring approximately 10 minutes of computer (Philco 212) time. Highlights of each iteration are presented in Table IV; these include (1) the fact that all fits over the last 72 hours (and probably greater intervals) defined a decay window of approximately one hour and (2) no iterations on any fit were divergent.* This latter property of the Spiral Decay program is readily appreciated when it is noted that, on fit #1 beginning with SPADAT mean elements, range-rate residuals of 3 km/sec and larger were common on the initial pass through the data. Visual confirmation of 707 decay in its early stages was provided by a weather observer in Duluth, Minn.; poor weather over the Eastern states and mid-Atlantic precluded sightings extending on into the most probable decay region (extending from the Azores into South Africa).

It is highly probable that 632 decayed in several fragments as in the case of 707. In order to evaluate the possible decay corridor for objects of various area/mass ratios, a sequence of decay trajectories was integrated, beginning with the visual evidence of decay over Duluth at 0726Z. In particular, a Moonwatch observation was reported about 0900Z from the Northeastern U.S. Based upon a fit including tracking data during this decay phenomenon, an object with an area/mass ratio even as low as $0.0002 \text{ m}^2/\text{kgm}$ would not complete another revolution. Since it is difficult to visualize a satellite component with these properties, and since both Moorestown and Prince Albert radars gave negative reports on this post-decay revolution, confirmation of this report is lacking.

*Since the observations accepted from iteration to iteration varied, divergence is arbitrarily defined as an increase in the weighted rms of five percent or more on successive iterations.

TABLE IV

SPACETRACK OBJECT 632 DECAY

PRE-DECAY ANALYSIS

<u>Fit</u>	<u>Data Interval</u> (Day: Zulu Time)	<u>Decay Time</u> (Day: Zulu Time)	<u>Drag Parameter</u> Meters ² kgm ⁻¹	<u>RMS Fit</u> (Weighted*)	<u>Divergent</u> <u>Iterations</u>
1	26:0446 - 27:1511	30:0817	0.01631	1.03	0
2	27:1758 - 28:1600	30:0911	0.01630	0.70	0
3	27:1753 - 28:1732	30:0856	0.01647	0.85	0
4	28:0400 - 29:1242	30:0818	0.01666	0.86	0
5	29:0351 - 29:1941	30:0803	**0.01694	1.06	0
6	29:0351 - 29:2113	***	**0.01684	1.22	0
22 7	29:0351 - 30:0016	30:0806	**0.01688	1.36	0
8	29:0351 - 30:0423	30:0757	**0.01698	2.02	0

POST-DECAY ANALYSIS

9	29:1701 - 30:0727	30:0747	**0.01746 (6 element fit)	2.84	0
---	-------------------	---------	------------------------------	------	---

* Generally based upon TIP bias/weight recommendations, as revised by results of the object 759 (1964 March 3-5) calibration effort

** Beginning with Fit 5, transitional drag effects were introduced

*** Although solution was convergent, convergence test failed to meet stringent (one percent) test on successive values of weighted rms before the pre-designated maximum number of iterations was exceeded.

4.2 OBJECT 803 DECAY

One of the better documented decay exercises involved the COSMOS 31 (Object 803) payload, launched on 6 June, 1964. A TIP exercise conducted at SPACETRACK during the week prior to decay successfully scheduled visual confirmations of decay during revolution 2161, along a corridor extending across the Northwestern U.S., at 20 October, 0516Z. Reports of unusual meteoritic phenomena on the previous revolution 2160 prompted an appeal in Canadian news media for detailed reports. Of the resulting fourteen reports submitted, a majority correlated with the timing and direction of 803, leaving little doubt that some component of 803 had decayed over Ottawa, Ontario, at approximately 2353 local time (20 October, 0353Z).

Further analysis was conducted to determine answers to the following questions:

- (1) What mechanism separated Object 803 at least one revolution before decay, and
- (2) What was the nature of the object that decayed prematurely?

The analysis presented here supports the conclusion that an array of solar cells was separated by aerodynamic forces near the ascending node, revolution 2160, and decayed twenty minutes later over Ottawa.

Examination of the ephemeris during the last few revolutions revealed that the perigee of the orbit was near the ascending node. A one-minute interval ephemeris was produced for the last revolutions to examine the altitude variation around the orbit; the following values were determined:

<u>Rev</u>	<u>Altitude in Vicinity of</u>			
	<u>Ascending Node</u>	<u>Northern Antinode</u>	<u>Descending Node</u>	<u>Southern Antinode</u>
2159	141 km	149 km	144 km	157 km
2160	133 km	137 km	132 km	142 km
2161	119 km	Decay		

Two mechanisms may be effective in removing a component of Object 803 near the ascending node of revolution 2160, aerodynamic and aerothermodynamic. The dynamic pressure is still quite low ($\sim 0.025 \text{ kg/m}^2$) but capable of inducing substantial vibration loading on structures of

poor aerodynamic design. The aerothermodynamic effects at 130 km border on heating rates sufficient to induce structural failure. The combination of these effects at 130 km should be sufficient to separate large surfaces with limited structure designed for deployment after orbit injection; antenna and solar cell arrays fall into this category.

To evaluate the nature of the object which decayed over Ottawa, a sequence of decay trajectories was run for a variety of drag coefficients, based upon position and velocity derived at the ascending node, revolution 2160. The area-to-mass ratio leading to visual decay phenomena over Ottawa (at 110 km) was $0.18 \text{ m}^2/\text{kgm}$, compared with 0.01 for typical payloads and 0.03 for typical rocket bodies. (A family of these trajectories is plotted in Figure 3.)

The final evidence suggesting the actual identity of the object lies in the reported visual phenomena. Some of the reports follow:

"...oblong in shape, with a long trail of sparks..."

"...lights were a vivid yellow and seemed to be like small illuminated windows in a long row. Smaller lights, like sparks, were seen beside the main body...approximately 20 lights strung out in a row resembling lights of a passenger train."

"...left a long trail of illumination behind it, resembling the trail left by an ascending rocket in a fireworks display."

"...a row of lights down the centre...looked like a distant train where the train's outline cannot be seen."

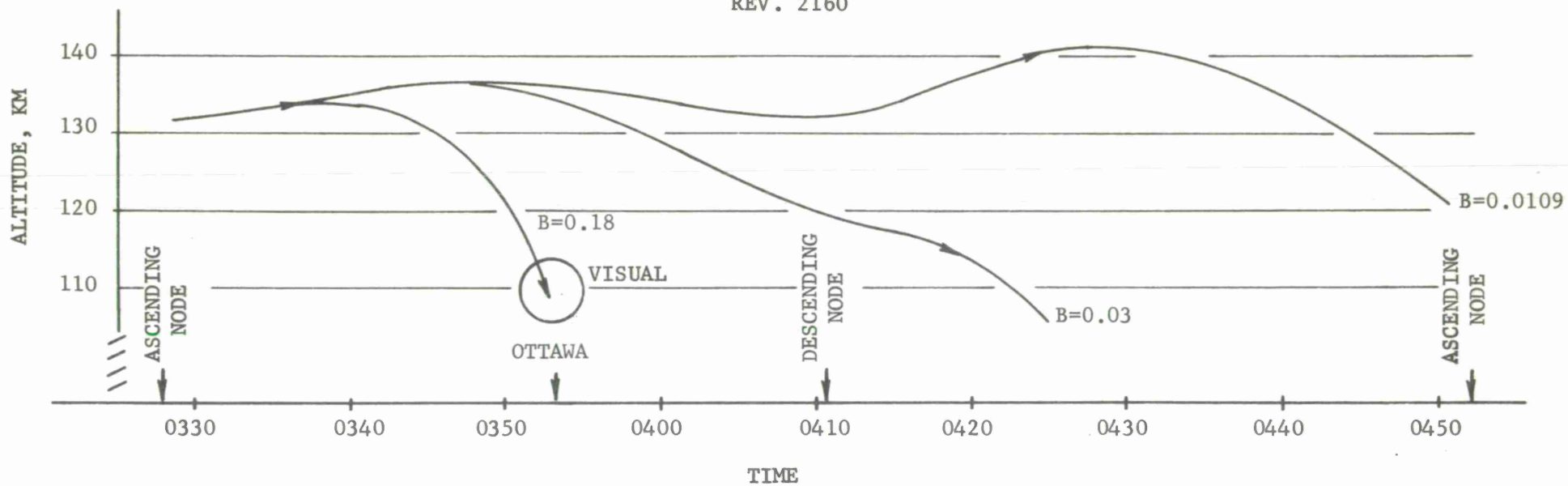
"...like a stream of lights in irregular pattern, those lights in front being quite bright...Each light seemed to hold its (relative) position."

"...a continuous bursting of multicoloured sparks, which appeared to be coming from a common object as they were in a straight line."

"...lights were white and surrounded by a yellowish luminosity with a long liminous tail..."

Materials commonly used for optical enhancement of reentry objects include the easily-ionized metallic oxides of such elements as cesium, selenium, indium, calcium and iron. As a corollary, some of these materials are also efficient photoelectric media and are used in solar energy converters. Thus the reported visual phenomena could be

REV. 2160



25

REV. 2161

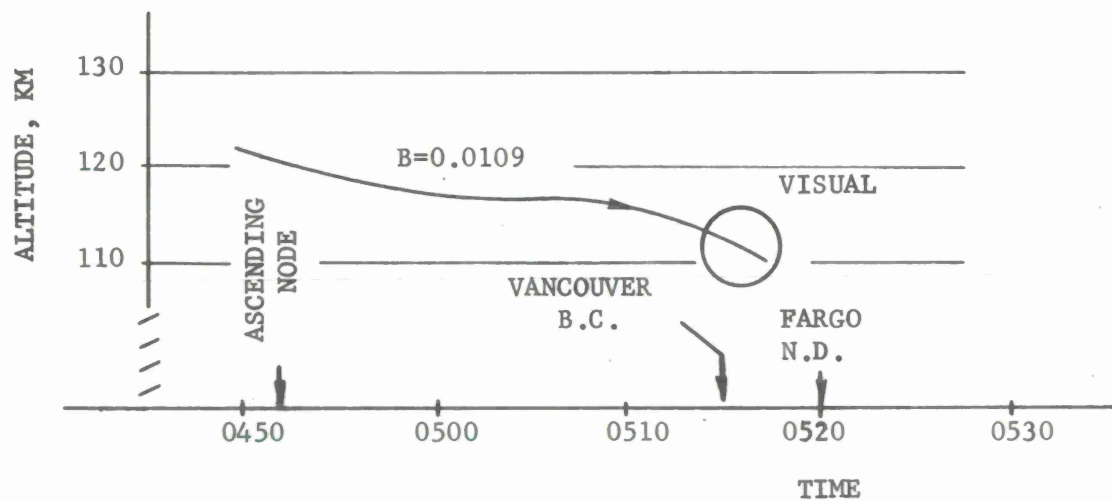


FIGURE 3. COSMOS 31 (OBJECT 803) DECAY

explained by a solar-cell panel, dispensing individual cells along the higher trajectory as the bonding material failed, which acted as efficient converters of heat to visual energy as the lower altitude range was reached. The area-to-mass ratio derived above tends to support this conclusion.

APPENDIX I

EPHEMERIS AND DIFFERENTIAL CORRECTION PROCEDURE

I.1 VARIATION-OF-PARAMETERS EPHEMERIS COMPUTATION

The formulation of the variation-of-parameters method for ephemeris computation is presented in this section.* In principle, the variation-of-parameters method formulates the equations of motion in terms of dependent variables which, in the absence of perturbative (non-two-body) forces, are constant. Such a formulation, used in a differential correction procedure, enhances the computational efficiency through (1) more efficient ephemeris integration, particularly where perturbations are small, and (2) effective application of differential correction based upon analytical expressions presented in Section I.2.

The variation-of-parameters method involves the steps shown in Figure I-1. Each of these steps is formulated below; in practice, they are programmed as subroutines which are called by a control program based upon the numerical integration procedure used. Each pass through the procedure advances time by a designated amount Δt ; repeated application will define future position and velocity from epoch elements.

a. Derivative Evaluation

(1) Oblateness (bulge)

A fairly general Earth model has been included in the SPIRDEC and CALIB programs, inclusive of zonal harmonics of the geopotential through the fifth order and tesseral (longitude-dependent) harmonics through the fourth order. The most efficient procedure for computing these terms is to define perturbative accelerations in the S (south), E (east) and Z (zenith) coordinate system, as follows:

$$\underline{\dot{r}}_B = \underline{S} g_S + \underline{E} g_E + \underline{Z} g_r$$

where g_S , g_E and g_r are defined, in terms of the potential function Φ , as shown in Table I-1.

* See also Appendix VI, Variation-of-Parameters for Low Eccentricity Orbits.

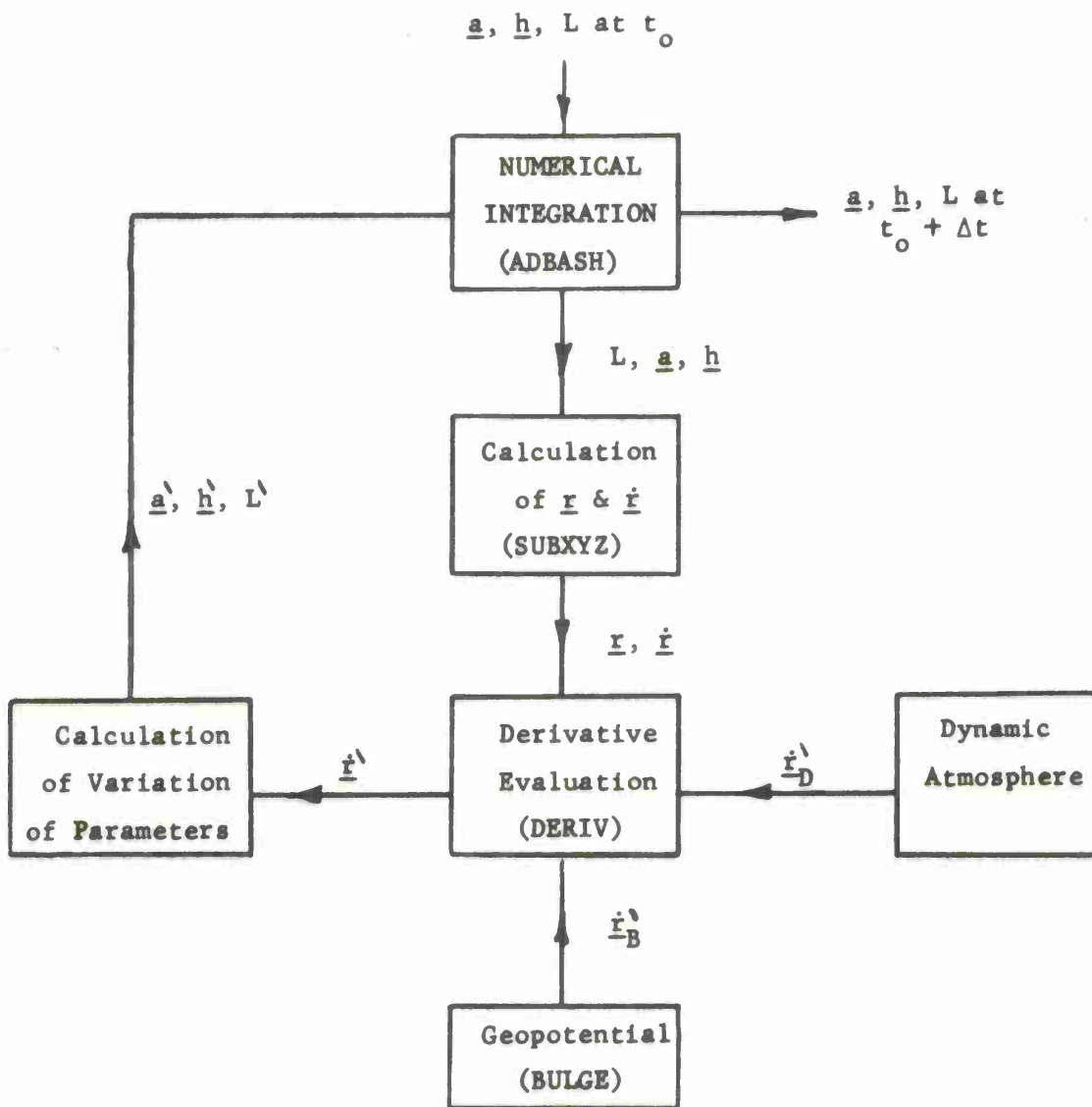


FIGURE I-1. VARIATION-OF-PARAMETERS METHOD FOR EPHEMERIS COMPUTATION

TABLE I-1. EXPRESSIONS FOR g_S , g_E , and g_r

$$\frac{1}{r} \frac{\partial \Phi}{\partial \theta} = g_S = + \frac{\mu}{r^2} \sum_{n=2}^{n_1} J_n \left(\frac{a_e}{r} \right)^n \left[P'_n (U_z) (1 - U_z^2)^{\frac{1}{2}} \right]$$

$$- \frac{\mu}{r^2} \sum_{n=2}^{n_2} \sum_{m=1}^n \left(\frac{a_e}{r} \right)^n \left[P'_{n,m} (U_z) (1 - U_z^2)^{\frac{1}{2}} \right] (C_{n,m} \cos m \lambda_E + S_{n,m} \sin m \lambda_E)$$

$$\frac{1}{r \cos \theta} \frac{\partial \Phi}{\partial \lambda_E} = g_E = - \frac{\mu}{r^2} \sum_{n=2}^{n_2} \sum_{m=1}^n m \left(\frac{a_e}{r} \right)^n \left[P_{n,m} (U_z) (1 - U_z^2)^{-\frac{1}{2}} \right] (C_{n,m} \sin m \lambda_E - S_{n,m} \cos m \lambda_E)$$

$$\frac{\partial \Phi}{\partial r} = g_r = + \frac{\mu}{r^2} \sum_{n=2}^{n_1} (n+1) J_n \left(\frac{a_e}{r} \right)^n P_n (U_z)$$

$$- \frac{\mu}{r^2} \sum_{n=2}^{n_2} \sum_{m=1}^n (n+1) \left(\frac{a_e}{r} \right)^n (1 - U_z^2)^{\frac{1}{2}} \left[P_{n,m} (U_z) (1 - U_z^2)^{-\frac{1}{2}} \right] (C_{n,m} \cos m \lambda_E + S_{n,m} \sin m \lambda_E)$$

Table I-2 conveys the series to evaluate the associated Legendre functions and the formula used to compute their derivatives. The derivatives always occur with the factor $\sqrt{1 - U_z^2}$ in Table I-1.

The series expressions are not presently used in the appropriate subroutine (MARTINI). That subroutine conforms to the specifications in the Milestone II Report*, Appendix A. A new subroutine (MONICS) with an extended potential ($n_1 = 9$ and $n_2 = 6$, presently) has been validated but not yet integrated into the operational program. MONICS uses the series, avoiding the singularities at the equator and poles by numerical checks.

The values of the sines and cosines of multiples of the East longitude may be found conveniently by the recursive relationships:

$$\sin n \lambda_E = 2 \sin (n-1) \lambda_E \cos \lambda_E - \sin (n-2) \lambda_E$$

$$\cos n \lambda_E = 2 \cos (n-1) \lambda_E \cos \lambda_E - \cos (n-2) \lambda_E$$

(2) Drag

The perturbations due to atmospheric drag are determined by entering the LJDRAG subroutine, which determines the atmospheric density corresponding to the satellite's altitude from a dynamic model atmosphere and translates this to a corresponding acceleration. The density model currently employed is due to Jacchia, with approximating curves in transitional regions provided by Lockheed. The formulation for this density model is given in Appendix II. (An additional entry into this subroutine is used to determine perigee density and scale height, in order to initialize the drag differential correction procedure.)

To compute the drag perturbation, the height H above the oblate spheroidal earth is first calculated (See Appendix V, Section 3):

$$H = (r-1) - \frac{3}{2} f^2 (U_z)^4 + (f + \frac{3}{2} f^2) U_z^2$$

The atmospheric density corresponding to this altitude is then determined.

The relative air velocity vector, v , is computed by assuming that the atmosphere is rotating at the same angular velocity as the Earth:

$$v_x = \dot{x} + y\dot{\theta}, \text{ where } \dot{\theta} = 0.058,834,47 \text{ radians/k}_e^{-1} \text{min}$$

$$v_y = \dot{y} - x\dot{\theta}$$

* Walters, L. G., Hilton, C. G., and Crossin, P. A., "Spiral Decay and Sensor Calibration Differential Correction Programs", Aeronutronic Publication No. U-2559, 31 March 1964.

TABLE I-2. ASSOCIATED LEGENDRE FUNCTIONS AND THEIR DERIVATIVES

Legendre Polynomials: $m = 0$

$$P_n(U_z) = P_{n,0}(U_z)$$

Associated Legendre Functions:

$$P_{n,m}(U_z) = \frac{(2n)!}{2^n n! (n-m)!} (1 - U_z^2)^{\frac{m}{2}} \sum_{r=0}^{\frac{n-m}{2}} c_r U_z^{n-m-2r}$$

where

$$c_0 = 1$$

and

$$\frac{c_r}{c_{r-1}} = - \frac{(n-m-2r+2)(n-m-2r+1)}{2r(2n+1-2r)}$$

Derivatives:

$$\sqrt{1 - U_z^2} P'_{n,m}(U_z) = P_{n,m+1}(U_z) - m U_z \frac{P_{n,m}(U_z)}{\sqrt{1 - U_z^2}}$$

Zonal: $m = 0$

$$P'_n(U_z) = \frac{P_{n,n+1}(U_z)}{\sqrt{1 - U_z^2}}$$

Sectorial: $m = n$

$$P_{n,n+1}(U_z) = 0$$

$$\sqrt{1 - U_z^2} P'_{n,n}(U_z) = - U_z \frac{(2n)!}{2^n (n-1)!} (1 - U_z^2)^{\frac{n-1}{2}}$$

$$v_z = \dot{z}$$

$$v = (\underline{v} \cdot \underline{v})^{\frac{1}{2}}$$

The drag acceleration then is

$$\underline{\dot{r}}_D = -\frac{1}{2} \rho v B \underline{v}$$

where $B = \frac{C_D A}{m}$ is the ballistic parameter.

(3) Radiation Pressure

The magnitude of the force acting on a satellite due to direct solar radiation pressure is

$$F_{\odot} = |\underline{F}_{\odot}| = \gamma P_{\odot} A$$

where A is the effective cross-sectional area of the satellite to radiation pressure

P_{\odot} is the solar radiation pressure in the vicinity of the Earth, assumed constant at $4.5 \times 10^{-5} \frac{\text{dynes}}{\text{cm}^2}$

γ is a factor depending on the reflecting characteristics of the satellite's surface; if the incident energy is reflected specularly or is absorbed and re-emitted isotropically, $\gamma = 1$

By neglecting the solar parallax, which is only 11 seconds of arc at 1000 miles altitude,

$$\underline{F}_{\odot} = -F_{\odot} \underline{L}_{\odot}$$

where \underline{L}_{\odot} is a unit vector directed to the Sun.

The points at which a satellite enters and leaves the Earth's shadow are continuously changing due to the apparent motion of the Sun and the perturbations on the orbit. The shadow effect can be handled very easily, however, in the special perturbations case. A check is made at each integration step to determine whether the satellite is illuminated or in the Earth's shadow. If the satellite is in the shadow, the radiation force does not act.

Consider the plane which passes through the centers of the Earth, Sun, and satellite as shown in Figure I-2. The Earth's shadow is assumed to be cylindrical. The dot product of \underline{L}_\odot and \underline{r} gives

$$\cos \psi = \frac{\underline{L}_\odot \cdot \underline{r}}{r}$$

Clearly, if $\cos \psi$ is positive, the satellite will be illuminated by the Sun. If $\cos \psi$ is negative, use is made of the triangle CES and the angle π , obtained from triangle TES:

$$\sin \pi = \frac{1}{r}$$

Consideration of Figure I-2 reveals that when $(\psi + \pi) < 180^\circ$, the satellite is still illuminated. However, when $(\psi + \pi) > 180^\circ$, the satellite will be in the Earth's shadow. In this case, the radiation force does not act. The test can readily be made on the sign of the quantity

$$\sin (\psi + \pi) = \sin \psi \cos \pi + \sin \pi \cos \psi$$

where $\sin \psi$ and $\cos \pi$ are always positive.

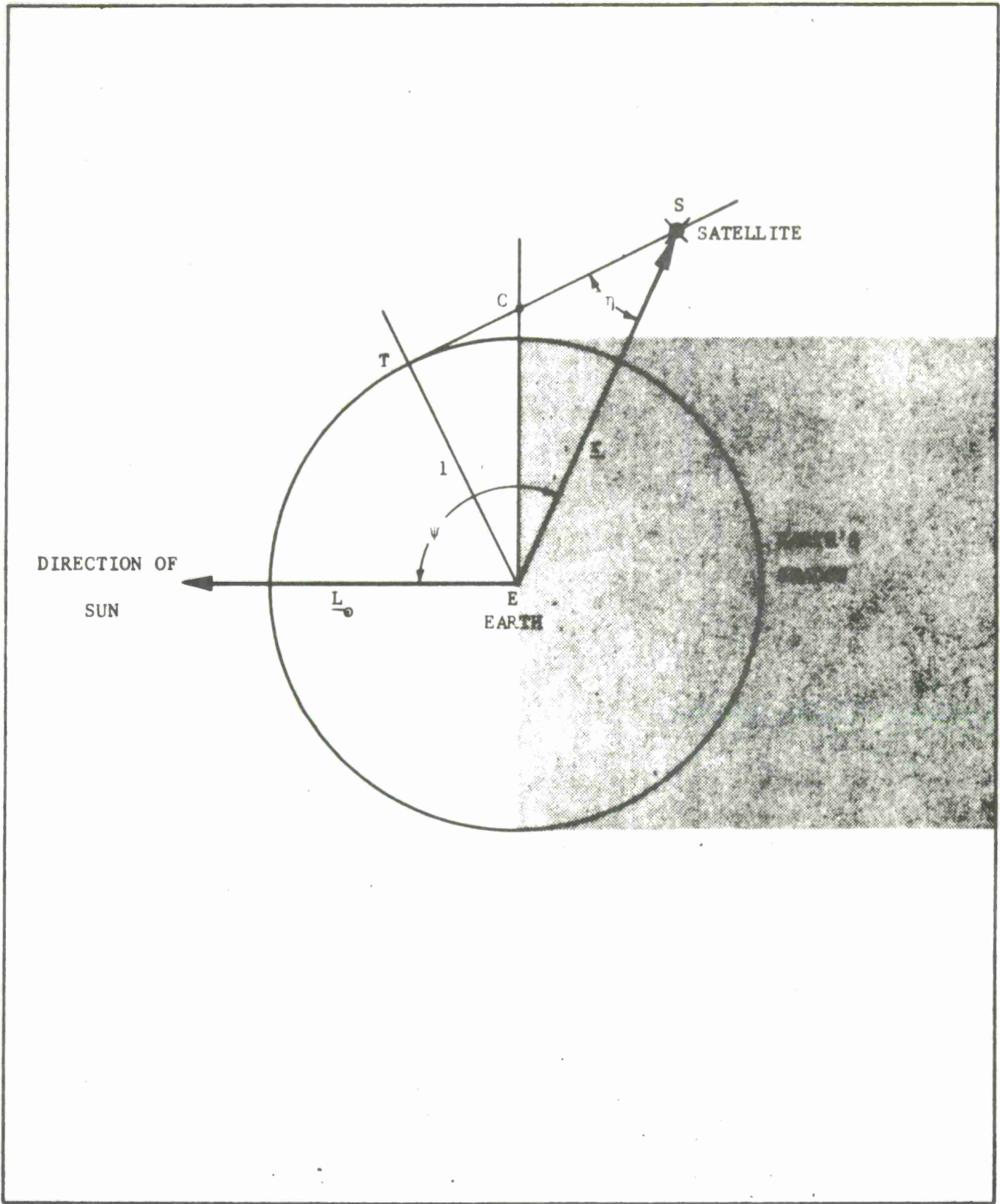


Figure I-2 Position of Satellite With Respect to Earth's Shadow

The acceleration due to direct solar radiation pressure, \ddot{r}_{sp} , is computed as follows. Initially, the mean longitude of the sun at the beginning of the current year $L_{\odot 0}$ is found by the system subroutine TLC.

$$L_{\odot} = L_{\odot 0} + n_{\odot} (t - t_0)$$

$$M_{\odot} = L_{\odot 0} + n_{\odot} (t - t_0) - \pi_{\odot}$$

$$l_{\odot} = L_{\odot 0} + n_{\odot} (t - t_0) + 2 e_{\odot} \sin M_{\odot} + \frac{5}{4} e_{\odot}^2 \sin 2M_{\odot}$$

$$L_{x_{\odot}} = \cos l_{\odot}$$

$$L_{y_{\odot}} = \cos \epsilon \sin l_{\odot}$$

$$L_{z_{\odot}} = \sin \epsilon \sin l_{\odot}$$

$$\cos \psi = \frac{l_{\odot} \cdot r}{r}$$

$$\frac{F_{\odot}}{m} = \frac{\gamma A}{m} p_{\odot}$$

If $\cos \psi > 0$, the satellite is illuminated.

If $\cos \psi < 0$, form $\sin(\psi + \eta) = \sin \psi \cos \eta + \sin \eta \cos \psi$

$$= \sqrt{(\cos^2 \psi - 1) \left(\frac{1}{r} - 1 \right)} + \left(\frac{1}{r} \right) \cos \psi$$

If $\sin(\psi + \eta) > 0$, the satellite is illuminated.

If the satellite is illuminated, calculate

$$\dot{x}_{RP}' = \left(\frac{F_0}{m}\right) L_{x0}$$

$$\dot{y}_{RP}' = \left(\frac{F_0}{m}\right) L_{y0}$$

$$\dot{z}_{RP}' = \left(\frac{F_0}{m}\right) L_{z0}$$

b. Calculation of Variation of Parameters

The total perturbative acceleration can now be used to determine the perturbative derivatives of the parameters, as follows:

$$\dot{\underline{r}} = \dot{\underline{r}}_B + \dot{\underline{r}}_D$$

$$r\dot{r}' = \underline{r} \cdot \dot{\underline{r}}'$$

$$\dot{s}\dot{s}' = \dot{\underline{r}} \cdot \dot{\underline{r}}'$$

$$r\dot{r} = \underline{r} \cdot \dot{\underline{r}}$$

$$D = \frac{r\dot{r}}{\sqrt{\mu}}$$

$$D' = \frac{r\dot{r}}{\sqrt{\mu}}$$

$$D'' = \frac{2\dot{s}\dot{s}}{\sqrt{\mu}}$$

$$r\dot{b}' = \underline{W} \cdot \dot{\underline{r}}'$$

$$e' = \frac{z(r\dot{b}')}{(1+W_z) \sqrt{\mu p}}$$

$$\underline{a}' = \frac{(D'' - D\dot{r}' - D\dot{r}')}{\sqrt{\mu}}$$

$$e\dot{Q} = \underline{W} \times \underline{a}$$

$$-e^2 \dot{v}' = e\dot{Q} \cdot \underline{a}'$$

$$L' = l' - \frac{2D'}{\sqrt{\mu a}} - \left[\frac{e^2 v'}{1 + \sqrt{1 - e^2}} \right]$$

$$\underline{h} = \frac{\underline{r} \times \underline{\dot{r}}}{\sqrt{\mu}}$$

The derivatives, as used in the Runge-Kutta routine, are:

$$\frac{dL}{dt} = k_e L' + n$$

$$\frac{da}{dt} = k_e a'$$

$$\frac{dh}{dt} = k_e \underline{h}'$$

c. Numerical Integration Procedure

The expression given above represent seven first-order differential equations, with time as the dependent variable. In the Milestone I and II versions of the SPIRDEC and CALIB programs, these are integrated by the Runge-Kutta procedure, utilizing an optional Simpson's rule test for truncation error to define an optimum variable time interval.

d. Calculation of Position and Velocity

At each time point where derivatives are to be evaluated, or where observations are to be represented, the space position and velocity are determined from the parameters a, h and L by the following procedure:

$$p = \underline{h} \cdot \underline{h}$$

$$e^2 = \underline{a} \cdot \underline{a}$$

$$a = \frac{p}{1 - e^2}$$

$$n = \frac{k_e \sqrt{\mu}}{a^{3/2}}$$

$$\underline{W} = \frac{h}{\sqrt{p}}, \quad W_z = \cos i$$

Define the nodal vectors \underline{M} and \underline{N}

$$M_x = -\frac{W_z W_x}{(1-W_z^2)^{\frac{1}{2}}}, \quad N_x = -\frac{W_y}{(1-W_z^2)^{\frac{1}{2}}}$$

$$M_y = -\frac{W_z W_y}{(1-W_z^2)^{\frac{1}{2}}}, \quad N_y = \frac{W_x}{(1-W_z^2)^{\frac{1}{2}}}$$

$$M_z = (1-W_z^2)^{\frac{1}{2}}, \quad N_z = 0$$

$$a_{xN} = \underline{a} \cdot \underline{N}$$

$$a_{yN} = \underline{a} \cdot \underline{M}$$

$$\Omega = \arctan \frac{N_y}{N_x} = \arctan \frac{W_x}{-W_y}$$

$$U = L - \Omega \text{ if } W_z \geq 0$$

$$L + \Omega \text{ if } W_z < 0$$

$$0 \leq U < 2\pi$$

Kepler's equation is solved by iteration using the Newton-Raphson method with an initial guess for $(E+\omega)$ of U [i.e., $(E+\omega)_1 = U$]

$$(E+\omega)_{i+1} = (E+\omega)_i - \frac{[U + e \sin E_i - (E+\omega)_i]}{e \cos E_i - 1} \text{ radians}$$

where

$$e \cos E_i = a_{xN} \cos (E+\omega)_i + a_{yN} \sin (E+\omega)_i$$

$$e \sin E_i = a_{xN} \sin (E+\omega)_i - a_{yN} \cos (E+\omega)_i$$

The iteration is concluded when

$$\left| (E+\omega)_{i+1} - (E+\omega)_i \right| < 10^{-8}$$

(If, after 50 iterations, the criterion is not met, the run is terminated. A comment to this effect is written on the output tape.)

After Kepler's equation is solved, the calculations continue:

$$r = a (1 - e \cos E)$$

$$\dot{r} = \frac{\sqrt{\mu a}}{r} (e \sin E)$$

$$r\dot{v} = \frac{\sqrt{\mu a}}{r} \sqrt{1 - e^2}$$

$$\cos u = \frac{a}{r} \left[\cos (E + \omega) - a_{xN} + a_{yN} \frac{e \sin E}{(1 + \sqrt{1 - e^2})} \right]$$

$$\sin u = \frac{a}{r} \left[\sin (E + \omega) - a_{yN} - a_{xN} \frac{e \sin E}{(1 + \sqrt{1 - e^2})} \right]$$

$$\underline{U} = \underline{N} \cos u + \underline{M} \sin u$$

$$\underline{V} = -\underline{N} \sin u + \underline{M} \cos u$$

$$\underline{r} = r \underline{U}$$

$$\underline{\dot{r}} = \dot{r} \underline{U} + r\dot{v} \underline{V}$$

This completes the calculation of position and velocity from the M, N parameters.

I.2 WEIGHTED DIFFERENTIAL CORRECTION

The differential correction procedure relates observation residuals to incremental changes in the orbit parameters. Raw observation data, corrected for known systematic (bias) errors, are compared against their representations, based upon the computed orbit. Their differences (residuals) are related by scalar differential expressions (equations of condition) to incremental changes in the parameters defining the computed orbit. This ordinarily heavily overdetermined system of equations is solved for parameter changes in the sense of weighted least squares, utilizing weights reflecting the statistical confidence in the corrected data, as determined from sensor calibration efforts.

a. Representation of Observations

Given the sensor latitude ϕ , east longitude λ_E and sea-level height H , the following procedure computes representations of range ρ_c , range-rate $\dot{\rho}_c$, and the direction cosines of the unit vector \underline{L} directed from the sensor to the satellite for time t , in minutes since epoch:

Compute local sidereal time θ at time t :

$$\theta = \lambda_E + \theta_{t_0} + 0.004,375,269,1 t \quad (\text{Mod } 2\pi)$$

Compute sensor location vector, \underline{R} :

$$X = - \left[(1 - \epsilon^2 \sin^2 \phi)^{-\frac{1}{2}} + H \right] \cos \phi \cos \theta$$

$$Y = - \left[(1 - \epsilon^2 \sin^2 \phi)^{-\frac{1}{2}} + H \right] \cos \phi \sin \theta$$

$$Z = - \left[(1 - \epsilon^2) (1 - \epsilon^2 \sin^2 \phi)^{-\frac{1}{2}} + H \right] \sin \phi$$

Compute the slant range, ρ_c :

$$\underline{\rho}_c = \underline{r} + \underline{R}, \text{ where } \underline{r} \text{ is the satellite's computed position at time } t.$$

$$\rho_c = (\underline{\rho}_c \cdot \underline{\rho}_c)^{\frac{1}{2}}$$

Compute unit vector from the station to the satellite in the equatorial coordinate system:

$$\underline{L}_c = \frac{\underline{\rho}_c}{\rho_c}$$

Compute range rate, $\dot{\rho}_c$, from

$\dot{\underline{\rho}}_c = \dot{\underline{x}} + \dot{\underline{R}}$, where the components of \underline{R} are given by

$$\underline{R} \begin{cases} \dot{x} = -y \dot{\theta}, & \dot{\theta} = 0.058,834,47 \\ \dot{y} = x \dot{\theta} \\ \dot{z} = 0 \end{cases}$$

then $\dot{\rho}_c = \underline{L} \cdot \dot{\underline{\rho}}_c = L_x (\dot{x} + \dot{X}) + L_y (\dot{y} + \dot{Y}) + L_z \dot{z}$,

b. Definition of Residuals

If range is observed, the residual is

$$R_1 = \rho - \rho_c$$

If azimuth, A, and elevation, h, are observed, the residuals are, respectively,

$$R_2 = \rho_c \tilde{\underline{A}} \cdot (\underline{L} - \underline{L}_c)$$

$$R_3 = \rho_c \tilde{\underline{D}} \cdot (\underline{L} - \underline{L}_c)$$

where

$$\tilde{\underline{A}} = \tilde{A}_{xh} \underline{S} + \tilde{A}_{yh} \underline{E} + \tilde{A}_{zh} \underline{Z}$$

$$\tilde{\underline{D}} = \tilde{D}_{xh} \underline{S} + \tilde{D}_{yh} \underline{E} + \tilde{D}_{zh} \underline{Z}$$

$$\underline{L} = L_{xh} \underline{S} + L_{yh} \underline{E} + L_{zh} \underline{Z}$$

The \underline{S} , \underline{E} , \underline{Z} unit vector system and the horizon oriented \underline{L}_h , $\tilde{\underline{A}}_h$, $\tilde{\underline{D}}_h$ unit vector system are defined by:

$$\underline{S} \begin{cases} S_x = \sin \phi \cos \theta \\ S_y = \sin \phi \sin \theta \\ S_z = -\cos \phi \end{cases} \quad \underline{L}_h \begin{cases} L_{xh} = -\cos A \cos h \\ L_{yh} = \sin A \cos h \\ L_{zh} = \sin h \end{cases}$$

$$\underline{E} \begin{cases} E_x = -\sin \theta \\ E_y = \cos \theta \\ E_z = 0 \end{cases} \quad \tilde{\underline{A}}_h \begin{cases} \tilde{A}_{xh} = \sin A \\ \tilde{A}_{yh} = \cos A \\ \tilde{A}_{zh} = 0 \end{cases}$$

$$\underline{Z} \begin{cases} Z_x = \cos \phi \cos \theta \\ Z_y = \cos \phi \sin \theta \\ Z_z = \sin \phi \end{cases} \quad \tilde{\underline{D}}_h \begin{cases} \tilde{D}_{xh} = \cos A \sin h \\ \tilde{D}_{yh} = -\sin A \sin h \\ \tilde{D}_{zh} = \cos h \end{cases}$$

If right ascension, α , and declination, δ , are observed, the residuals are:

$$R_4 = \rho_c \underline{A} \cdot (\underline{L} - \underline{L}_c)$$

$$R_5 = \rho_c \underline{D} \cdot (\underline{L} - \underline{L}_c)$$

where

$$\underline{L} \begin{cases} L_x = \cos \delta \cos \alpha \\ L_y = \cos \delta \sin \alpha \\ L_z = \sin \delta \end{cases}$$

$$\underline{A} \begin{cases} A_x = -\sin \alpha \\ A_y = \cos \alpha \\ A_z = 0 \end{cases}$$

$$\underline{D} \begin{cases} D_x = -\sin \delta \cos \alpha \\ D_y = -\sin \alpha \sin \delta \\ D_z = \cos \delta \end{cases}$$

See Figure I-2 for these vector relationships.

If range rate, $\dot{\rho}$, is observed,

$$R_6 = \rho_c \Delta \dot{\rho} = (\dot{\rho} - \dot{\rho}_c) \rho_c$$

c. Differential Correction

The residuals in the observations are related to the changes in the elements through first-order scalar differential expressions of the form

$$R_i = \left(C \frac{\Delta n}{n} \right)_i \frac{\Delta n_o}{n_o} + \left(C \Delta a_{xn} \right)_i \Delta a_{xn_o} + \left(C \Delta a_{yn} \right)_i \Delta a_{yn_o} + \left(C \Delta U_o \right)_i \Delta U_o \\ + \left(C \Delta \Omega \right)_i \Delta \Omega_o + \left(C \Delta i \right)_i \Delta i_o + \left(C \frac{\Delta B}{B} \right)_i \frac{\Delta B}{B}$$

where the form of the coefficients, C_i , depend on the observation type, time of observation, and the observation weights. These coefficients, which have been developed by means of first-order partials, are functions of the orbit elements and computed observations.

The coefficients are computed by first establishing the R and U coefficients at time t.

Celestial Sphere
Centered At
Observer

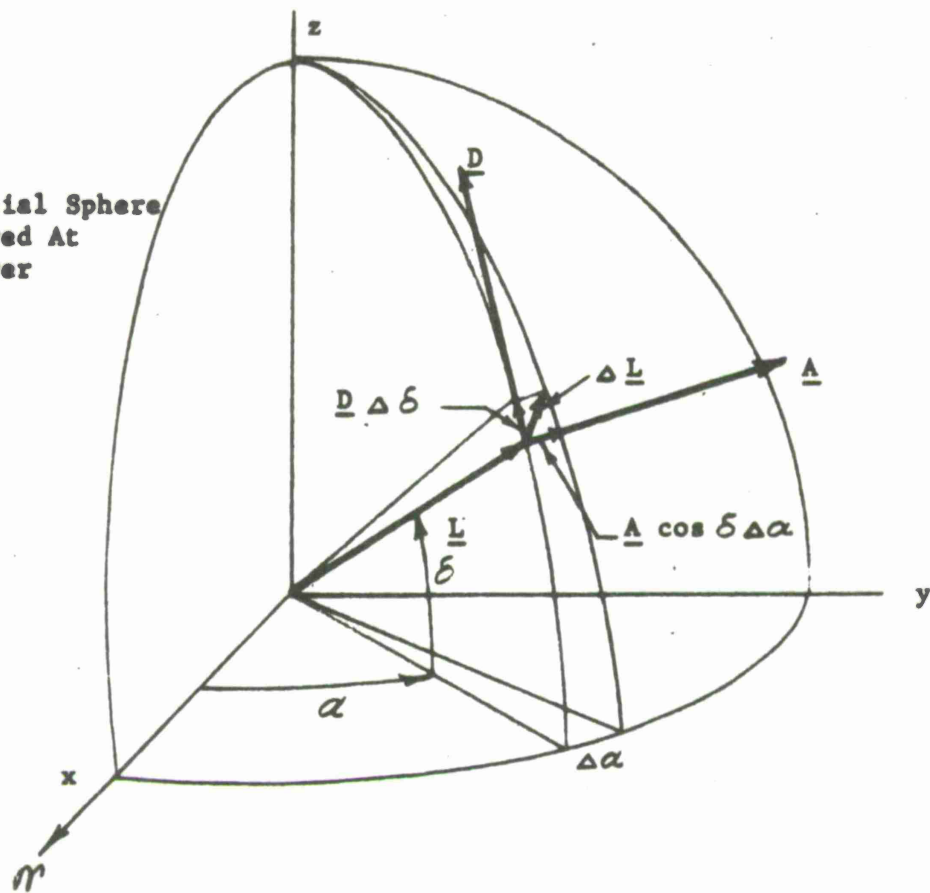


FIGURE I-3. VECTOR RELATIONSHIPS

$$R_u = \left(\frac{a}{r}\right)^2 e \sin E$$

$$R_n = -\frac{2}{3} r + (U - U_o) R_u$$

$$R_{xN} = \left(\frac{a}{r}\right)^2 \left[a_{xN} - \cos (E + \omega) \right]$$

$$R_{yN} = \left(\frac{a}{r}\right)^2 \left[a_{yN} - \sin (E + \omega) \right]$$

$$U_u = \left(\frac{a}{r}\right)^2 \sqrt{1 - e^2}$$

$$U_n = (U - U_o) U_u$$

$$U_{xN} = \frac{a^2}{r} \left\{ \left(1 + \frac{r}{a}\right) \sin (E + \omega) + \right. \\ \left. a_{xN} e \sin E \left[\frac{e^2 - (1 + \sqrt{1-e^2}) e \cos E}{(1 + \sqrt{1-e^2})^2 \sqrt{1-e^2}} \right] - \frac{a_{yN}}{1 + \sqrt{1-e^2}} \right\}$$

$$U_{yN} = \frac{a^2}{r} \left\{ - \left(1 + \frac{r}{a}\right) \cos (E + \omega) + \right. \\ \left. a_{yN} e \sin E \left[\frac{e^2 - (1 + \sqrt{1-e^2}) e \cos E}{(1 + \sqrt{1-e^2})^2 \sqrt{1-e^2}} \right] + \frac{a_{xN}}{1 + \sqrt{1-e^2}} \right\}$$

(1) Coefficients for slant range observation

When the slant range is observed, the residual and coefficients are given by the expressions:

$$R = R_1 \sigma_\rho^{-1}$$

$$C_{\frac{\Delta n}{n}} = \left[\underline{L}_c \cdot \underline{U} R_n + \underline{L}_c \cdot \underline{V} U_n \right] \sigma_\rho^{-1}$$

$$C_{\Delta a_{xN}} = \left[\underline{L}_c \cdot \underline{U} R_{xN} + \underline{L}_c \cdot \underline{V} U_{xN} \right] \sigma_\rho^{-1}$$

$$C_{\Delta a_{yN}} = \left[\underline{L}_c \cdot \underline{U} R_{yN} + \underline{L}_c \cdot \underline{V} U_{yN} \right] \sigma_\rho^{-1}$$

$$C_{\Delta U_o} = \left[\underline{L}_c \cdot \underline{U} R_u + \underline{L}_c \cdot \underline{V} U_u \right] \sigma_\rho^{-1}$$

$$C_{\Delta \Omega} = \left[\underline{L}_c \cdot \underline{V} r \cos i - \underline{L}_c \cdot \underline{W} r \sin i \cos u \right] \sigma_\rho^{-1}$$

$$C_{\Delta i} = \left[\underline{L}_c \cdot \underline{W} r \sin u \right] \sigma_\rho^{-1}$$

The expressions for $C_{\frac{\Delta B}{B}}$ are presented in Appendix IV.

(2) Coefficients for azimuth and elevation observations

When azimuth A is observed, then $R = R_2 (\rho_c \sigma_A)^{-1}$ and the coefficients are obtained by replacing L by \tilde{A} and σ_ρ by $\rho_c \sigma_A$, where σ_A is the standard deviation in the azimuth measurement.

For elevation observations, $R = R_3 (\rho_c \sigma_h)^{-1}$ and the corresponding coefficients are obtained by replacing L with \tilde{D} . σ_ρ is replaced by $\rho_c \sigma_h$, where σ_h is the standard deviation in elevation angle.

(3) Coefficients for range-rate observations

For range rate observations, preliminary coefficients are computed from:

$$\dot{R}_u = \left(\frac{\mu}{a} \right)^{\frac{1}{2}} \left(\frac{a}{r} \right)^3 (e \cos E - e^2)$$

$$\dot{R}_N = \frac{\dot{r}}{3} + (U - U_0) \dot{R}_u$$

$$\dot{R}_{xN} = \left(\frac{\mu}{a}\right)^{\frac{1}{2}} \left(\frac{a}{r}\right)^3 \left[\sin(E + \omega) - a_{xN} e \sin E - a_{yN} \right]$$

$$\dot{R}_{yN} = \left(\frac{\mu}{a}\right)^{\frac{1}{2}} \left(\frac{a}{r}\right)^3 \left[-\cos(E + \omega) - a_{yN} e \sin E + a_{xN} \right]$$

$$\dot{U}_u = \left(\frac{\mu}{a}\right)^{\frac{1}{2}} \left(\frac{a}{r}\right)^3 \sqrt{1 - e^2} e \sin E$$

$$\dot{U}_n = \frac{r\dot{v}}{3} + (U - U_0) \dot{U}_u$$

$$\dot{U}_{xN} = \left(\frac{\mu}{a}\right)^{\frac{1}{2}} \left(\frac{a}{r}\right)^3 \sqrt{1 - e^2} \left[\cos(E + \omega) - a_{xN} \left(1 + \frac{r^2}{ap}\right) \right]$$

$$\dot{U}_{yN} = \left(\frac{\mu}{a}\right)^{\frac{1}{2}} \left(\frac{a}{r}\right)^3 \sqrt{1 - e^2} \left[\sin(E + \omega) - a_{yN} \left(1 + \frac{r^2}{ap}\right) \right]$$

The range rate coefficients are then computed as

$$C_{\frac{\Delta n}{n}} = \left\{ \underline{L}_c \cdot \underline{U} \left[\rho_c (\dot{R}_n - \dot{v}U_n) - \dot{\rho}_c R_n \right] + \dot{\rho}_c \cdot \underline{U} R_n \right. \\ \left. + \underline{L}_c \cdot \underline{V} \left[\rho_c (\dot{U}_n + \frac{\dot{r}}{r} U_n) - \dot{\rho}_c U_n \right] + \dot{\rho}_c \cdot \underline{V} U_n \right\} \sigma_{\dot{\rho}}^{-1}$$

$$C_{\Delta a_{xN}} = \left\{ \underline{L}_c \cdot \underline{U} \left[\rho_c (\dot{R}_{xN} - \dot{v}U_{xN}) - \dot{\rho}_c R_{xN} \right] + \dot{\rho}_c \cdot \underline{U} R_{xN} \right. \\ \left. + \underline{L}_c \cdot \underline{V} \left[\rho_c (\dot{U}_{xN} + \frac{\dot{r}}{r} U_{xN}) - \dot{\rho}_c U_{xN} \right] + \dot{\rho}_c \cdot \underline{V} U_{xN} \right\} \sigma_{\dot{\rho}}^{-1}$$

$$C_{\Delta a_{yN}} = \left\{ \begin{aligned} & \underline{L}_c \cdot \underline{U} [\rho_c (\dot{R}_{yN} - \dot{V} U_{yn} - \dot{\rho}_c R_{yN})] + \dot{\rho}_c \cdot \underline{U} R_{yN} \\ & + \underline{L}_c \cdot \underline{V} [\rho_c (U_{nN} + \frac{\dot{r}}{r} U_{yN}) - \dot{\rho}_c U_{yN}] + \dot{\rho}_c \cdot \underline{V} U_{yN} \end{aligned} \right\} \sigma_{\dot{\rho}}^{-1}$$

$$C_{\Delta U_o} = \left\{ \begin{aligned} & \underline{L}_c \cdot \underline{U} [\rho_c (\dot{R}_u - \dot{V} U_u) - \dot{\rho}_c R_u] + \dot{\rho}_c \cdot \underline{U} R_u \\ & + \underline{L}_c \cdot \underline{V} [\rho_c (U_u + \frac{\dot{r}}{r} U_u) - \dot{\rho}_c U_u] + \dot{\rho}_c \cdot \underline{V} U_u \end{aligned} \right\} \sigma_{\dot{\rho}}^{-1}$$

$$C_{\Delta \Omega} = \left\{ \begin{aligned} & - \rho_c \underline{L}_c \cdot \underline{U} r \dot{v} \cos i + \underline{L}_c \cdot \underline{V} \cos i [\rho_c \dot{r} - \dot{\rho}_c r] \\ & + \dot{\rho}_c \cdot \underline{V} r \cos i + \underline{L}_c \cdot \underline{W} \sin i [\rho_c (r \dot{v} \sin u - \dot{r} \cos u \\ & + \dot{\rho}_c r \cos u)] - \dot{\rho}_c \cdot \underline{W} r \sin i \cos u \end{aligned} \right\} \sigma_{\dot{\rho}}^{-1}$$

$$C_{\Delta i} = \left\{ \begin{aligned} & \underline{L}_c \cdot \underline{W} [\rho_c (r \dot{v} \cos u + r \sin u) - \dot{\rho}_c r \sin u] \\ & + \dot{\rho}_c \cdot \underline{W} r \sin u \end{aligned} \right\} \sigma_{\dot{\rho}}^{-1}$$

The coefficient $C_{\frac{\Delta B}{B}}$ is given in Appendix IV.

(4) Differential Correction Solution

$$\text{Let } \sum_{j=1}^N C_{ij} \Delta_j = R_{ij}$$

represent all such equations of condition, where C_{ij} are the coefficients, R_{ij} are the accepted observation residuals, Δ_j are the corrections to the orbital elements, and N is the number of elements to be corrected and is the number of accepted observation residuals. The resulting matrix equation is solved to give the correction, Δ_j in a least square sense, to the orbital elements at time, t_o . These corrections are applied as follows (primes denote corrected elements):

$$n'_o = n_o \left(1 + \frac{\Delta n_o}{n_o} \right)$$

$$U'_o = U_o + \Delta U_o$$

$$B'_o = B_o + \Delta B_o$$

$$a'_{xNo} = a_{xNo} + \Delta a_{xN}$$

$$a'_{yNo} = a_{yNo} + \Delta a_{yN}$$

$$\Omega'_o = \Omega_o + \Delta \Omega$$

$$i'_o = i_o + \Delta i$$

$$L'_o = U'_o + \Omega'_o \text{ if } W'_z = \cos i \geq 0$$

$$L'_o = U'_o - \Omega'_o \text{ if } W'_z = \cos i < 0$$

Following the above calculation of the corrected elements, another representation of the observations is performed, on the basis of the corrected elements, and another set of residuals is formed by using the same input observations. The weighted RMS values of sets of consecutive residuals are compared to define convergence of the computational process.

APPENDIX II

JACCHIA-NICOLET DYNAMIC ATMOSPHERE MODEL

The physical properties of the outer atmosphere are governed by two relations between pressure P, and density, ρ . The first is the equation of hydrostatic equilibrium

$$\frac{dP}{dh} = -g\rho$$

where g is the acceleration of gravity at height h . The second is the ideal gas law.

$$MP = k\rho T$$

Here k is the Boltzmann constant, but M , the mean molecular mass, and T , the temperature, are additional variables. Fortunately, the temperature is practically independent of h above a level called the thermopause. The variations of mean molecular mass, however, must be assumed according to some theory. This theory concerns itself with the dissociation of molecules and the diffusion of atmospheric constituents. The resulting atmospheric model, obtained by integrating the above equations is a static atmosphere. It depends also on the boundary conditions assumed at the lower boundary. Upon this static model, variations due to solar activity can be effected.

By employing Nicolet's¹ model for density variations with height and temperature, Jacchia² has demonstrated excellent correlation between solar, geomagnetic and geographic phenomena and exospheric temperature, the latter derived from satellite accelerations using Nicolet's static model. By reversing this procedure, temperature may be derived using Jacchia's formulas, and the density from Nicolet's model; this procedure has been implemented in the Spiral Decay Program to provide a flexible dynamic atmosphere model.

II.1 RELATION OF SOLAR, GEOMAGNETIC AND GEOGRAPHIC PHENOMENA TO TEMPERATURE.

Temperature is computed from Jacchia's expressions, beginning with the input quantities.

F_{10}	10.7 cm flux
\bar{F}_{10}	F_{10} averaged over three solar rotations
A_p	Geomagnetic index
The following are provided by the program:	
D	Day number
α_0, δ_0	Position of the sun (right ascension and declination)
θ	Sidereal time at vehicle
ϕ	Geocentric latitude of vehicle
h	Height above sea level

¹Nicolet, M., "Density of the Heterosphere related to Temperature" SAO Special Report 75, 19 September 1961. (SAO has furnished an improved tabulation of this model.)

²Jacchia, L. G., "The Temperature above the Thermopause" SAO Special Report 150, 22 April 1964.

Temperature is computed as follows:

Compute the average night time minimum temperature ($^{\circ}\text{K}$)

$$\bar{T}_O = 974^{\circ} + 4.0^{\circ}2 (\bar{F}_{10} - 150) + 0.0004 (\bar{F}_{10} - 150)^2$$

Compute the night time minimum for the day

$$T'_O = \bar{T}_O + 1.0^{\circ}9 (F_{10} - \bar{F}_{10})$$

Add the semiannual term

$$T_O = T'_O + \left[0.039 + 0.015 \sin 2\pi \left(\frac{D-150}{365} \right) \right] \\ \times \bar{F}_{10} \sin 4\pi \left(\frac{D-60}{365} \right)$$

Correct for latitude and elongation from sun (see figure II-1)

Define: $2 \eta = (\theta' - \delta_{\theta})$

$$2 \xi = (\theta' + \delta_{\theta})$$

the maximum daytime temperature at latitude θ' is

$$T_D = T_O (1 + R \cos^m \eta)$$

and the minimum nighttime temperature at latitude θ' is

$$T_N = T_O (1 + R \sin^m \xi)$$

where T_O is the global minimum in the exosphere.

Empirical values for R and m , derived by Jacchia and Slowey, are 0.3 and 2.5 respectively.

$$H_{\theta} = \theta - \alpha_{\theta} \text{ (radians)}$$

$$\tau \triangleq H_{\theta} - \frac{\pi}{4} + 0.21 \sin \left(H_{\theta} + \frac{\pi}{4} \right) \quad -\pi < \tau < +\pi$$

$$T' - T_O = 0.3 T_O \left\{ \sin^{2.5} \xi \left[1 - \cos^{2.5} \frac{\tau}{2} \right] + \cos^{2.5} \eta \cos^{2.5} \frac{\tau}{2} \right\}$$

Finally the geomagnetic effect is added

$$T = T' + 1.0^{\circ}2 A_P$$

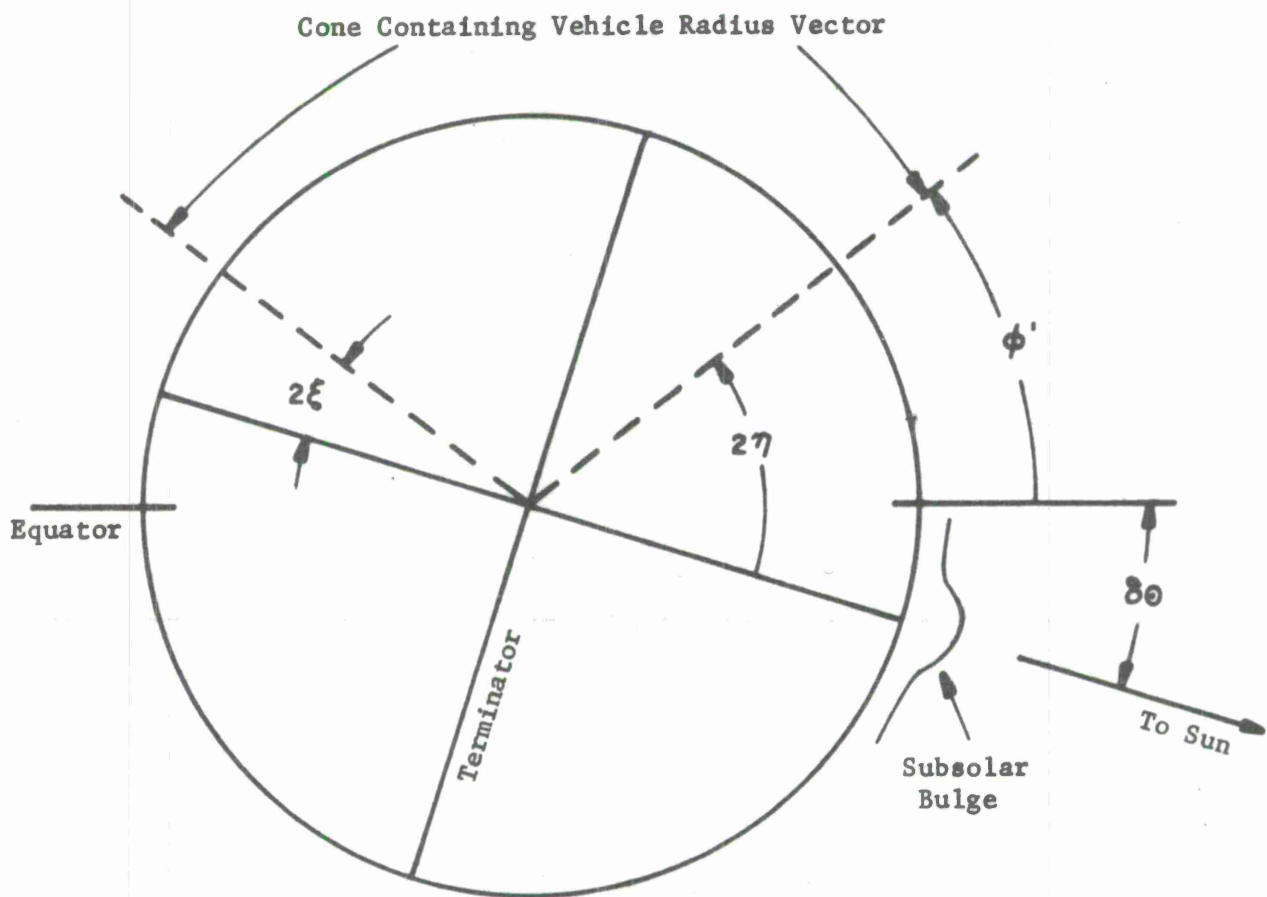


FIGURE II-1. RELATION OF VEHICLE LATITUDE TO SUBSOLAR BULGE

II.2 APPLICATION OF NICOLET'S STEADY-STATE MODEL

Given the altitude and temperature, density is determined by interpolation in Nicolet's steady-state model. This model, tabulated for 10 km altitude and 50° temperature increments, involves almost 3000 storage locations. In order to reduce this number to a reasonable value, series representations were evaluated. In particular, for each altitude, a third order polynomial provides a satisfactory representation for the variations of log density with temperature, i.e.

$$\log \rho (h,T) - \log \rho (h,1100) = A \left[\frac{T-1100}{400} \right] + B \left[\frac{T-1100}{400} \right]^2 + C \left[\frac{T-1100}{400} \right]^3$$

The four values needed to determine log density from temperature -- $\log \rho (h,1100)$, A, B, C -- for each altitude increment are compacted, two words to each cell, into the 48 bit word structure of the Philco 2000, requiring less than 300 core locations. Below 120 km, the limit of the Nicolet II tables, values of $\log \rho$ derived from the COESA 1962 model are used; the densities at 100 and 110 km have been adjusted slightly to assure a smooth transition. At 120 km, the SAO density has also been decreased slightly. This is in the direction indicated by Slowey's reduction of Explorer 17 data.³

Given the temperature, four values of density are derived for two altitude increments above and below the actual satellite altitude. Density and scale-height for the satellite altitude are derived from these points.

This model follows Nicolet's selection of molecular temperature as the essential parameter. Any refinements in the relationship between this temperature and geophysical parameters can easily be incorporated into the model in the future. For instance, the indication³ that the geomagnetic index, K_p , is better correlated with atmospheric fluctuations than is A_p may result in a different "geomagnetic effect" formula.

II.3 INTERPOLATION FORMULAS

Given the temperature, four consecutive values of $\log \rho$ are derived, two for altitudes higher than the satellite altitude h , and two below. (Near the ends of the table, more values will be used on one side than the other). These altitudes are designated by the subscripts -1, 0, 1, and 2. Then, defining $s = 0.1 (h-h_0)$ for 10 km tabular intervals in altitude,

³Slowey, J. "Atmospheric Densities and Temperatures from the Drag Analysis of the Explorer 17 Satellite" SAO Special Report 157, 1 July 1964.

$$\begin{aligned} \log \rho (h, T) = & -\frac{(s)(s-1)(s-2)}{6} \log \rho (h_{-1}, T) \\ & + \frac{(s+1)(s-1)(s-2)}{2} \log \rho (h_0, T) \\ & - \frac{(s+1)(s)(s-2)}{2} \log \rho (h_1, T) \\ & + \frac{(s+1)(s)(s-1)}{6} \log \rho (h_2, T) \end{aligned}$$

The density scale height, H_ρ , is given in km. by

$$\begin{aligned} \frac{1}{H_\rho} &= - \frac{\Delta \log_e \rho}{\Delta h} \\ &= - \frac{\log_e 10}{10} \left[- \frac{3s^2 - 6s + 2}{6} \log \rho (h_{-1}, T) \right. \\ &\quad + \frac{3s^2 - 4s - 1}{2} \log \rho (h_0, T) \\ &\quad - \frac{3s^2 - 2s - 2}{2} \log \rho (h_1, T) \\ &\quad \left. + \frac{3s^2 - 1}{6} \log \rho (h_2, T) \right] \end{aligned}$$

II.4 DENSITY ABOVE 1000 km

Above 1000 km, the density is extrapolated from tabular values at 1000 km by assuming an isothermal atmosphere with constant scale height as determined at 1000 km, i.e.

$$\log \rho (h, T) = \log \rho (1000, T) - \frac{h - 1000}{H(1000, T)} \log e$$

Thus, the normal interpolation procedure is used to derive $H(1000, T)$ from four values of $\log \rho (h, T)$ for $h = 970, 980, 990,$ and 1000 km.

Since $s = 2$,

$$\frac{\log_{10} e}{H(1000, T)} = \sum_{i=-1}^2 a_i \log \rho (h_i, T)$$

where

h_{-1}	$= 970 \text{ km}$	a_{-1}	$= + 1/30$
h_0	$= 980$	a_0	$= - 3/20$
h_1	$= 990$	a_1	$= + 3/10$
h_2	$= 1000$	a_2	$= - 11/60$

Thus, above 1000 km

$$\log \rho (h, T) = \log \rho (1000, T) - (h - 1000) \sum_{i=-1}^2 a_i \log \rho (h_i, T)$$

APPENDIX III

SCALAR DIFFERENTIAL EXPRESSIONS FOR ORBIT PARAMETERS

An orbit determination is a procedure for translating observations into a theory of the orbit suitable for producing a prediction or ephemeris. The orbit determination method employed herein is based upon differential correction preceded by a "representation" or calculation of the observations from a preliminary or approximate theory. The representation is accomplished by special perturbations or numerical integration of selected equations that define the motion or departures from an initial reference orbit. In the interests of computational efficiency, two departures from the engineering practice of differential orbit correction have been made:

- (1) The linear differential correction formulae are obtained analytically by differentiating relationships between the observations and the orbit, and
- (2) The representation of the observations from a preliminary orbit, required for the computation of observation residuals, is carried out by the variation-of-parameters method, thus avoiding the time-consuming aspects of the numerical integration of the total acceleration into an orbit.

The resulting method has demonstrated outstanding computational efficiency, as evidenced in the experimentation described in a subsequent volume, and ability to cope with a wide variety of observation patterns.

This section deals with the choice of parameters utilized in the orbit theory and presents a derivation of the linear correction formulae for translating topocentric observation residuals into corrections of the orbit parameters utilized in the representation of the observations.

III.1 SELECTION OF ORBIT PARAMETERS

The degree of success of a differential correction depends largely upon the perspicacity of the choice of the parameters that represent the orbit in the correction process. Any choice of parameters which leads to nearly linear relationships between cause (errors in the parameters) and effect (topocentric observation residuals) over the expected range of the values of the parameters forms the basis for an adequate orbit theory. Additional considerations of computational simplicity and compatibility with other aspects of the representation or correction procedures serve further to restrict appropriate choices of the parameters. A conventional choice, including eccentricity, e , and argument of perigee, ω , is unsatisfactory because of the inevitable tendency toward lower eccentricities of geocentric satellites interacting with the upper atmosphere. As the eccentricity approaches zero, prior to decay, the argument of perigee becomes more poorly defined and loses its value as a reference direction from which the position (anomaly) of the object is measured. Alternatively, a choice of parameters involving nodal longitude, Ω , and inclination, i , leads to a singularity as i approaches zero, for Ω becomes poorly defined. The latter consideration is not important in the present application but must be considered prior to the appearance of equatorial satellites.

The choice of parameters utilized in the development of this theory involves quantities identified with a coordinate system based upon orthogonal unit vectors, \underline{N} , \underline{M} , \underline{W} (Figure III-1) directed respectively to the ascending node, the northern antinode, and normal to the orbit plane.

The six parameters selected are the following:

L_0 mean longitude of the satellite measured in
two planes from the vernal equinox (i.e.
 $\Omega + \omega + M_0$)

$$a_{xN} = e \cos \omega$$

$$a_{yN} = e \sin \omega$$

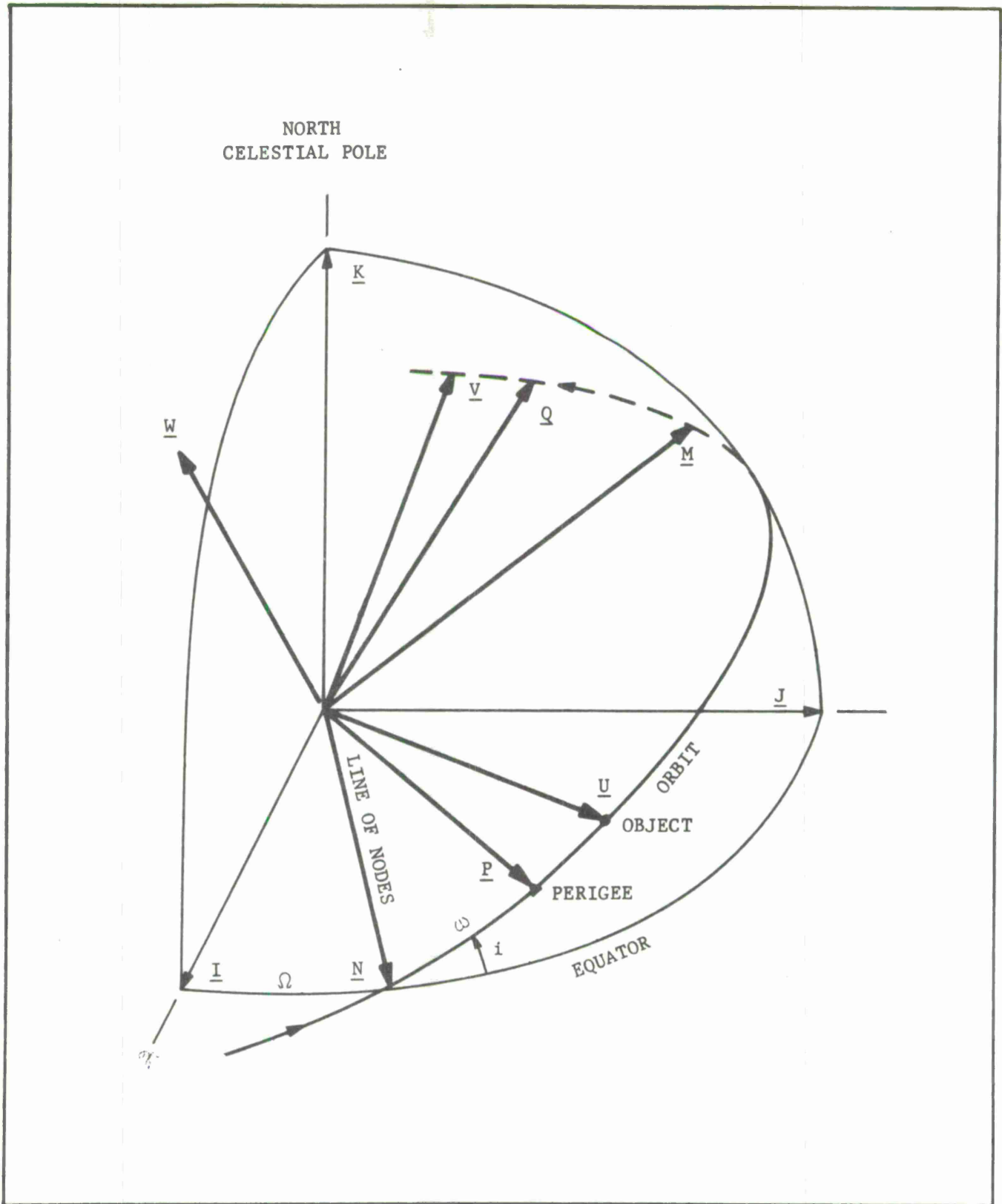


FIG. III-1. PROJECTION OF ORBIT ON CELESTIAL SPHERE, WITH ORIENTATION UNIT VECTORS AND ANGLES DISPLAYED

- a semi-major axis of the osculating orbit
- Ω longitude of the ascending node
- i inclination of the orbit from the equator plane.

The choice of the \underline{M} , \underline{N} and \underline{W} coordinate system and of Ω and i as parameters are subject to revision when equatorial orbits are considered. These parameters are wholly adequate, however, for the satellites which are the subjects of the present study.

Another argument governing the choice of orbit parameters is the compatibility with the ephemeris integration program. In the variation of parameters procedure employed in this study, the derivatives of L_0 , \underline{a} and the angular momentum $\underline{h} = \sqrt{\mu} \underline{W}$ are determined from the perturbative (non two-body) force field; their integrals then do not involve the dominant central-mass gravitational term and an extremely efficient ephemeris program results. The duplication of parameters between the correction formulae and the ephemeris integration formulae leads to minimum of translation steps between the two.

III.2. THE DIFFERENTIAL RELATIONSHIPS

This presentation is logically divided into three parts. The first is a derivation of the differential expressions relating position and orbit parameters in the orbit plane and involves the properties of a two-body orbit. The second extends the differentiation to the orientation of the orbit plane (specified by Ω and i in this formulation). The third step brings in the observer and leads to the final differential correction formulae employed in this study.

a. Differential Expressions for Position Components in the Orbit Plane

This section is concerned with the derivation of the differential relationships between the adopted parameters and the position components in

the orbit plane. These derivations are conveniently separable from the broader problem in that these quantities depend only on four of the six parameters, i.e., a , $U_0 = M_0 + \omega = L_0 - \Omega$, $a_{xN} = e \cos \omega$, $a_{yN} = e \sin \omega$, and the analysis involves only scalar two-body formulae. The remaining differential relationships are derived in section III.2b from the expressions for the vectors defining the orientation of the orbit plane.

The whole of the analysis will employ the \underline{N} , \underline{M} and \underline{W} unit vectors to specify the orientation of the orbit plane and the reference directions in this plane. The \underline{N} and \underline{M} vectors lie in the orbit plane with \underline{N} directed to the node as shown in Figure III-1. The sense of \underline{W} is determined by that of the angular momentum, northerly for direct (eastward) motion. Position in this plane is denoted by the components x_N and y_N defined by:

$$x_N = r \cos u = \underline{N} \cdot \underline{r} \quad (1)$$

$$y_N = r \sin u = \underline{M} \cdot \underline{r} \quad (2)$$

where u , the "argument of the latitude," is given by

$$u = v + \omega \quad (3)$$

These angles and other quantities used in this section are defined in Figure III-1. Other two-body expressions used in this development include:

$$n = k' \sqrt{\mu} a^{-\frac{3}{2}} \quad (4)$$

$$U = U_0 + n (t - t_0) \quad (5)$$

$$E - e \sin E = M = U - \omega \quad (6)$$

$$r = a (1 - e \cos E) \quad (7)$$

$$r \cos v = a (\cos E - e) \quad (8)$$

$$r \sin v = a \sqrt{1 - e^2} \sin E \quad (9)$$

Reference to the glossary* will clarify the meanings of these quantities.

The differential expressions for x_N and y_N are obtained by differentiating (1) and (2).

$$\Delta x_N = \Delta r \cos u - r \Delta u \sin u \quad (10)$$

$$\Delta y_N = \Delta r \sin u + r \Delta u \cos u \quad (11)$$

The determination of Δr follows from (7). The determination of $r \Delta u$ is made in terms of its components $r \Delta v$ and $r \Delta \omega$, the first of these from the derivatives of (8) and (9) and the latter from the derivatives of the parameters $e \cos \omega$ and $e \sin \omega$. These parameters will be denoted a_{xN} and a_{yN} , respectively, in subsequent developments. They are the components, referred to axes determined by \underline{N} and \underline{M} , of a vector \underline{a} directed to perigee with magnitude e .

The procedure outlined above is relatively straightforward and will be summarized in this section. Starting with the parameters a_{xN} and a_{yN} :

$$\Delta a_{xN} = \Delta(e \cos \omega) = \Delta e \cos \omega - e \Delta \omega \sin \omega$$

$$\Delta a_{yN} = \Delta(e \sin \omega) = \Delta e \sin \omega + e \Delta \omega \cos \omega$$

Expressions for Δe and $e \Delta \omega$ follow directly:

$$\Delta e = \Delta a_{xN} \cos \omega + \Delta a_{yN} \sin \omega \quad (12)$$

$$e \Delta \omega = -\Delta a_{xN} \sin \omega + \Delta a_{yN} \cos \omega \quad (13)$$

Next, the differential of (7) yields Δr :

$$\Delta r = \frac{r \Delta a}{a} + ae \Delta E \sin E - a \Delta e \cos E \quad (14)$$

The term ΔE follows from (4), (5), and (6), for

* Appendix VII

$$\frac{\Delta n}{n} = -\frac{3}{2} \frac{\Delta a}{a}$$

$$\Delta U = \Delta U_0 + (t - t_0) \Delta n = \Delta U_0 - \frac{3}{2} (U - U_0) \frac{\Delta a}{a}$$

and finally

$$\Delta E = \frac{a}{r} \Delta U_0 - \frac{a}{r} \Delta \omega - \frac{3}{2} (U - U_0) \frac{a}{r} \frac{\Delta a}{a} + \frac{a}{r} \sin E \Delta e .$$

Substitution for ΔE in (14) leads to

$$\begin{aligned} \Delta r = & \frac{\Delta a}{a} \left[r - \frac{3}{2} (U - U_0) \frac{a^2}{r} e \sin E \right] + \Delta U_0 \left[\frac{a^2}{r} e \sin E \right] \\ & + \Delta \omega \left[-\frac{a^2}{r} e \sin E \right] + \Delta e \left[-a \cos E + \frac{a^2}{r} e \sin^2 E \right] \end{aligned}$$

Further substitution for $\Delta \omega$ and Δe from (12) and (13) leads to the form

$$\Delta r = R_u \Delta U_0 + R_a \frac{\Delta a}{a} + R_{xN} \Delta a_{xN} + R_{yN} \Delta a_{yN} \quad (15)$$

The R's are the partial derivatives of r with respect to the indicated parameters and are tabulated below:

$$R_u = \frac{a^2}{r} e \sin E$$

$$R_a = r - \frac{3}{2} (U - U_0) R_u$$

$$R_{xN} = \frac{a^2}{r} [a_{xN} - \cos (E + \omega)]$$

$$R_{yN} = \frac{a^2}{r} [a_{yN} - \sin (E + \omega)]$$

Alternative expressions may be derived for use in special circumstances, but the present form is well suited to the low-eccentricity orbits of the present analysis.

For the partial derivatives entering into $r\Delta u$, the differentials of $r\Delta v$ are obtained from equations (8) and (9) as follows:

$$\Delta r \cos v - r \Delta v \sin v = \Delta a (\cos E - e) - a \Delta e - a \sin E \Delta E$$

and

$$\begin{aligned} \Delta r \sin v + r \Delta v \cos v = & \Delta a \sqrt{1 - e^2} \sin E - \frac{a e \sin E}{\sqrt{1 - e^2}} \Delta e \\ & + a \sqrt{1 - e^2} \cos E \Delta E \end{aligned}$$

from which

$$r \Delta v = a \sqrt{1 - e^2} \Delta E + \frac{a \sin E}{\sqrt{1 - e^2}} \Delta e$$

Following the substitution pattern established above for Δe and ΔE leads to

$$r \Delta v = v_u \Delta U_o + v_a \frac{\Delta a}{a} + v_{xN} \Delta a_{xN} + v_{yN} \Delta a_{yN} \quad (16)$$

where the coefficients or partial derivatives are

$$v_u = \frac{a^2}{r} \sqrt{1 - e^2}$$

$$v_a = -\frac{3}{2} (U - U_o) v_u$$

$$V_{xN} = \frac{a^2}{r} \left[\sqrt{1-e^2} \sin E \cos \omega \left(1 + \frac{r}{p}\right) + \frac{\sqrt{1-e^2}}{e} \sin \omega \right]$$

$$V_{yN} = \frac{a^2}{r} \left[\sqrt{1-e^2} \sin E \sin \omega \left(1 + \frac{r}{p}\right) - \frac{\sqrt{1-e^2}}{e} \cos \omega \right]$$

The instability of these derivatives for low-eccentricity is a reflection of the indeterminate nature of perigee in a nearly circular orbit.

The $r\Delta\omega$ component of $r\Delta u$ follows directly from (13). In combination with (16) there results

$$\begin{aligned} r\Delta u &= r\Delta v + r\Delta\omega \\ &= U_u \Delta U_o + U_a \frac{\Delta a}{a} + U_{xN} \Delta a_{xN} + U_{yN} \Delta a_{yN} \end{aligned} \quad (17)$$

with the coefficients

$$U_u = V_u = \frac{a^2}{r} \sqrt{1-e^2}$$

$$U_a = V_a = -\frac{3}{2} (U - U_o) U_u$$

$$\begin{aligned} U_{xN} = \frac{a^2}{r} \left[\left(1 + \frac{r}{a}\right) \sin (E + \omega) + a_{xN} e \sin E \frac{e^2 - (1 + \sqrt{1-e^2}) e \cos E}{\sqrt{1-e^2} (1 + \sqrt{1-e^2})^2} \right. \\ \left. - \frac{a_{xN}^2}{1 + \sqrt{1-e^2}} \right] \end{aligned}$$

$$U_{yN} = \frac{a^2}{r} \left[- \left(1 + \frac{r}{a} \right) \cos (E + \omega) + a_{yN} e \sin E \frac{e^2 - (1 + \sqrt{1 - e^2}) e \cos E}{\sqrt{1 - e^2} (1 + \sqrt{1 - e^2})^2} + \frac{a_{xN}}{1 + \sqrt{1 - e^2}} \right]$$

In the above expressions, special care has been taken in the arrangement of terms so that no computational problems arise as the eccentricity approaches zero. These expressions for Δr and $r \Delta u$ will be combined in the following section with the differential expressions involving orbit plane orientation.

b. Differential Expression Extended to the Orientation of the Orbit Plane

The orbit plane orientation enters into the analysis through the expression for the observation vector $\underline{\rho}$, shown in Figure III-2 and defined by

$$\underline{\rho} = \underline{r} + \underline{R} = r \underline{U} + \underline{R}$$

where \underline{R} is the "station" vector from observer to geocentric. Differentiating leads to

$$\Delta \underline{\rho} = \Delta r \underline{U} + r \Delta \underline{U} + \Delta \underline{R} \quad (18)$$

For the present analysis, $\Delta \underline{R}$ is assumed zero, and no attempt to correct station location will be made. The expression for Δr is given in Eq. (15); the expression for $\Delta \underline{U}$ remains to be determined.

The changes in \underline{U} can be attributed to two sources; the change in orientation of the orbit plane and the change in position of the object within this plane. These can be determined from the identity

$$\underline{U} = \underline{N} \cos u + \underline{M} \sin u$$

$$\Delta \underline{U} = \Delta \underline{N} \cos u + \Delta \underline{M} \sin u + \Delta u (\underline{M} \cos u - \underline{N} \sin u) \quad (19)$$

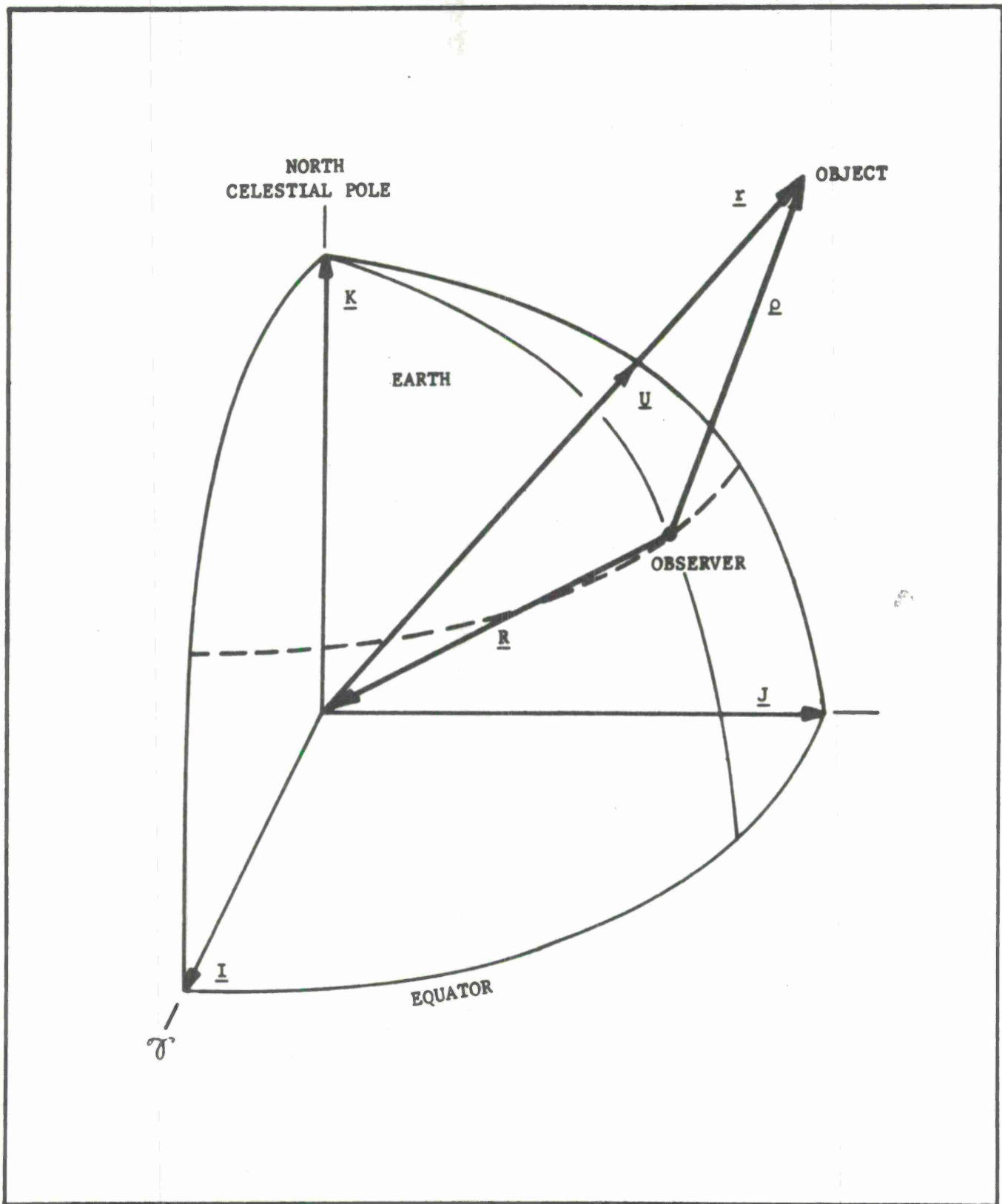


FIG. III-2. OBSERVATIONAL FRAMEWORK

The quantities of $\Delta \underline{N}$ and $\Delta \underline{M}$ can be related to the parameters $\Delta \Omega$ and Δi through the following line of reasoning. Starting with the definition of the orientation parameters in terms of \underline{W}

$$\underline{W}: \begin{cases} W_x = \sin \Omega \sin i \\ W_y = -\cos \Omega \sin i \\ W_z = \cos i \end{cases} \quad (20)$$

Differentiation leads to

$$\Delta W_x = \cos \Omega \sin i \Delta \Omega + \sin \Omega \cos i \Delta i$$

$$\Delta W_y = \sin \Omega \sin i \Delta \Omega - \cos \Omega \cos i \Delta i$$

$$\Delta W_z = -\sin i \Delta i$$

The coefficients of $\Delta \Omega$ and of Δi can be expressed in terms of \underline{M} and \underline{N} from their components.

$$\underline{N}: \begin{cases} N_x = \cos \Omega \\ N_y = \sin \Omega \\ N_z = 0 \end{cases} \quad (21)$$

$$\underline{M}: \begin{cases} M_x = -\sin \Omega \cos i \\ M_y = \cos \Omega \cos i \\ M_z = \sin i \end{cases} \quad (22)$$

Thus

$$\Delta \underline{W} = \underline{N} \Delta \Omega \sin i - \underline{M} \Delta i$$

Similarly, by differentiating (21) and (22) expressions for $\Delta \underline{N}$ and $\Delta \underline{M}$ follow.

$$\Delta \underline{N} = \underline{M} \Delta \Omega \cos i - \underline{W} \Delta \Omega \sin i \quad (23)$$

$$\Delta \underline{M} = -\underline{N} \Delta \Omega \cos i + \underline{W} \Delta i \quad (24)$$

By combining (18), (19), (23) and (24), the expression for $\Delta \underline{\rho}$ assumes the form:

$$\begin{aligned} \Delta \underline{\rho} &= \Delta r \underline{U} + r \Delta u (\underline{M} \cos u - \underline{N} \sin u) \\ &\quad + r \Delta \Omega [\cos i (\underline{M} \cos u - \underline{N} \sin u) - \underline{W} \sin i \cos u] \\ &\quad + r \Delta i (\underline{W} \sin u) \end{aligned} \quad (25)$$

or, expressed in terms of the \underline{U} , \underline{V} , \underline{W} unit vectors

$$\begin{aligned} \Delta \underline{\rho} &= \Delta r \underline{U} + (r \Delta u + r \Delta \Omega \cos i) \underline{V} \\ &\quad + (r \Delta i \sin u - r \Delta \Omega \sin i \cos u) \underline{W} \end{aligned} \quad (26)$$

The six orbit parameters enter this differential expression explicitly as Δi and $\Delta \Omega$, and implicitly through Δr and $r \Delta u$ as given by (15) and (17). Then combination leads to:

$$\begin{aligned}
\Delta \rho &= \Delta U_o (\underline{U} R_u + \underline{V} U_u) + \frac{\Delta a}{a} (\underline{U} R_a + \underline{V} U_a) \\
&+ \Delta a_{xN} (\underline{U} R_{xN} + \underline{V} U_{xN}) + \Delta a_{yN} (\underline{U} R_{yN} + \underline{V} U_{yN}) + \\
&+ \Delta \Omega (\underline{V} r \cos i - \underline{W} r \sin i \cos u) \\
&+ \Delta i (\underline{W} r \sin u)
\end{aligned} \tag{27}$$

where the partial derivatives denoted by R_u , U_u , etc., have been previously defined.

c. Extension to Topocentric Observation Residuals

The final step in the derivation of the differential relationships involves the translation of $\Delta \rho$, as expressed in (27), into differential expressions expressed in the topocentric observer's geometry. Appropriate observed quantities include pairs of angles, such as topocentric right ascension and declination or altitude and azimuth, and range. These observation residuals may be recognized in the $\Delta \rho$ expression by writing

$$\Delta \rho = \Delta(\rho \underline{L}) = \Delta \rho \underline{L} + \rho \Delta \underline{L} \tag{28}$$

and the definition of \underline{L} in terms of topocentric right ascension and declination:

$$\underline{L}: \begin{cases} L_x = \cos \delta \cos \alpha \\ L_y = \cos \delta \sin \alpha \\ L_z = \sin \delta \end{cases} \tag{29}$$

The differential $\Delta \underline{L}$ is expressed by

$$\Delta \underline{L}: \begin{cases} \Delta L_x = -\cos \delta \sin \alpha \Delta \alpha - \sin \delta \cos \alpha \Delta \delta \\ \Delta L_y = \cos \delta \cos \alpha \Delta \alpha - \sin \delta \sin \alpha \Delta \delta \\ \Delta L_z = \cos \delta \Delta \delta \end{cases}$$

By defining two additional orthogonal vectors, \underline{A} and \underline{D} , both mutually perpendicular to \underline{L} and with \underline{A} lying parallel to the equatorial plane

$$\underline{A}: \begin{cases} A_x = -\sin \alpha \\ A_y = \cos \alpha \\ A_z = 0 \end{cases} \quad (30)$$

$$\underline{D}: \begin{cases} D_x = -\sin \delta \cos \alpha \\ D_y = -\sin \delta \sin \alpha \\ D_z = \cos \delta \end{cases} \quad (31)$$

the $\Delta \underline{L}$ can be expressed as

$$\Delta \underline{L} = \underline{A} \cos \delta \Delta \alpha + \underline{D} \Delta \delta$$

or

$$\Delta \underline{\rho} = \underline{L} \Delta \rho + \underline{A} \rho \cos \delta \Delta \alpha + \underline{D} \rho \Delta \delta \quad (32)$$

Thus the successive dot products of $\Delta \underline{\rho}$ with the vector triad \underline{L} , \underline{A} and \underline{D} leads to scalar differential expressions for $\Delta \rho$, $\rho \cos \delta \Delta \alpha$ and $\rho \Delta \delta$ respectively. In practice, the vectors \underline{L} , \underline{A} and \underline{D} may be defined either

by the observation or by the representation; with incomplete observations, i.e., only one or two of the coordinates such as obtained by range-only or angle-only instruments, the \underline{L} , \underline{A} , \underline{D} triad must be obtained from the representation.

Differential expressions involving altitude and azimuth observations may be similarly obtained by defining the horizon system vector triad \underline{L} , \underline{A} and \underline{D} , whose horizon components are

$$\underline{L}: \begin{cases} L_{xh} = -\cos A \cos h \\ L_{yh} = +\sin A \cos h \\ L_{zh} = +\sin h \end{cases} \quad (33)$$

$$\underline{A}: \begin{cases} A_{xh} = +\sin A \\ A_{yh} = +\cos A \\ A_{zh} = 0 \end{cases} \quad (34)$$

$$\underline{D}: \begin{cases} D_{xh} = +\cos A \sin h \\ D_{yh} = -\sin A \sin h \\ D_{zh} = +\cos h \end{cases} \quad (35)$$

where A is the azimuth angle measured east from north, and h the altitude angle measured from the local horizon.

These horizon components must be rotated into the equator system, to which the components of $\Delta \underline{\rho}$ are referred, by

$$\left. \begin{aligned} L_x &= L_{xh} S_x + L_{yh} E_x + L_{zh} Z_x \\ L_y &= L_{xh} S_y + L_{yh} E_y + L_{zh} Z_y \\ L_z &= L_{xh} S_z + L_{yh} E_z + L_{zh} Z_z \end{aligned} \right\} \underline{L} \rightarrow \underline{\tilde{A}}, \underline{\tilde{D}}$$

where

$$\underline{S}: \begin{cases} S_x = \sin \phi \cos \theta \\ S_y = \sin \phi \sin \theta \\ S_z = -\cos \phi \end{cases}$$

$$\underline{E}: \begin{cases} E_x = -\sin \theta \\ E_y = +\cos \theta \\ E_z = 0 \end{cases}$$

$$\underline{Z}: \begin{cases} Z_x = \cos \phi \cos \theta \\ Z_y = \cos \phi \sin \theta \\ Z_z = \sin \phi \end{cases}$$

and where ϕ is the astronomical latitude and θ is the local sidereal time.

Then

$$\Delta \underline{L} = \underline{\tilde{A}} \cos h \Delta A + \underline{\tilde{D}} \Delta h$$

and

$$\Delta \underline{\rho} = \underline{L} \Delta \rho + A \rho \cos h \Delta A + \underline{\tilde{D}} \Delta h \quad (36)$$

Thus scalar differential expressions relating the orbit parameters to topocentric altazimuth observation residuals are readily obtained by successive dot products of $\Delta \underline{\rho}$, given by (27), with \underline{L} , $\underline{\tilde{A}}$ and $\underline{\tilde{D}}$ again determined either from observation or representation.

APPENDIX IV

SCALAR DIFFERENTIAL EXPRESSIONS FOR DRAG

The development of the secular drag perturbations for a satellite moving about a spherical earth has received considerable attention in the literature ^{1,2,3}. In order to adapt these theories to a differential-correction procedure for earth satellites executing grazing entry, where drag represents the primary perturbative influence, this theory has been extended to include, in the determination of density variations along the path, the altitude variations arising from motion over an oblate earth. This altitude variation is significant for highly inclined satellites, amounting to 21 km. at the poles.

IV.1 DETERMINATION OF DENSITY VARIATIONS ALONG PATH

Altitude variations over the earth's surface arise from two factors, as illustrated in Fig. IV-1. The variation due to eccentricity is

$$r - q = ae (1 - \cos E)$$

from the perigee distance q . A second altitude variation is that due to oblateness, where the earth radius varies over the earth as

$$R = a_e \left[1 - f U_z^2 + \frac{3}{2} f^2 (U_z^4 - U_z^2) \right], U_z = \sin i \sin (v + \omega)$$

where f is the flattening coefficient ($= 1/298.3$). Combining these effects, the altitude variation along the path from that determined at the two-body perigee point is given, to first order in flattening, by

$$ae (1 - \cos E) + f (U_z^2 - P_e^2) a_e$$

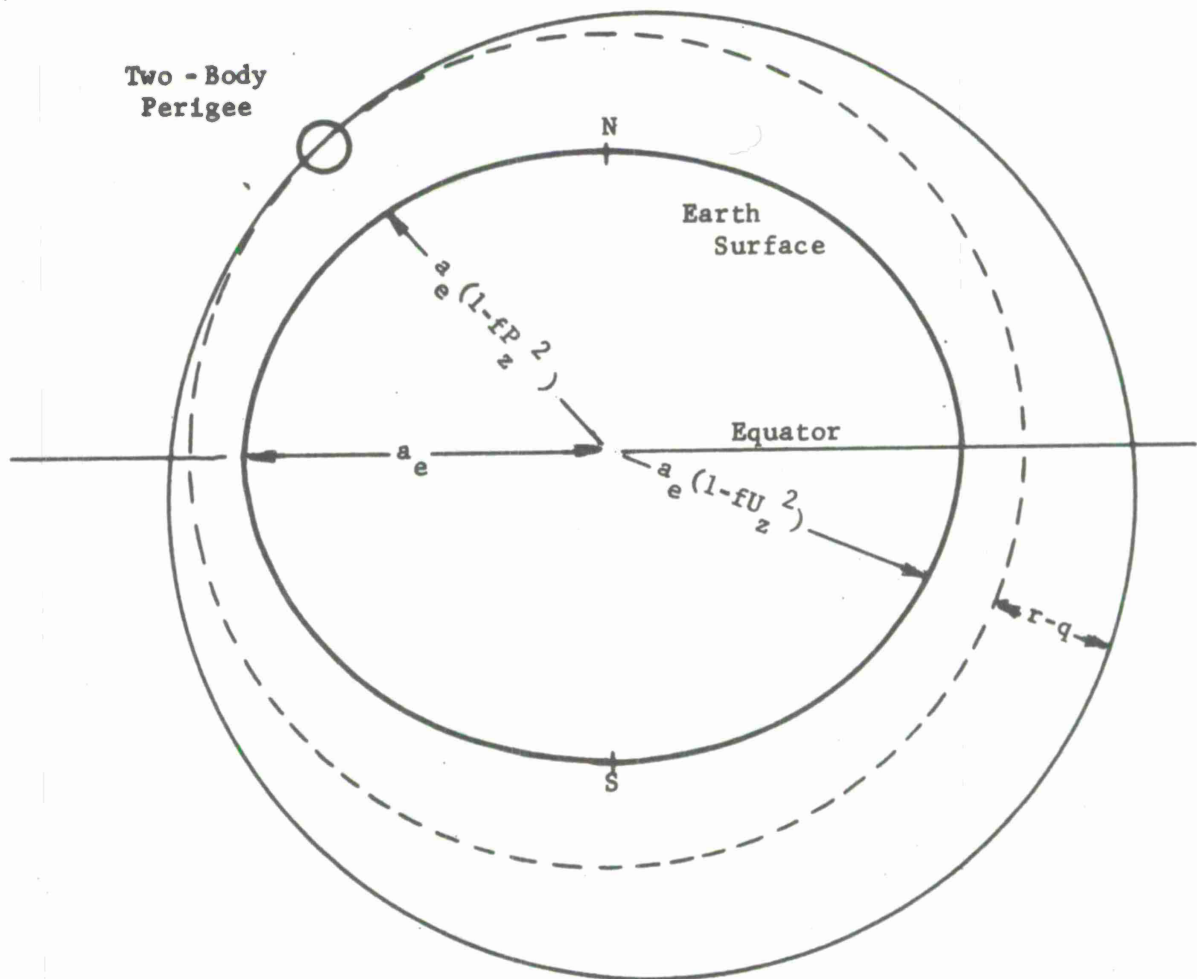


FIGURE IV-1. HEIGHT ABOVE OBLATE EARTH

where P_z is determined at the two-body perigee point. This expression may be expressed in terms of the single variable E by the substitution

$$v = E + e \sin E + \dots$$

For a first order theory in flattening and eccentricity, this sequence is terminated at $v = E$, and

$$U_z = \sin i \sin (v + \omega) \approx \sin i \sin (E + \omega)$$

Further manipulation leads to an altitude variation along the path given by

$$ae (1 - \cos E) + \frac{f \sin^2 i}{2} a_e [\cos 2\omega - \cos 2(E + \omega)]$$

The density variations along the path, assuming an isothermal (exponential) atmosphere in the vicinity of perigee altitude is then given by

$$\rho = \rho_\pi \exp \left\{ -k \left[ae (1 - \cos E) + \frac{f \sin^2 i}{2} a_e (\cos 2\omega - \cos 2E \cos 2\omega + \sin 2E \sin 2\omega) \right] \right\} \quad (1)$$

where ρ_π is the perigee density, determined from an appropriate density model, and k^{-1} is the scale height, similarly determined.

IV.2 SECULAR VARIATION IN SEMI-MAJOR AXIS

Differentiation of the vis-viva (energy) integral leads to the expression for variations in semi-major axis, as follows:

$$\dot{s}^2 = \mu \left[\frac{2}{r} - \frac{1}{a} \right] = \frac{\mu}{a} \left[\frac{1 + e \cos E}{1 - e \cos E} \right]$$

$$\text{and } 2\dot{\underline{r}} \cdot \dot{\underline{r}}' = 2\dot{s}\dot{s}' = \frac{\mu}{a^2} \dot{a}', \text{ or } \dot{a}' = \frac{2a^2}{\mu} \dot{s}\dot{s}'$$

where $\dot{\underline{r}}$ is the velocity vector and $\dot{\underline{r}}'$ is the perturbative acceleration.

For drag, the acceleration component \dot{s} along the path is given by

$$\dot{s} = -\frac{1}{2} B \rho \dot{s}^2 = -\frac{1}{2} B \rho \frac{\mu}{a} \cdot \frac{1 + e \cos E}{1 - e \cos E}$$

Following the procedure outlined in ref. (1), the variation in semi-major axis, with eccentric anomaly, is derived:

$$\frac{da}{dE} = \frac{r\sqrt{a}}{\sqrt{\mu}} \dot{s} = -B \rho a^2 \left[\frac{1 + e \cos E}{1 - e \cos E} \right]^{3/2} (1 - e \cos E) \quad (2)$$

①
②
③

as given in ref. (1). Three variable expressions are involved, and the following comments are germane:

- ① The variations in density, due to orbital eccentricity and/or oblateness, are very large. Eccentricity effects can represent many scale heights even for relatively low (~ 0.01) eccentricities, and oblateness can lead to density variations of the order of one scale height for highly inclined orbits.
- ② This second term arises from variations in satellite velocity, and is very small ($\sim 3e$) for low eccentricity orbits.
- ③ This third term arises from radial distance variations. In addition to the small variation ($\sim e$) for orbits of interest, this term partially offsets the second term above.

Thus, the significant variations in semi-major axis arise from the variations in density encountered along the path. In the following analysis, the secular variation in semi-major axis shall be determined, and subsequently used to define the scalar differential expression for the differential correction of drag.

The introduction of the density variations along the path, eqn. (1), into (2) leads to

$$\frac{da}{dE} = -B \rho_{\pi} a^2 \exp(-kae) \left\{ \exp(kae \cos E) \cdot (1 + 2e \cos E + \dots) \right. \\ \left. \exp \left[-kfa_e \frac{\sin^2 i}{2} (\cos 2\omega - \cos 2\omega \cos 2E + \sin 2\omega \sin 2E) \right] \right\}.$$

The last exponential term is expanded in a Taylor series involving terms of the form:

$$\frac{\alpha^n}{n!} \left[(1 - \cos 2E) + \sin 2E \tan 2\omega \right]^n, \alpha = - \frac{k f \sin^2 i}{2} a_e \cos 2\omega$$

with the observations:

- (1) Despite the factor f in α , α is not a small number, but rather approaches unity at altitudes representative of terminal decay. This arises from the factor k , the reciprocal scale height, and requires that sufficient terms be carried to permit the factorial term to define convergence.
- (2) In the binomial expansion of the bracketed quantity, and the subsequent integration on a per-revolution basis to define the secular variations in the parameters, all odd functions of E (and ω) vanish.

The expansion of the bracketed quantity leads to even functions of E of the form:

$$\cos^r E (1 - \cos 2E)^s$$

Their subsequent integration, on a per-revolution basis, defines a sequence of integrals of the form:

$$\frac{1}{2\pi} \int_0^{2\pi} \exp(z \cos E) F(\cos E, 1 - \cos 2E) dE$$

where $z = kae$

These integrals define Bessel functions of imaginary argument; Table IV-1 provides a table of these integrals and the generating series for the $B_n(z)$ terms, for small argument ($z \leq 2$). For large argument, asymptotic series for related functions are available.¹

By performing these operations, the sequence of terms for the secular variation in semi-major axis is derived, as given in Table IV-2. Terms of order e have not been included, for the reasons given earlier.

TABLE IV-1

BESSEL FUNCTIONS OF IMAGINARY ARGUMENT

Integrals of the Form

$$\frac{1}{2\pi} \int_0^{2\pi} \exp(z \cos E) F(\cos E, 1-\cos 2E) dE$$

Kernel, F	Integral
1	$B_0(z)$
$(1-\cos 2E)$	$B_1(z)$
$(1-\cos 2E)^2$	$3 \cdot B_2(z)$
$(1-\cos 2E)^3$	$3 \cdot 5 \cdot B_3(z)$
$(1-\cos 2E)^4$	$3 \cdot 5 \cdot 7 \cdot B_4(z)$
$(1-\cos 2E)^5$	$3 \cdot 5 \cdot 7 \cdot 9 \cdot B_5(z)$
2 cos E	$z B_1(z)$
$2\cos E (1-\cos 2E)$	$z B_2(z)$
$2\cos E (1-\cos 2E)^2$	$3 \cdot z B_3(z)$
$2\cos E (1-\cos 2E)^3$	$3 \cdot 5 \cdot z B_4(z)$
$2\cos E (1-\cos 2E)^4$	$3 \cdot 5 \cdot 7 \cdot z B_5(z)$
$\cos^2 E$	$B_0(z) - \frac{1}{2} B_1(z)$
$\cos^2 E (1-\cos 2E)$	$B_1(z) - \frac{1}{2} [3 \cdot B_2(z)]$
$\cos^2 E (1-\cos 2E)^2$	$3 \cdot B_2(z) - \frac{1}{2} [3 \cdot 5 \cdot B_3(z)]$
$\cos^2 E (1-\cos 2E)^3$	$3 \cdot 5 \cdot B_3(z) - \frac{1}{2} [3 \cdot 5 \cdot 7 \cdot B_4(z)]$
$\cos^2 E (1-\cos 2E)^4$	$3 \cdot 5 \cdot 7 \cdot B_4(z) - \frac{1}{2} [3 \cdot 5 \cdot 7 \cdot 9 \cdot B_5(z)]$

For small argument ($z \leq 2$):

$$B_n(z) = \sum_{r=0}^{\infty} \frac{(z/2)^{2r}}{r! (n+r)!}$$

TABLE IV-2

EXPRESSION FOR SECULAR VARIATION IN SEMI-MAJOR AXIS

$$\frac{\delta a}{\delta t} = -B\rho_{\pi} na^2 \exp(-z) \left\{ \left[B_0 + \alpha B_1 + \frac{\alpha^2}{2!} (3 \cdot B_2) + \frac{\alpha^3}{3!} (3 \cdot 5 \cdot B_3) + \frac{\alpha^4}{4!} (3 \cdot 5 \cdot 7 \cdot B_4) + \dots \right] + \right. \\ \left. + (\alpha \tan 2\omega)^2 \left[(B_1 - \frac{1}{2} 3 \cdot B_2) + \alpha (3 \cdot B_2 - \frac{1}{2} 3 \cdot 5 \cdot B_3) + \frac{\alpha^2}{2!} (3 \cdot 5 \cdot B_3 - \frac{1}{2} 3 \cdot 5 \cdot 7 \cdot B_4) + \dots \right] + \right. \\ \left. + \frac{1}{6} (\alpha \tan 2\omega)^4 \left[(3 \cdot B_2 - 3 \cdot 5 \cdot B_3 + \frac{1}{4} 3 \cdot 5 \cdot 7 \cdot B_4) + \alpha (3 \cdot 5 \cdot B_3 - 3 \cdot 5 \cdot 7 \cdot B_4 + \frac{1}{4} 3 \cdot 5 \cdot 7 \cdot 9 \cdot B_5) + \dots \right] \right\}$$

08

TABLE IV-3

EXPRESSION FOR SECULAR VARIATION IN ECCENTRICITY

$$\frac{1}{e} \frac{\delta e}{\delta t} = -B\rho_{\pi} pn \exp(-z) \frac{a}{2H} \left\{ \left[B_1 + \alpha B_2 + \frac{\alpha^2}{2} 3 \cdot B_3 + \frac{\alpha^3}{3!} 3 \cdot 5 \cdot B_4 + \frac{\alpha^4}{4!} 3 \cdot 5 \cdot 7 \cdot B_5 + \dots \right] + \right. \\ \left. + (\alpha \tan 2\omega)^2 \left[(B_2 - \frac{1}{2} 3 \cdot B_3) + \alpha (3 \cdot B_3 - \frac{1}{2} 3 \cdot 5 \cdot B_4) + \frac{\alpha^2}{2!} (3 \cdot 5 \cdot B_4 - \frac{1}{2} 3 \cdot 5 \cdot 7 \cdot B_5) + \dots \right] + \right. \\ \left. + \frac{1}{6} (\alpha \tan 2\omega)^4 \left[(3 \cdot B_3 - 3 \cdot 5 \cdot B_4 + \frac{1}{4} 3 \cdot 5 \cdot 7 \cdot B_5) + \alpha (3 \cdot 5 \cdot B_4 - 3 \cdot 5 \cdot 7 \cdot B_5 + \frac{1}{4} 3 \cdot 5 \cdot 7 \cdot 9 \cdot B_6) + \dots \right] \right\}$$

IV.3 SECULAR VARIATION IN ECCENTRICITY

A similar procedure* leads to the secular variation in eccentricity, given in Table IV.3, preceding page.

The apparent tangent terms in Tables IV.2 and IV.3 present no difficulty, since they are associated with factors of α to give:

$$\alpha \tan 2\omega = -kf \frac{\sin^2 i}{2} \sin 2\omega$$

IV.4 SCALAR DIFFERENTIAL EXPRESSIONS

Secular variations in semi-major axis and eccentricity have been presented above; additional secular variations in inclination perigee and node arise from atmospheric rotation, but are of minor importance in differential correction. In addition, the computational investment required to include short-period terms is unwarranted for the range of eccentricities considered here.

Orbit parameters included in the differential correction include mean motion n , $a_{xN} = e \cos \omega$ and $a_{yN} = e \sin \omega$. The differential correction for drag is incorporated by expanding the scalar differential expressions (given in Appendix I for the two-body parameters) to include terms in $\frac{\Delta B}{B}$,

as follows, where Δf represents an observation residual.

$$\begin{aligned} \Delta f = & C_{\frac{\Delta n}{n}} \left(\frac{\Delta n_o}{n_o} - \frac{3}{2} \cdot \frac{1}{a} \cdot \frac{\delta a}{\delta t} (t-t_o) \cdot \frac{\Delta B}{B} \right) \\ & + C_{\Delta a_{xN}} \left(\Delta a_{xN_o} + a_{xN} \frac{1}{e} \frac{\delta e}{\delta t} (t-t_o) \frac{\Delta B}{B} \right) \\ & + C_{\Delta a_{yN}} \left(\Delta a_{yN_o} + a_{yN} \frac{1}{e} \frac{\delta e}{\delta t} (t-t_o) \frac{\Delta B}{B} \right) \\ & + C_{\Delta \Omega} \Delta \Omega + C_{\Delta i} \Delta i + C_{\Delta U_o} \Delta U_o \end{aligned}$$

*See Reference (1) for partial derivation.

The expressions for $\frac{\delta a}{\delta t}$ and $\frac{\delta e}{\delta t}$ are given in Tables IV.2 and IV.3. The apparent indeterminacy of the $C_{\Delta a_{xN}}$ and $C_{\Delta a_{yN}}$ coefficients for circular orbits is more

apparent than real, for the $\frac{\delta e}{\delta t}$ expression contains a factor $z = kae$. In practice, the e term in z is associated with the $\cos \omega$ and $\sin \omega$ terms to avoid division by e .

REFERENCES

- ¹Arsenault, J., Koskela, P., and Walters, L. G., "Earth Satellite Ephemerides by General Perturbations", Aeronutronic Report U-970, August 25, 1960. (Also published as Section 8.3 in Koelle, "Handbook of Astronautical Engineering", McGraw-Hill Book Company, 1961)
- ²Sterne, T. E., "An Introduction to Celestial Mechanics", Interscience, 1961, page 161.
- ³El'Yasberg, P. E., "Dependence of Secular Variations of Orbit Elements on Air Resistance," ARS Journal, V. 30, 1960, pp 672-675.

APPENDIX V

SCALAR DIFFERENTIAL EXPRESSIONS FOR SENSOR CALIBRATION

This appendix develops the 4×7 matrix of coefficients relating residuals in the four observation components - range, range-rate, azimuth and elevation - to corrections to sensor coordinates, latitude, longitude, and height above the reference ellipsoid, and to biases in range, azimuth, elevation and station time. Although the determination of bias in range-rate is a trivial extension of this theory, the existence of a scale factor error is more probable, and is revealed in a characteristic range-rate residual pattern.

V.1 SCALAR DIFFERENTIAL EXPRESSIONS FOR SENSOR LOCATION*

The problem presented is that of correcting a geodetic position by using observations of a satellite for which a definitive orbit has been determined. To elaborate, assume that an observation network has been established. The stations comprising this network are assumed to be tied together exceedingly well; that is, their geodetic positions are assumed to be accurately known. Further, it is assumed that observations from the stations of this network have resulted in the determination of a definitive orbit for the satellite. Observations of this satellite are also made from an isolated observing site, of which the approximate location is known. Corrections to the site's assumed position

* Koskela, P., Nicola, L., and Walters, L. G., "Station Coordinates from Satellite Observations," ARS Journal, Vol. 32, p. 253, February 1962.

must now be obtained by using the satellite observations. The position obtained in this way is referred directly to the reference spheroid and therefore has the advantage of being independent of local gravitational anomalies.

The problem may be visualized with the aid of Figure V-1. As the satellite describes its orbit about Earth, its position with respect to the dynamical center is defined by the known vector \underline{r} , tabulated as a function of time. The observer's position is given by \underline{R} , a vector conveniently represented by the components x_c and y_c in the meridian plane and by the local sidereal time or hour angle of the vernal equinox θ . For a fixed observation point on Earth, only the sidereal time varies as Earth rotates.

The observations are components of the vector $\underline{\rho}$, either its magnitude, slant range ρ , or direction cosines \underline{L} , expressed in terms of the topocentric angles right ascension and declination or elevation angle and azimuth.

The station vector \underline{R} can be written as

$$\underline{R} = -x_c \cos \theta \underline{I} - x_c \sin \theta \underline{J} - y_c \underline{K} \quad (1)$$

where \underline{I} , \underline{J} , and \underline{K} are unit vectors directed along the x, y, and z axes respectively.

$$\theta = \theta_{GR} + \lambda_E$$

where λ_E is the longitude of the observer measured positively to the east, and θ_{GR} is the Greenwich sidereal time. θ_{GR} may be calculated from

$$\theta_{GR} = \theta_{GR_0} + 0.004,375,26905 (t-t_0)$$

where θ_{GR_0} is the Greenwich sidereal time in radians at some arbitrary epoch, and $(t-t_0)$ is the mean solar time interval, in minutes, since that epoch. The observer's coordinates in the meridian plane are

$$\begin{aligned} x_c &= (C + H) \cos \phi \\ y_c &= (S + H) \sin \phi \end{aligned}$$

where (See Section V.3)

$$\begin{aligned} C &= \frac{a_e}{(1 - e^2 \sin^2 \phi)^{\frac{1}{2}}} \\ S &= (1 - e^2) C \end{aligned}$$

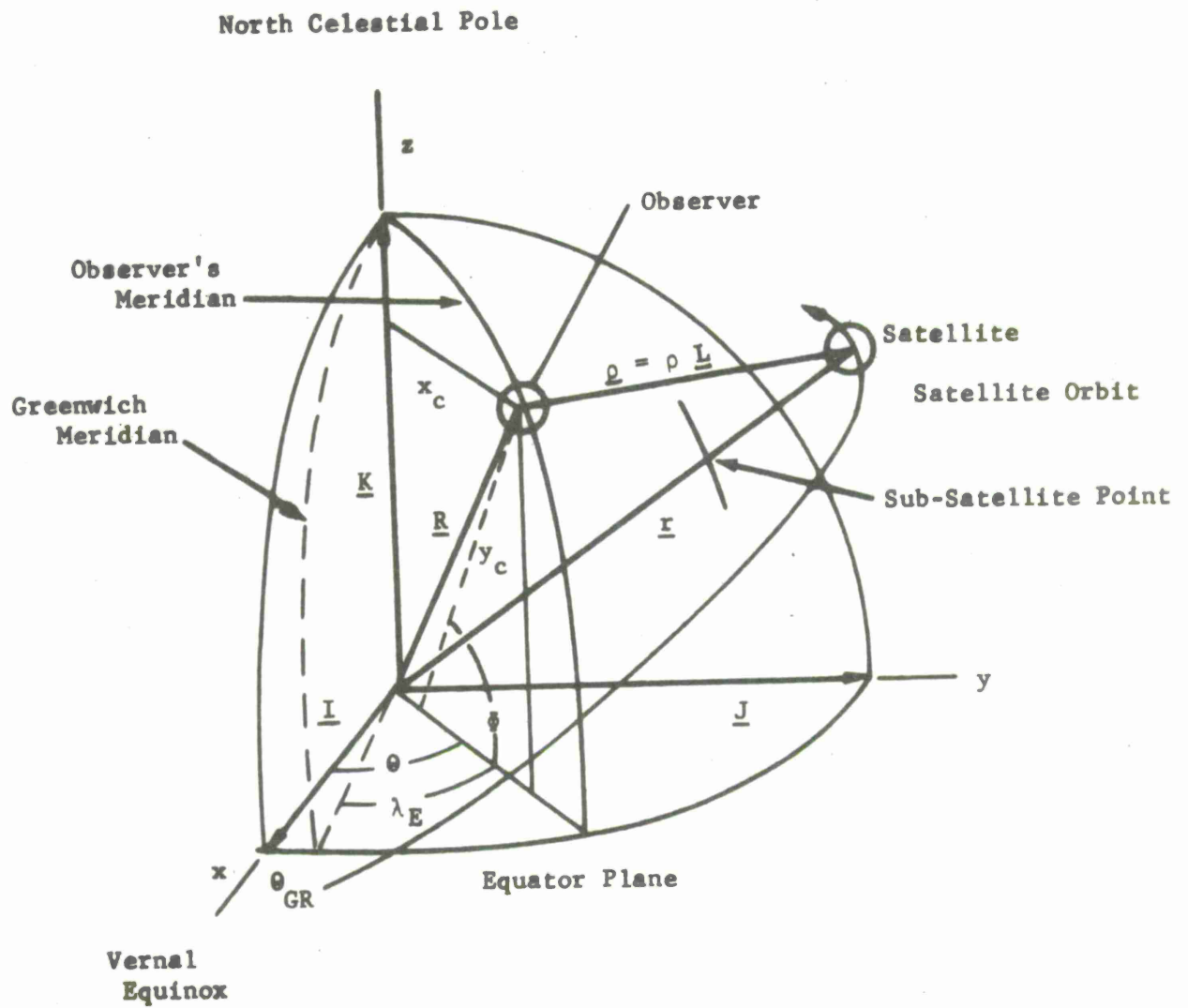


FIGURE V-1. POSITION RELATIONSHIP OF OBSERVER, SATELLITE AND DYNAMICAL CENTER

H is the height above the reference ellipsoid in Earth equatorial radii, and

$$e^2 = 2f - f^2$$

where f is the flattening or oblateness, e the eccentricity of the adopted reference ellipsoid, ϕ the geodetic latitude, and a_e Earth's equatorial radius.

The fundamental relationship between the positions of the observer, dynamical center, and satellite may now be written as (see Figure V-1)

$$\underline{\rho} = \underline{r} + \underline{R}$$

or, using Eq. 1

$$\underline{\rho} = \underline{r} - x_c \cos \theta \underline{I} - x_c \sin \theta \underline{J} - y_c \underline{K}$$

This equation may be differentiated to relate the incremental changes $\Delta \underline{\rho}$, residuals in range or angular position of the satellite generally taken in the sense observed minus computed, to the corresponding changes $\Delta \underline{r}$ (orbit uncertainties) and to $\Delta \underline{R}$ (station errors). If it is assumed that the orbit is adequately known, it will remain uncorrected during the station correction procedure, and the incremental changes $\Delta \underline{r}$ can be set to zero. Following this procedure

$$\Delta \underline{\rho} = \Delta x_c [-\underline{I} \cos \theta - \underline{J} \sin \theta] - \Delta y_c \underline{K} +$$

$$\Delta \lambda_E [\underline{I} x_c \sin \theta - \underline{J} x_c \cos \theta]$$

This differential expression may be transformed into the more familiar spherical coordinates involving latitude and height above the reference ellipsoid; neglecting second and higher order terms, the vector differential expression becomes

$$\Delta \underline{\rho} = [y_c (\underline{I} \cos \theta + \underline{J} \sin \theta) - x_c \underline{K}] \Delta \phi$$

$$+ [x_c (\underline{I} \sin \theta - \underline{J} \cos \theta)] \Delta \lambda_E$$

$$+ [- x_c (\underline{I} \cos \theta + \underline{J} \sin \theta) - y_c \underline{K}] \frac{\Delta H}{C + H}$$

An alternative expression, in terms of the vector triad \underline{S} , \underline{E} and \underline{Z} defining the observers south, east and zenith directions may be written, again ignoring terms of order e^2 (flattening) in the coefficients for this differential expression:

$$\Delta \underline{\rho} = (C + H) \Delta \phi \underline{S} - (C + H) \cos \phi \Delta \lambda_E \underline{E} - \Delta H \underline{Z}$$

Successive dot products of this vector expression with the triad of vectors \underline{L} , \underline{A}_h , \underline{D}_h , defined by the observed quantities, leads to the coefficients for sensor location in terms of range, azimuth and elevation, as given in Table V-1.

The comparable coefficients for range-rate may be derived from

$$\rho \Delta \rho = \underline{\rho} \cdot \Delta \underline{\rho} = \underline{\rho} \cdot \Delta \underline{R}, \text{ since } \Delta \underline{r} = 0.$$

Taking the time derivative,

$$\rho \Delta \dot{\rho} = (\dot{\underline{\rho}} - \dot{\rho} \underline{L}) \cdot \Delta \underline{R} + \underline{\rho} \cdot \Delta \dot{\underline{R}}$$

From

$$\underline{R} = - (C + H) \underline{Z}$$

$$\Delta \underline{R} = (C + H) \Delta \phi \underline{S} - (C + H) \cos \lambda_E \Delta \theta \underline{E} - \Delta H \underline{Z}$$

and from

$$\dot{\underline{R}} = \underline{\Omega} \times \underline{R}, \underline{\Omega} = \dot{\theta} \underline{K}$$

$$\begin{aligned} \Delta \dot{\underline{R}} &= (C + H) \Delta \phi [\dot{\theta} (s_{xJ} - s_{yI})] \\ &\quad - (C + H) \cos \phi \Delta \lambda_E [\dot{\theta} (E_{xJ} - E_{yI})] \\ &\quad + \Delta H [\dot{\theta} (z_{xJ} - z_{yI})] \end{aligned}$$

These substitutions in the equation for $\rho\Delta\dot{\rho}$, above, lead to

$$\begin{aligned}\rho\Delta\dot{\rho} &= (C + H) \Delta\phi [\underline{S} \cdot (\underline{\dot{\rho}} - \dot{\rho}\underline{L} + \underline{\rho} \times \underline{\Omega})] \\ &\quad - (C + H) \cos\phi \Delta\lambda_E [\underline{E} \cdot (\underline{\dot{\rho}} - \dot{\rho}\underline{L} + \underline{\rho} \times \underline{\Omega})] \\ &\quad - \Delta H [\underline{Z} \cdot (\underline{\dot{\rho}} - \dot{\rho}\underline{L} + \underline{\rho} \times \underline{\Omega})]\end{aligned}$$

These expressions are given in Table V-1.

V.2 SCALAR DIFFERENTIAL EXPRESSIONS FOR TIME AND OBSERVATION BIAS

The sensor timing error ΔT may be identified by the equivalent orbital ΔU ($= n\Delta T$) required to bring the orbit timing into agreement with the sensor observation times. These coefficients are identical to those employed in the orbit differential correction. In theory, the relation of timing to ΔU through the mean motion n is strictly valid for low-eccentricity orbits; in practice, the iterative application of these expressions produce rapid convergence.

The additional terms in Table V-1 relating to biases in the observed quantities, are trivial.

V.3 COORDINATES OF THE SENSOR AND THE SATELLITE

This section is appended to derive the expressions for sensor location used in the program and the expression for the height of a satellite above the oblate spheroid. The last expression is cited on Page 4 of Appendix I and Page 1 of Appendix IV.

The meridian section of the earth is assumed to be an ellipse. The coordinates of the intersection of the radius vector with the spheroid are

$$\begin{aligned}x_c &= r_c \cos \phi' = a_e \cos E \\ y_c &= r_c \sin \phi' = a_e \sqrt{1-e^2} \sin E\end{aligned}$$

TABLE V-1. SCALAR DIFFERENTIAL EXPRESSIONS FOR SENSOR CALIBRATION

	SENSOR LOCATION ERROR			TIMING	OBSERVATION BIASES		
	$(C+H) \Delta\phi$	$-(C+H) \cos \phi \Delta\lambda$	$-\Delta H$	$n \Delta T$	$\Delta\rho_B$	ΔA_B	Δh_B
RANGE $\Delta\rho$	$\underline{S} \cdot \underline{L}_h$	$\underline{E} \cdot \underline{L}_h$	$\underline{Z} \cdot \underline{L}_h$	$\underline{L}_h \cdot (\underline{U}R_u + \underline{V}U_u)$	1	0	0
AZIMUTH $\rho \cos h \Delta A$	$\underline{S} \cdot \underline{A}_h$	$\underline{E} \cdot \underline{A}_h$	$\underline{Z} \cdot \underline{A}_h (=0)$	$\underline{A}_h \cdot (\underline{U}R_u + \underline{V}U_u)$	0	$\rho \cos h$	0
ELEVATION $\rho \Delta h$	$\underline{S} \cdot \underline{D}_h$	$\underline{E} \cdot \underline{D}_h$	$\underline{Z} \cdot \underline{D}_h$	$\underline{D}_h \cdot (\underline{U}R_u + \underline{V}U_u)$	0	0	ρ
RANGE-RATE $\rho \Delta \dot{\rho}$	$\underline{S} \cdot (\dot{\underline{\rho}} - \dot{\underline{\rho}}_L + \underline{\rho} \times \underline{\Omega})$	$\underline{E} \cdot (\dot{\underline{\rho}} - \dot{\underline{\rho}}_L + \underline{\rho} \times \underline{\Omega})$	$\underline{Z} \cdot (\dot{\underline{\rho}} - \dot{\underline{\rho}}_L + \underline{\rho} \times \underline{\Omega})$	$(\dot{\underline{\rho}} - \dot{\underline{\rho}}_L) \cdot (\underline{U}R_u + \underline{V}U_u) + \underline{\rho} [\underline{U}(\dot{R}_u + \dot{v}U_u) + \underline{V}(\dot{U}_u + \dot{v}R_u)]$	0	0	0

06

where x_c , y_c , a_e and e are the same as in V.1 above and ϕ' is the geocentric latitude. E , the eccentric (or reduced) latitude, corresponds to the eccentric anomaly in the orbital ellipse.

$$(1-e^2) x_c^2 + y_c^2 = r_c^2 (1-e^2 \cos^2 \phi') = a_e^2 (1-e^2)$$

a. Geodetic Sensor Location

Consider a small change of eccentric latitude. This will produce (see Figure V-2) the coordinate changes

$$-dx_c = ds \sin \phi = a_e dE \sin E$$

$$dy_c = ds \cos \phi = a_e dE \sqrt{1-e^2} \cos E$$

where ds is the displacement along the meridian.

Thus,

$$(1-e^2) (dx_c)^2 + (dy_c)^2 = (ds)^2 (1-e^2 \sin^2 \phi) = (a_e dE)^2 (1-e^2)$$

from which

$$\sin E = \frac{ds}{a_e dE} \quad \sin \phi = \frac{\sqrt{1-e^2} \sin \phi}{\sqrt{1-e^2} \sin^2 \phi}$$

and

$$\sqrt{1-e^2} \cos E = \frac{ds}{a_e dE} \cos \phi = \frac{\sqrt{1-e^2} \cos \phi}{\sqrt{1-e^2} \sin^2 \phi}$$

For a point on the spheroid then

$$x_c = \frac{a_e \cos \phi}{\sqrt{1-e^2 \sin^2 \phi}} = C \cos \phi$$

and

$$y_c = \frac{a_e (1-e^2) \sin \phi}{\sqrt{1-e^2 \sin^2 \phi}} = S \sin \phi$$

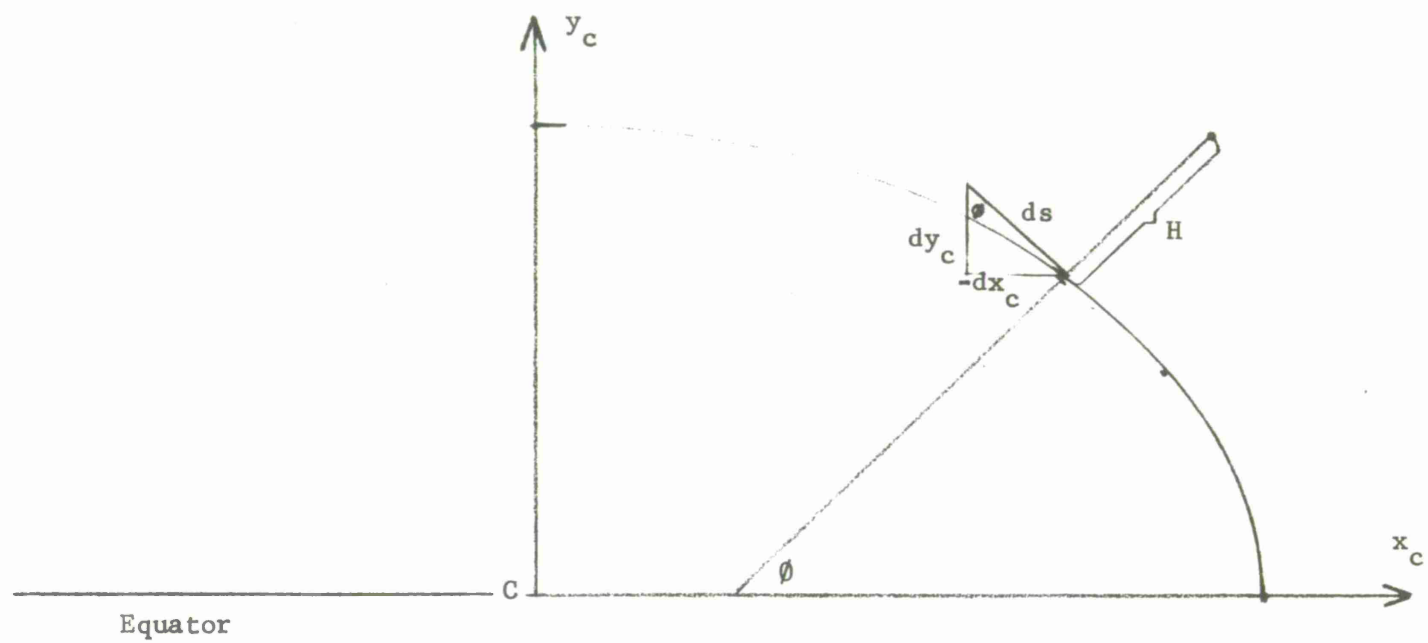


FIGURE V-2. MERIDIAN CROSS-SECTION OF EARTH

Since height, H, is ordinarily measured opposite to the direction of gravity, for a general point and in particular for the sensor

$$x_c = (C + H) \cos \phi$$

$$y_c = (S + H) \sin \phi$$

as in V.1 above.

b. Height Above Oblate Spheroid

In terms of geodetic latitude, the distance from the center of the earth is

$$r_c = a_e \sqrt{1-e^2} \left[1 - e^2 \cos^2 \phi' \right]^{-\frac{1}{2}}$$

$$r_c = a_e \sqrt{1-e^2} \left[(1 - e^2) + e^2 \sin^2 \phi' \right]^{-\frac{1}{2}}$$

$$r_c = a_e \left[1 + \frac{e^2}{1-e^2} U_z^2 \right]^{-\frac{1}{2}}$$

since

$$U_z = \sin \phi'$$

$$r_c = a_e \left[1 + \frac{2f-f^2}{(1-f)^2} U_z^2 \right]^{-\frac{1}{2}}$$

$$r_c = a_e \left\{ 1 + (2f-f^2) \left[1 + 2f + O(f^2) \right] U_z^2 \right\}^{-\frac{1}{2}}$$

$$r_c = a_e \left\{ 1 + \left[2f+3f^2 + O(f^3) \right] U_z^2 \right\}^{-\frac{1}{2}}$$

$$r_c = a_e \left\{ 1 - (f+\frac{3}{2}f^2) U_z^2 + \frac{3}{2}f^2 U_z^4 + O(f^3) \right\}$$

APPENDIX VI
VARIATION-OF-PARAMETERS FOR
NON EQUATORIAL ORBITS

In the variation-of-parameters technique, the parameters of an osculating orbit are determined by the actual position and velocity at a given instant. These parameters describe the two-body orbit that the object would follow if all subsequent perturbations were removed. Thus, in Fig. VI-1, the full curve represents the actual disturbed path of an object, and the two dotted ellipses represent the osculating two-body orbits derived from position and velocity at the points A and B, respectively.

When the two points are close together, the elements of the two osculating ellipses will differ by relatively small amounts. Hence, these elements may be visualized as parameters that vary with time because of the disturbing forces.

The ephemeris program employs the variation-of-parameters technique and thereby overcomes the computational inefficiency of numerical integration methods where the total acceleration is computed and integrated step-by-step. Computational efficiency is achieved by replacing the integrated variables by parameters which, in the two-body case, are invariant. Thus, the numerical integration required relates only to the components of the force field which disturb the two-body motion. These perturbations are extremely small in comparison to the central force term during normal orbiting flight. An alternative perturbation technique, the so called "Encke" method which integrates departures from the two-body orbit, is not well adapted to the integration of a satellite orbit when the object is exposed to continuous drag over the orbit.

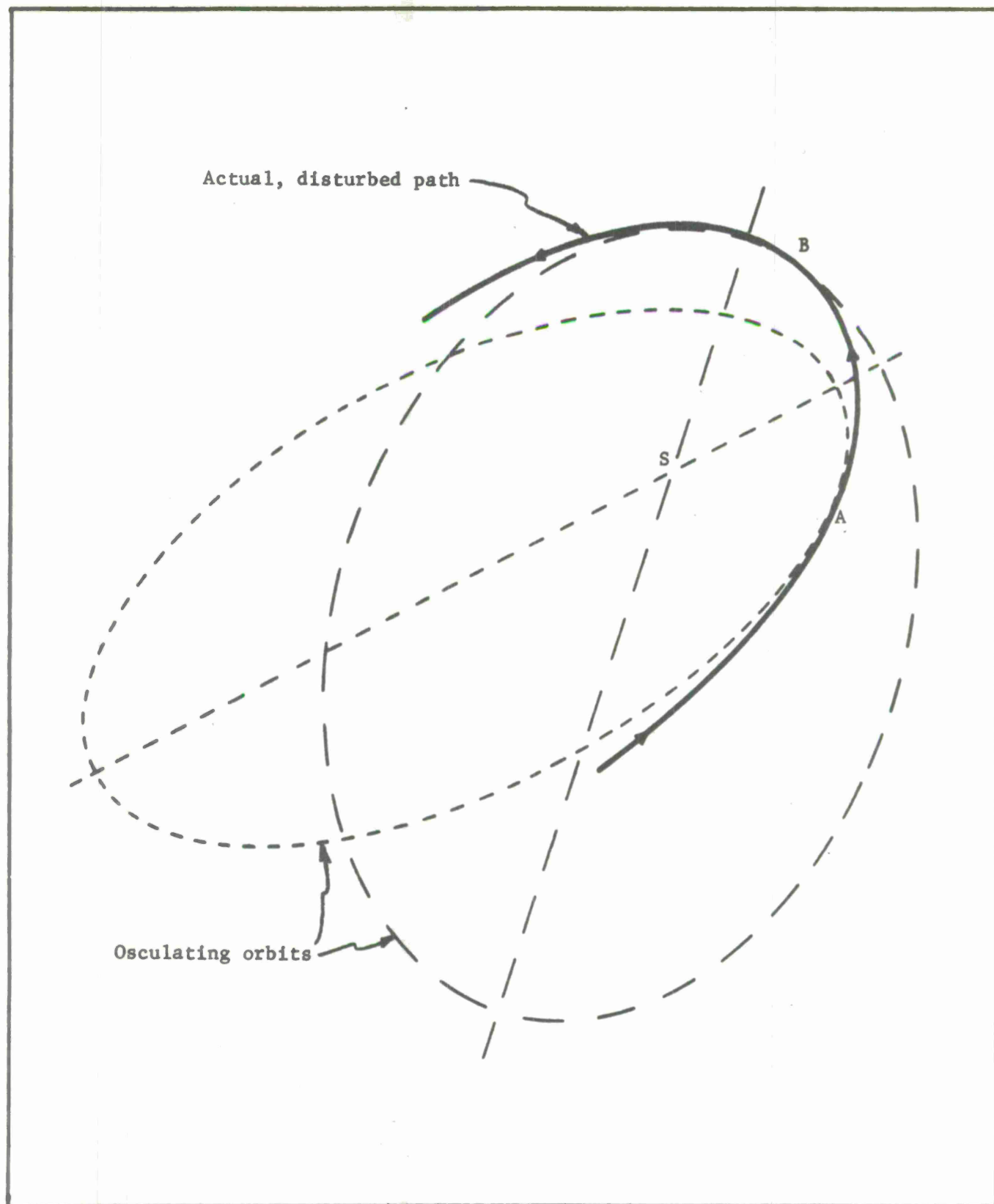


FIGURE VI-1. OSCULATING ORBIT DEFINITION

In the following analysis, the time rate-of-change or variation of functions will be divided into two parts as follows:

If f is any function,

$$\frac{1}{k_e} \frac{df}{dt} = \frac{df}{d\tau} = \dot{f} + \grave{f} \quad (1)$$

where $\tau = k_e (t-t_0)$, the normalized time.

In Eq. (1) \dot{f} (f -dot) is the "two-body variation" that would hold at the instant if all subsequent perturbations were suddenly removed, i.e., the variation in the instantaneous osculating orbit; and \grave{f} (f -grave) is the perturbative variation, i.e., the part of the variation caused by the disturbing forces (in this case the atmospheric drag and Earth's bulge).

For some functions the perturbative variations are zero because the instantaneous osculating orbit is defined so as to yield for their variations the same values as the actual orbit. Thus, for x , y , and z referred to non-rotating axes,

$$\frac{dx}{d\tau} = \dot{x}, \quad \grave{x} = 0, \quad x \rightarrow y, z^* \quad (2)$$

and for velocity functions independent of orientation,

$$\frac{dr}{d\tau} = \dot{r}, \quad \grave{r} = 0 \quad (3)$$

*Denotes that similar relations hold for y and z components.

$$\frac{ds}{d\tau} = \dot{s} , \quad \ddot{s} = 0 \quad (4)$$

For the elements that would be constant in two-body motion, the variations are consequences of the disturbing forces alone. For example,

$$\frac{da}{d\tau} = \dot{a} , \quad \ddot{a} = 0 \quad (5)$$

$$\frac{dn}{d\tau} = \dot{n} , \quad \ddot{n} = 0 \quad (6)$$

The anomalies, v and E , and the mean longitude, L , have both kinds of variation because they are referred to a perturbed or "accelerated" origin. Thus,

$$\frac{dv}{d\tau} = \dot{v} + v' , \quad \dot{v} = r^{-2} \sqrt{\mu p} \quad (7a,b)$$

$$\frac{dE}{d\tau} = \dot{E} + E' , \quad \dot{E} = r^{-1} \sqrt{\mu/a} \quad (8a,b)$$

$$\frac{dL}{d\tau} = \dot{L} + L' \quad (9a)$$

Since $\dot{L} = \dot{M} = n/k_e$, the last of these expressions is more familiar in the form

$$\frac{dL}{dt} = n + k_e L' \quad (9b)$$

The parameters which are integrated in the low-eccentricity ephemeris program are:

- $\underline{h} = \sqrt{p} \underline{W}$ - the orbital angular momentum vector per unit mass
- $\underline{a} = e \underline{P}$ - a vector defining eccentricity and perigee location

$$L = M + \omega + \Omega \quad - \quad \text{the mean longitude of the object}$$

The vector, \underline{h} , is a logical choice for satellite orbits since it embodies the orientation of the orbit plane as well as the two-body properties of the orbit. The vector, \underline{a} , combines the effects of eccentricity and perigee location in a way which maintains continuity through zero eccentricity. The remaining parameters define the position of the object in its orbit. Seven quantities are integrated, including six components of the two vectors, rather than the minimum six, to avoid complications in the evaluation of some of the parameters.

In the application of the variation-of-parameters technique, the perturbative variations in the parameters must be related to the components of the disturbing accelerations. The perturbative variation in n , the mean motion, follows from the definition,

$$n = k_e \sqrt{\mu} a^{-3/2} \quad (10)$$

leading to

$$\dot{n} = -\frac{3}{2} n a^{-1} \dot{a} \quad (11)$$

To relate \dot{n} to the force field, it is necessary to express \dot{a} in terms of the perturbative variations in velocity, $\underline{\dot{r}}$. This is readily accomplished through the vis-viva integral,

$$\dot{s}^2 = \underline{\dot{r}} \cdot \underline{\dot{r}} = \mu \left[\frac{2}{r} - \frac{1}{a} \right] \quad (12)$$

Differentiation yields

$$2\dot{\underline{r}} \cdot \frac{d\dot{\underline{r}}}{d\tau} = -\frac{2\mu}{r^2} \frac{dr}{d\tau} + \frac{\mu}{a^2} \frac{da}{d\tau} \quad (13)$$

However, r is independent of orientation, and the semi-major axis and mean motion are constants in two-body motion. Therefore, using Eqs. (3) and (5), and the definition given in Eq. (1), leads to

$$2\dot{\underline{r}} \cdot (\ddot{\underline{r}} + \hat{\underline{r}}) = -\frac{2\mu}{r^2} \dot{r} + \frac{\mu}{a^2} \dot{a} \quad (14)$$

The first terms on each side of Eq. (14) are equivalent, since they arise in the differentiation of the two-body problem. The perturbative component of a is therefore

$$\dot{a} = \frac{2a^2}{\mu} \dot{\underline{r}} \cdot \hat{\underline{r}} \quad (15)$$

Combining Eq. (15) with Eq. (11) yields

$$\mu \dot{n} = -3na \dot{\underline{r}} \cdot \hat{\underline{r}} \quad (16)$$

Eq. (16) then relates \dot{n} to the forces tending to disturb the two-body motion. These forces are embodied in $\hat{\underline{r}}$ and include contributions from drag and the Earth's bulge. It is interesting to note that the mean motion is affected only by the tangential component of $\hat{\underline{r}}$; drag is, therefore, responsible for the secular variations in n .

By similar reasoning, other parameters may be related to the non two-body components of the force field. The angular momentum, \underline{h} , is immediately expressed through its definition,

$$\sqrt{\mu} \underline{h} = \underline{r} \times \dot{\underline{r}} \quad (17)$$

Therefore, by a shortcut differentiation process that may be inferred from the foregoing differentiation of $\dot{\underline{r}} \cdot \hat{\underline{r}}$,

$$\sqrt{\mu} \dot{\mathbf{h}} = \underline{\mathbf{r}} \times \dot{\underline{\mathbf{r}}} \quad (18)$$

because $\dot{\mathbf{h}}$ and $\dot{\underline{\mathbf{r}}}$ are both zero.

Next, the vector, $\underline{\mathbf{a}}$, can be expressed as

$$\sqrt{\mu} \underline{\mathbf{a}} = \dot{D} \underline{\mathbf{r}} - D \dot{\underline{\mathbf{r}}} \quad (19)$$

where D is defined as follows:

$$\sqrt{\mu} D = \underline{\mathbf{r}} \cdot \dot{\underline{\mathbf{r}}} \quad \text{and} \quad \sqrt{\mu} \dot{D} = \dot{\underline{\mathbf{r}}} \cdot \dot{\underline{\mathbf{r}}} - \frac{\sqrt{\mu}}{r} \quad (20)$$

Differentiation leads to the expression for $\dot{\underline{\mathbf{a}}}$,

$$\mu \dot{\underline{\mathbf{a}}} = (2\dot{\underline{\mathbf{r}}} \cdot \dot{\underline{\mathbf{r}}}) \underline{\mathbf{r}} - (\underline{\mathbf{r}} \cdot \dot{\underline{\mathbf{r}}}) \dot{\underline{\mathbf{r}}} - (\underline{\mathbf{r}} \cdot \dot{\underline{\mathbf{r}}}) \dot{\underline{\mathbf{r}}} \quad (21)$$

The perturbative expression for the mean longitude, L, is complicated by its dependence upon the rotation of the orbit plane about the instantaneous radius vector, $\underline{\mathbf{r}}$, as well as the transverse acceleration components. Thus,

$$\dot{L} = \dot{M} + \dot{\omega} + \dot{\Omega} \quad (22)$$

for direct motion.

While each of the three angles on the right-hand side in Eq. (22) behaves badly for small eccentricity or small inclination, their sum \dot{L} is well behaved.

The vectors, $\underline{\mathbf{r}}$ and $\underline{\mathbf{U}}$, are not instantaneously affected by the perturbations, so $\dot{\nu}$ arises solely from the perturbations of the orbital axes. From Fig. VI-2(a)

$$\dot{\nu} = \underline{\mathbf{P}} \cdot \dot{\underline{\mathbf{Q}}} = -\underline{\mathbf{Q}} \cdot \dot{\underline{\mathbf{P}}}$$

but $\underline{a} = e \underline{P}$

so $-e\dot{v} = \underline{Q} \cdot \underline{\dot{a}} = Q_x \dot{a}_x + Q_y \dot{a}_y + Q_z \dot{a}_z$ (23)

The orthogonal component of the perturbative acceleration is

$$r\dot{b} = \underline{W} \cdot \underline{\dot{r}} = W_x \dot{x} + W_y \dot{y} + W_z \dot{z} \quad (24)$$

where \underline{W} is the unit vector perpendicular to the instantaneous orbit plane.

The perturbations of the orientation angles are caused by the rotation of the orbit plane about the instantaneous radius vector, \underline{r} .
From Fig. VI-2(c)

$$\underline{N} = \underline{U} \cos u - \underline{V} \sin u, \quad (25)$$

and

$$\underline{M} = \underline{U} \sin u + \underline{V} \cos u, \quad (26)$$

where

$$u = v + \omega. \quad (27)$$

From Fig. VI-2(b), looking along the instantaneous line of nodes,

$$u' = -\Omega' \cos i \quad (28)$$

Now, at any instant, the true longitude is

$$l = u + \Omega \quad (29)$$

so that

$$l' = u' + \Omega' = \Omega' (1 - \cos i) \quad (30)$$

But from Fig. VI-2(b), Eq.(25), and the fact that $\underline{U}^{\dot{\lambda}} = 0$, so that

$$\underline{U} \cdot \underline{W}^{\dot{\lambda}} = -\underline{W} \cdot \underline{U}^{\dot{\lambda}} = 0,$$

$$\Omega^{\dot{\lambda}} \sin i = -\underline{W} \cdot \underline{N}^{\dot{\lambda}} = \underline{N} \cdot \underline{W}^{\dot{\lambda}} = -\underline{V} \cdot \underline{W}^{\dot{\lambda}} \sin u \quad (31)$$

Now, $\underline{V} = \underline{W} \times \underline{U}$ so $\sqrt{p} \underline{V} = \underline{h} \times \underline{U} = \underline{r} \times \underline{\dot{r}} \times \underline{U}$

or $\sqrt{p} \underline{V} = (\underline{r} \underline{\dot{r}} - \underline{\dot{r}} \underline{r}) / \sqrt{\mu}$

so that

$$\sqrt{p}^{\dot{\lambda}} \underline{V} + \sqrt{p} \underline{V}^{\dot{\lambda}} = (\underline{r} \underline{\dot{r}}^{\dot{\lambda}} - \underline{\dot{r}}^{\dot{\lambda}} \underline{r}) / \sqrt{\mu} \quad (32)$$

because $\underline{r}^{\dot{\lambda}} = 0$ and $\underline{\dot{r}}^{\dot{\lambda}} = 0$.

Now dotting \underline{W} into Eq. (32) above and noting that

$$\underline{W} \cdot \underline{V} = 0,$$

$$\underline{W}^{\dot{\lambda}} \cdot \underline{V} = -\underline{W} \cdot \underline{V}^{\dot{\lambda}},$$

and

$$\underline{W} \cdot \underline{r} = 0$$

because of orthogonality,

$$\underline{V}^{\dot{\lambda}} \cdot \underline{W} = \underline{r} \frac{\underline{W} \cdot \underline{\dot{r}}^{\dot{\lambda}}}{\sqrt{\mu} p} = -\underline{V} \cdot \underline{W}^{\dot{\lambda}}. \quad (33)$$

Substituting Eq. (33) into Eq. (31) and recalling Eq. (24),

$$\Omega^{\dot{\lambda}} = \frac{r^2 \dot{b}^{\dot{\lambda}} \sin u}{\sqrt{\mu} p \sin i}. \quad (34)$$

Finally, entering these relationships into Eq. (30),

$$\dot{\lambda} = \frac{r \sin u (1 - \cos i) r \dot{b}^{\dot{\lambda}}}{\sqrt{\mu} p \sin i},$$

or

$$\ell' = \frac{(r \sin u \sin i) r b^3}{\sqrt{\mu p} (1 + \cos i)} .$$

But

$$z = r \sin u \sin i$$

and

$$\cos i = W_z ,$$

so

$$\ell' = \frac{z (r b^3)}{(1 + W_z) \sqrt{\mu p}} . \quad (35)$$

The following fundamental relationships are used in deriving \dot{L} :

$$M = E - e \sin E , \quad (36)$$

$$e \sin E = \frac{r \dot{r}}{\sqrt{\mu a}} , \quad (37)$$

$$r \cos v = a (\cos E - e) , \quad (38)$$

$$r \sin v = a \sqrt{1 - e^2} \sin E , \quad (39)$$

$$\frac{r}{a} = (1 - e \cos E) , \quad (40)$$

$$L = M + \omega + \Omega = M + \Pi , \quad (41)$$

$$\Pi = \omega + \Omega . \quad (42)$$

Differentiating Eq. (42),

$$\dot{\Pi} = \dot{\omega} + \dot{\Omega} = \dot{\ell}' - v' , \quad (43)$$

so that

$$\dot{L} = \dot{M}' + \dot{\ell}' - v' . \quad (44)$$

Differentiating Eq. (40) and Eq. (37),

$$(e \cos E)' = e' \cos E - e E' \sin E = \frac{r}{a^2} a', \quad (45)$$

$$(e \sin E)' = e' \sin E + e E' \cos E = \frac{r r'}{\sqrt{\mu a}} - \frac{1}{2} \frac{a'}{a} e \sin E, \quad (46)$$

from which

$$e' = \frac{r r'}{\sqrt{\mu a}} \sin E + \frac{1}{2} \frac{a'}{a} \left[\left(\frac{r}{a} + 1 \right) \cos E - e \right], \quad (47)$$

and

$$e E' = \frac{r r'}{a} \cos E - \frac{1}{2} \frac{a'}{a} \left(\frac{r}{a} + 1 \right) \sin E. \quad (48)$$

Now differentiating Eq. (38) and rearranging terms,

$$a E' \sin E = r v' \sin v + a' (\cos E - e) - a e'. \quad (49)$$

Substituting Eq. (39) and Eq. (40) and dividing out $a \sin E$,

$$E' = v' \sqrt{1-e^2} - \frac{r r'}{\sqrt{\mu a}} - \frac{1}{2} \frac{a'}{a} e \sin E. \quad (50)$$

Differentiating Eq. (36) and introducing Eq. (46),

$$M' = E' - (e \sin E)' = E' - \frac{r r'}{\sqrt{\mu a}} + \frac{1}{2} \frac{a'}{a} e \sin E. \quad (51)$$

Combining Eq. (50) and Eq. (51),

$$M' = v' \sqrt{1-e^2} - \frac{2 r r'}{\sqrt{\mu a}}. \quad (52)$$

Finally, using Eq. (44) and Eq. (52),

$$\dot{L} = \dot{\ell} - \frac{2 r r'}{\sqrt{\mu a}} - \frac{e^2 v'}{1 + \sqrt{1-e^2}}. \quad (53)$$

APPENDIX VII

LIST OF SYMBOLS

Many of the symbols used in this document occur with the same meaning throughout the various volumes. These have been defined below. We have attempted to avoid inventing new notation wherever possible. The symbology is closest to that of Baker and Makemson, Introduction to Astrodynamics, Academic Press, 1960. This in turn is based on the notation of Herrick, who follows closely the recommendations of the International Astronomical Union.

Some symbols, which are used only once, are defined at that place and not in this list. Subscripts are sometimes an obvious use of a symbol defined in this list to delimit another symbol. Such a subscript is not generally defined separately. For any other omissions apologies are offered.

Vectors are denoted by underlines. While most vectors symbolized with capital letters are unit vectors, \underline{R} , for instance, is not.

Superscripts

· (Dot)	Derivative with respect to τ (canonical time)
' (Grave)	Perturbative derivative with respect to
- (Bar)	Average

LIST OF SYMBOLS

A	Azimuth angle, measured eastward from north in the horizon plane
A	Effective cross-sectional area of the satellite
\underline{A}	Unit vector perpendicular to the line-of-sight vector, \underline{L} , in the direction of increasing right ascension
$\widetilde{\underline{A}}$	Unit vector perpendicular to the line-of-sight vector, \underline{L} , in the direction of increasing azimuth
A_ρ	Geomagnetic index
a	Semi-axis major of ellipse or hyperbola, mean distance
a_e	Mean equatorial radius of the earth
\underline{a}	$e\underline{P}$, vector integral of the equations of motion
a_{XN}	$e \cos \omega = \underline{a} \cdot \underline{N}$
a_{YN}	$e \sin \omega = \underline{a} \cdot \underline{M}$
B	Subscript denoting bulge (asphericity) perturbations
B	Ballistic parameter, $\frac{C_D A}{m}$
B_n	Modified Bessel function of imaginary argument, Z: $B_n(z) = \frac{2}{z} I_n^n(Z)$
B_i	Bias in O_i stored in BIBUF
b	Semi-axis minor: $b = a \sqrt{1-e^2}$

- C Auxiliary quantity used to find station coordinates:
- $$C = a_e \sqrt{1 - e^2 \sin^2 \vartheta}$$
- C_D Total atmospheric drag coefficient
- $C_{\Delta i}$ Coefficient of Δi in the equations of condition (differential correction), where i is a parameter to which correction is sought
- $C_{i,j}$ Coefficient of $\cos j \lambda$ in tesseral harmonic of order i
- c Speed of light
- c Subscript indicating computed value or a quantity derived from the ephemeris computation
- D Auxiliary variable: $\sqrt{\mu} \quad D = r\dot{r}$
- D Day Number
- D Subscript denoting drag (atmospheric) perturbations
- \underline{D} Unit vector perpendicular to line-of-sight vector, \underline{L} , in direction of increasing declination
- $\tilde{\underline{D}}$ Unit vector perpendicular to line-of-sight vectors, \underline{L} , in direction of increasing elevation angle
- d Differential operator
- E Eccentric anomaly
- \underline{E} Unit vector to east point of horizon

F_{10}	Flux of solar radiation at 10.7 cm
\bar{F}_{10}	F_{10} averaged over three solar rotations
F_{\odot}	Magnitude of the force of solar radiation pressure
f	Flattening of earth spheroid
g	Acceleration of gravity
g_E	Components of the perturbative acceleration due to the earth's asphericity in the easterly, southerly and radial directions. Note that radial is defined here in the geocentric, not geodetic, sense and thus southerly is perpendicular to the geocentric radius and not in the local horizon plane
g_S	
g_r	
g_r	Subscript denoting Greenwich meridian
H	Scale Height
\underline{H}	Unit vector perpendicular to line of nodes in the equator plane
H_{\odot}	Hour angle of the sun
H_{ρ}	Density scale height
h	Height above sea level
h	Subscript indicating horizon coordinate system
h	Elevation angle
\underline{h}	Vector integral of the equations of motion: $\sqrt{\mu} \underline{h}$ is the angular momentum per unit mass \underline{W}

<u>I</u>	Unit vector toward the foot of the mean vernal equinoctial colure of epoch on the true equator of date
$I_n(z)$	Bessel Function of imaginary argument and order n
i	inclination of the satellite orbit to the equator plane
<u>J</u>	Unit vector to foot of summer solstitial colure on the true equator of date
<u>K</u>	Unit vector to the north pole of the true equator of date
k	reciprocal of scale height
k_e	Gaussian gravitational constant, square root of the product of the universal constant of gravitation and the mass of the earth. $k_e = 0.07436662$ (earth radii) ^{3/2} per minute
k'	Dimensionless number equal to k_e , ratio of canonical to ordinary solar time.
L	Mean orbital longitude
<u>L</u>	Line-of-sight unit vector
l	True orbital longitude
M	Mean anomaly
<u>M</u>	Unit Vector toward northern antinode of the orbit

m	mass of satellite
\underline{N}	Unit vector toward ascending node
n	Mean angular motion of satellite
O_i	General notation for an observed quantity
o	Subscript referring to epoch, t_o
o	Subscript indicating observed value or a quantity derived from observed values
θ	Subscript denoting sun
P	Period of revolution
P	Pressure
\underline{P}	Unit vector to perigee
P_θ	Solar radiation pressure
P_n	Legendre polynomial order n
$P_{n,m}$	Associated Legendre function
P'_n	Derivative of the Legendre polynomial with respect to its argument
$P'_{n,m}$	Derivative of the associated Legendre function with respect to its argument
p	Semi-latus rectum, parameter of conic section
P_j	General notation for a parameter describing the satellite motion

Q	apogee distance
\underline{Q}	Unit vector parallel to velocity at perigee
q	perifocal distance
R	Distance of observing station from center of earth
R	Subscript denoting radiation pressure perturbations
\underline{R}	Vector from observing station to center of earth. Its components are X, Y, Z
$R_{n,m}$	$P_{n,m} (1 - U_z^2)^{-1/2}$
$R'_{n,m}$	$P'_{n,m} (1 - U_z^2)^{1/2}$
r	Radial distance from center of earth to satellite
\underline{r}	Position vector of satellite. Its components are x, y, z
$r_{i,j}$	Correlation between corrections to elements i and j
S	$C(1 - e)^2$, auxiliary quantity used in finding station coordinates
\underline{S}	Unit Vector to South point of horizon or similar unit vector perpendicular to radius vector.
S_{ij}	Coefficient of $\sin j \lambda$ in tesseral harmonic of order i

s	Fraction of interpolation interval
s	arc length
\dot{s}	speed, magnitude of velocity vector
T	Temperature
t	time
U	Mean argument of latitude
\underline{U}	Unit vector toward satellite
u	True argument of latitude
\underline{V}	Unit vector in orbit plane perpendicular to radius vector in direction of increasing anomaly, transverse unit vector
v	true anomaly
\underline{W}	Unit vector perpendicular to orbit plane in same direction as angular momentum vector
X	$\underline{R} \cdot \underline{I}$, component of station vector
x	$\underline{r} \cdot \underline{I}$, component of satellite position vector

\bar{Y}	$\underline{J} \cdot \underline{R}$ component of station vector
y	$\underline{J} \cdot \underline{r}$ component of satellite position vector
Z	$\underline{K} \cdot \underline{R}$ component of station vector
z	$\underline{K} \cdot \underline{r}$ component of satellite position vector
z	$\frac{ae}{H_p}$ argument in the analytic integration of drag
α	right ascension
α	$1/2kf \sin^2 i_e a_e \cos 2\omega$, argument in the expansion of the analytical drag perturbations to account for the oblateness of the atmosphere
γ	Reflectivity of satellite
Δ	Differential operator producing a small finite increment, especially a residual
δ	Declination
ϵ	Small criterion for convergence or error test
ϵ	Obliquity of the ecliptic

η	$\sin^{-1} (r^{-1})$, auxiliary angle used in radiation pressure perturbations
π	Minimum angular distance from subsolar bulge (Appendix II, Volume I)
θ	Sidereal time
κ	Upper bound (fraction) for correction to ballistic parameter
κ_B	Tabular coefficient of ballistic parameter to account for variation of drag coefficient with altitude
λ, λ_E	Geographic longitude measured east from Greenwich
λ_W	Longitude west of Greenwich
μ	Gravitation constant, usually unity
v	speed with respect to atmosphere, ground speed
\underline{v}	Velocity with respect to atmosphere, ground velocity
ξ	Maximum angular distance from subsolar bulge (Appendix II, Volume I)
Π	Longitude of perigee
π	subscript denoting perigee value

ρ	Atmospheric density
ρ	Range, distance from sensor to satellite
$\underline{\rho}$	Position vector of satellite with respect to sensor
Σ	Summation operator
σ	Standard deviation
τ	canonical time $\tau = k'(t - t_0)$
τ	Modified hour angle of subsolar bulge (Appendix II, Volume I)
Φ	Potential
\emptyset	Geodetic or astronomical latitude
\emptyset'	Geocentric latitude
ψ	Elongation from Sun
Ω	Right ascension of the ascending node
ω	Argument of perigee

DOCUMENT CONTROL DATA - R&D

(Security classification of title, body of abstract and indexing annotation must be entered when the overall report is classified)

1. ORIGINATING ACTIVITY (Corporate author) Philco Corporation, Newport Beach, California		2a. REPORT SECURITY CLASSIFICATION Vol I-III Uncl, Vol IV Secret	
		2b. GROUP Vol IV-4	
3. REPORT TITLE Spiral Decay and Sensor Calibration Differential Correction Programs Volumes I, II, III, and IV.			
4. DESCRIPTIVE NOTES (Type of report and inclusive dates)			
5. AUTHOR(S) (Last name, first name, initial) Gaa, T G VanderStucken, P A Hilton, C G Walters, L G			
6. REPORT DATE Feb 65		7a. TOTAL NO. OF PAGES 123	7b. NO. OF REFS 0
8a. CONTRACT OR GRANT NO. AF19(628)3377		8a. ORIGINATOR'S REPORT NUMBER(S) ESD-TDR-65-76 4VOLS	
b. PROJECT NO. 496L SPO		8b. OTHER REPORT NO(S) (Any other numbers that may be assigned this report)	
c.			
d.			
10. AVAILABILITY/LIMITATION NOTICES Qualified requesters may obtain copies from DDC. Vol IV Not releasable to OTS.			
11. SUPPLEMENTARY NOTES None		12. SPONSORING MILITARY ACTIVITY 496L SPO, Hq ESD, L G Hanscom Fld., Bedford, Mass.	
13. ABSTRACT This documents presents the theory, operation, and coding details of and experience with a computer program for the accurate prediction of the reentry corridor of an earth satellite undergoing orbital decay due to atmospheric friction. This program is also useful in the precision prediction of satellite positions for other purposes such as sensor calibration and weapon systems.			

14. KEY WORDS	LINK A		LINK B		LINK C	
	ROLE	WT	ROLE	WT	ROLE	WT
<p>Orbit Determination Computer Programming EDP SPACETRACK Satellites</p>						

INSTRUCTIONS

1. **ORIGINATING ACTIVITY:** Enter the name and address of the contractor, subcontractor, grantee, Department of Defense activity or other organization (*corporate author*) issuing the report.
- 2a. **REPORT SECURITY CLASSIFICATION:** Enter the overall security classification of the report. Indicate whether "Restricted Data" is included. Marking is to be in accordance with appropriate security regulations.
- 2b. **GROUP:** Automatic downgrading is specified in DoD Directive 5200.10 and Armed Forces Industrial Manual. Enter the group number. Also, when applicable, show that optional markings have been used for Group 3 and Group 4 as authorized.
3. **REPORT TITLE:** Enter the complete report title in all capital letters. Titles in all cases should be unclassified. If a meaningful title cannot be selected without classification, show title classification in all capitals in parenthesis immediately following the title.
4. **DESCRIPTIVE NOTES:** If appropriate, enter the type of report, e.g., interim, progress, summary, annual, or final. Give the inclusive dates when a specific reporting period is covered.
5. **AUTHOR(S):** Enter the name(s) of author(s) as shown on or in the report. Enter last name, first name, middle initial. If military, show rank and branch of service. The name of the principal author is an absolute minimum requirement.
6. **REPORT DATE:** Enter the date of the report as day, month, year; or month, year. If more than one date appears on the report, use date of publication.
- 7a. **TOTAL NUMBER OF PAGES:** The total page count should follow normal pagination procedures, i.e., enter the number of pages containing information.
- 7b. **NUMBER OF REFERENCES:** Enter the total number of references cited in the report.
- 8a. **CONTRACT OR GRANT NUMBER:** If appropriate, enter the applicable number of the contract or grant under which the report was written.
- 8b, 8c, & 8d. **PROJECT NUMBER:** Enter the appropriate military department identification, such as project number, subproject number, system numbers, task number, etc.
- 9a. **ORIGINATOR'S REPORT NUMBER(S):** Enter the official report number by which the document will be identified and controlled by the originating activity. This number must be unique to this report.
- 9b. **OTHER REPORT NUMBER(S):** If the report has been assigned any other report numbers (*either by the originator or by the sponsor*), also enter this number(s).
10. **AVAILABILITY/LIMITATION NOTICES:** Enter any limitations on further dissemination of the report, other than those

imposed by security classification, using standard statements such as:

- (1) "Qualified requesters may obtain copies of this report from DDC."
- (2) "Foreign announcement and dissemination of this report by DDC is not authorized."
- (3) "U. S. Government agencies may obtain copies of this report directly from DDC. Other qualified DDC users shall request through _____."
- (4) "U. S. military agencies may obtain copies of this report directly from DDC. Other qualified users shall request through _____."
- (5) "All distribution of this report is controlled. Qualified DDC users shall request through _____."

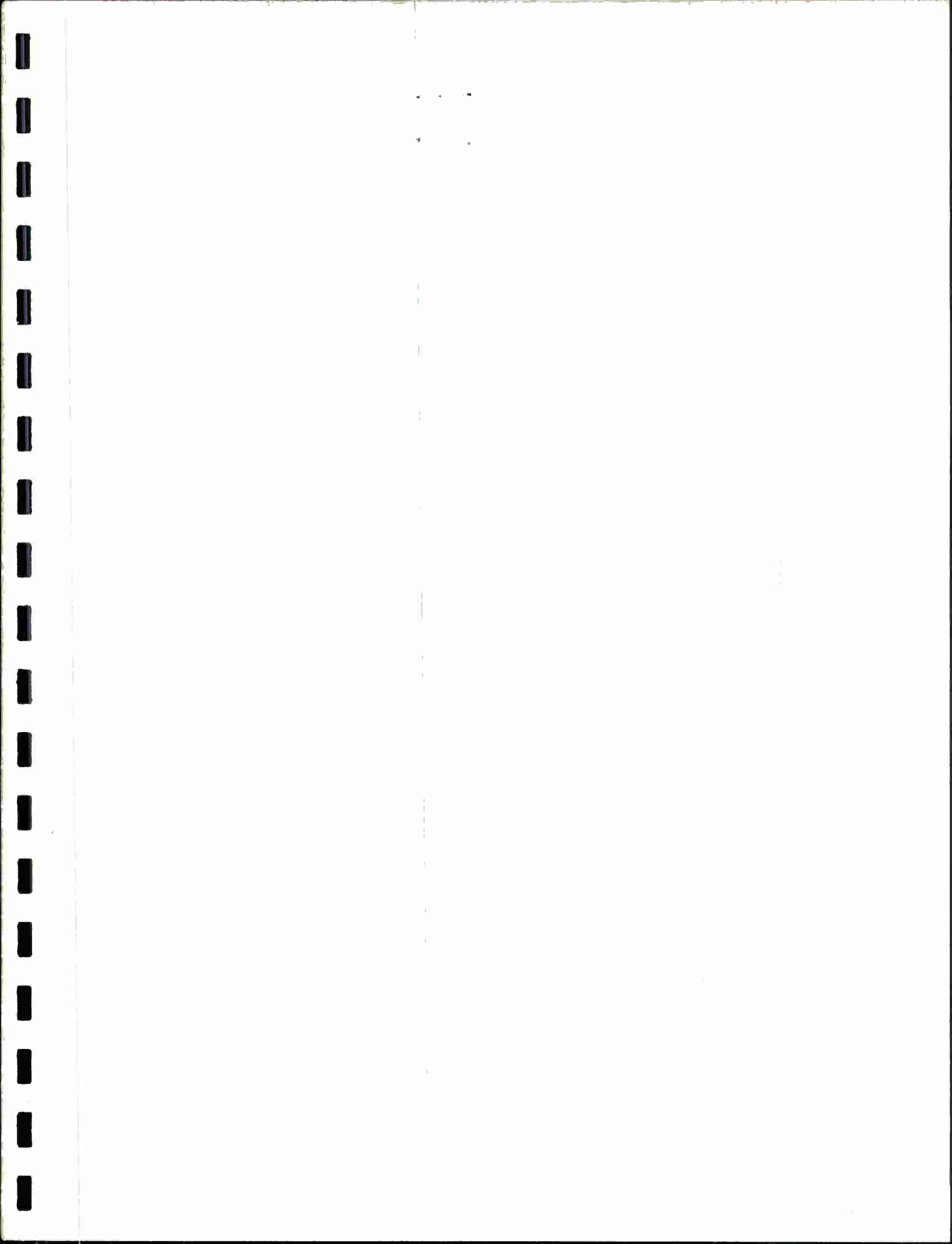
If the report has been furnished to the Office of Technical Services, Department of Commerce, for sale to the public, indicate this fact and enter the price, if known.

11. **SUPPLEMENTARY NOTES:** Use for additional explanatory notes.
12. **SPONSORING MILITARY ACTIVITY:** Enter the name of the departmental project office or laboratory sponsoring (*paying for*) the research and development. Include address.
13. **ABSTRACT:** Enter an abstract giving a brief and factual summary of the document indicative of the report, even though it may also appear elsewhere in the body of the technical report. If additional space is required, a continuation sheet shall be attached.

It is highly desirable that the abstract of classified reports be unclassified. Each paragraph of the abstract shall end with an indication of the military security classification of the information in the paragraph, represented as (TS), (S), (C), or (U).

There is no limitation on the length of the abstract. However, the suggested length is from 150 to 225 words.

14. **KEY WORDS:** Key words are technically meaningful terms or short phrases that characterize a report and may be used as index entries for cataloging the report. Key words must be selected so that no security classification is required. Identifiers, such as equipment model designation, trade name, military project code name, geographic location, may be used as key words but will be followed by an indication of technical context. The assignment of links, rules, and weights is optional



100
100

100
100

